Nuclear Safety
NEA/CSNI/R(2017)1
April 2017
www.oecd-nea.org

Reactivity-initiated Accident Fuel-rod-code Benchmark Phase II: Uncertainty and Sensitivity Analyses

OECD
BETTER POLICIES FOR BETTER LIVES

NEA
NUCLEAR ENERGY AGENCY

Unclassified **NEA/CSNI/R(2017)1**

Organisation de Coopération et de Développement Économiques
Organisation for Economic Co-operation and Development **22-May-2017**

English text only

NUCLEAR ENERGY AGENCY
COMMITTEE ON THE SAFETY OF NUCLEAR INSTALLATIONS

Cancels & replaces the same document of 10 April 2017

Reactivity-Initiated Accident (RIA) Fuel-Codes Benchmark Phase II: Uncertainty and Sensitivity Analyses

JT03414540

Complete document available on OLIS in its original format

NEA/CSNI/R(2017)1
Unclassified

English text only

ORGANISATION FOR ECONOMIC CO-OPERATION AND DEVELOPMENT

The OECD is a unique forum where the governments of 35 democracies work together to address the economic, social and environmental challenges of globalisation. The OECD is also at the forefront of efforts to understand and to help governments respond to new developments and concerns, such as corporate governance, the information economy and the challenges of an ageing population. The Organisation provides a setting where governments can compare policy experiences, seek answers to common problems, identify good practice and work to co-ordinate domestic and international policies.

The OECD member countries are: Australia, Austria, Belgium, Canada, Chile, the Czech Republic, Denmark, Estonia, Finland, France, Germany, Greece, Hungary, Iceland, Ireland, Israel, Italy, Japan, Latvia, Luxembourg, Mexico, the Netherlands, New Zealand, Norway, Poland, Portugal, the Republic of Korea, the Slovak Republic, Slovenia, Spain, Sweden, Switzerland, Turkey, the United Kingdom and the United States. The European Commission takes part in the work of the OECD.

OECD Publishing disseminates widely the results of the Organisation's statistics gathering and research on economic, social and environmental issues, as well as the conventions, guidelines and standards agreed by its members.

NUCLEAR ENERGY AGENCY

The OECD Nuclear Energy Agency (NEA) was established on 1 February 1958. Current NEA membership consists of 31 countries: Australia, Austria, Belgium, Canada, the Czech Republic, Denmark, Finland, France, Germany, Greece, Hungary, Iceland, Ireland, Italy, Japan, Luxembourg, Mexico, the Netherlands, Norway, Poland, Portugal, the Republic of Korea, the Russian Federation, the Slovak Republic, Slovenia, Spain, Sweden, Switzerland, Turkey, the United Kingdom and the United States. The European Commission also takes part in the work of the Agency.

The mission of the NEA is:

- to assist its member countries in maintaining and further developing, through international co-operation, the scientific, technological and legal bases required for a safe, environmentally friendly and economical use of nuclear energy for peaceful purposes;
- to provide authoritative assessments and to forge common understandings on key issues, as input to government decisions on nuclear energy policy and to broader OECD policy analyses in areas such as energy and sustainable development.

Specific areas of competence of the NEA include the safety and regulation of nuclear activities, radioactive waste management, radiological protection, nuclear science, economic and technical analyses of the nuclear fuel cycle, nuclear law and liability, and public information. The NEA Data Bank provides nuclear data and computer program services for participating countries.

COMMITTEE ON THE SAFETY OF NUCLEAR INSTALLATIONS

The NEA Committee on the Safety of Nuclear Installations (CSNI) is an international committee made up of senior scientists and engineers with broad responsibilities for safety technology and research programmes, as well as representatives from regulatory authorities. It was created in 1973 to develop and co-ordinate the activities of the NEA concerning the technical aspects of the design, construction and operation of nuclear installations insofar as they affect the safety of such installations.

The committee's purpose is to foster international co-operation in nuclear safety among NEA member countries. The main tasks of the CSNI are to exchange technical information and to promote collaboration between research, development, engineering and regulatory organisations; to review operating experience and the state of knowledge on selected topics of nuclear safety technology and safety assessment; to initiate and conduct programmes to overcome discrepancies, develop improvements and reach consensus on technical issues; and to promote the co-ordination of work that serves to maintain competence in nuclear safety matters, including the establishment of joint undertakings.

The priority of the CSNI is on the safety of nuclear installations and the design and construction of new reactors and installations. For advanced reactor designs, the committee provides a forum for improving safety-related knowledge and a vehicle for joint research.

In implementing its programme, the CSNI establishes co-operative mechanisms with the NEA Committee on Nuclear Regulatory Activities (CNRA), which is responsible for issues concerning the regulation, licensing and inspection of nuclear installations with regard to safety. It also co-operates with other NEA Standing Technical Committees, as well as with key international organisations such as the International Atomic Energy Agency (IAEA), on matters of common interest.

ACKNOWLEDGEMENTS

This report is prepared by the RIA Benchmark Phase II Task Group of the Working Group of Fuel Safety (WGFS).

Special gratitude is expressed to Olivier Marchand (IRSN, France) for drafting the report, to Jean Baccou and Vincent Georgenthum (IRSN, France) for their efforts in drafting Chapter 4 of the report, as well as to Asko Aekoma, (VTT, Finland), Marco Cherubini (NINE, Italy), Luis Enrique Herranz (CIEMAT, Spain), Lars Olof Jernkvist (Quantum Technologies, Sweden), Marc Petit (IRSN, France) Ian Porter (NRC, USA) , and Jinzhao Zhang (TRACTEBEL, Belgium) for reviewing the report.

The following WGFS members and experts performed calculations and provided valuable input to various chapters of the report:

Masaki AMAYA	JAEA,	Japan
Asko ARKOMA,	VTT,	Finland
Felix BOLDT,	GRS,	Germany
Heng BAN,	INL,	United States
Marco CHERUBINI,	NINE,	Italy
Adrien DETHIOUX,	TRACTEBEL,	Belgium
Thomas DRIEU,	TRACTEBEL,	Belgium
Charles FOLSOM,	INL,	United States
Vincent GEORGENTHUM,	IRSN,	France
Patrick GOLDBRONN,	CEA,	France
Luis Enrique HERRANZ,	CIEMAT,	Spain
Lars Olof JERNKVIST,	Quantum Technologies,	Sweden
Hyedong JEONG,	KINS,	Korea
Jan KLOUZAL, UJV,	Czech	Republic
Olivier MARCHAND,	IRSN,	France
Fabio MORETTI,	NINE,	Italy
István PANKA,	MTA EK,	Hungary
Ian PORTER,	NRC,	United States
José M. REY GAYO	CSN,	Spain
Inmaculada C. SAGRADO GARCIA,	CIEMAT,	Spain
Jérôme SERCOMBE,	CEA,	France,
Heinz Günther SONNENBERG,	GRS,	Germany
Yutaka UDAGAWA,	JAEA,	Japan
Jinzhao ZHANG,	TRACTEBEL,	Belgium

LIST OF ABBREVIATIONS AND ACRONYMS

CABRI	test reactor in France
CIEMAT	Centro de Investigaciones Energéticas, Medioambientales y Tecnológicas (Spain)
CSN	Consejo de Seguridad Nuclear (Spain)
CSNI	Committee on the Safety of Nuclear Installations (NEA)
DHR	variation of radial average enthalpy
DNB	departure from nucleate boiling
ECT	clad total axial elongation
ECTH	clad total (thermal + elastic + plastic) hoop strain
EFT1	fuel column total axial elongation
FGR	fission-gas release
FWHM	full width at half maximum
GRS	Gesellschaft für Anlagen- und Reaktorsicherheit (Germany)
HZP	hot zero power
INL	Idaho National Laboratory (United States)
IRSN	Institut de Radioprotection et de Sûreté Nucléaire (France)
JAEA	Japan Atomic Energy Agency
KINS	Korean Institute of Nuclear safety
LUB/UUB	lower/upper uncertainty bound
LUB_{min}/UUB_{max}	minimum/maximum of the LUBs/UUBs provided by all participants
MOX	mixed oxide fuel (U and Pu)
MTA EK	Centre of Energy Research, Hungarian Academy of Sciences
NEA	Nuclear Energy Agency (OECD)
NINE	Nuclear and INdustrial Engineering (Italy)
NRC	Nuclear Regulatory Commission (United States)
NSRR	Nuclear Safety Research Reactor (Japan)
OECD	Organisation for Economic Co-operation and Development

PCC	partial correlation coefficient
PCMI	pellet-cladding mechanical interaction
PDF	probability density function
PRCC	partial rank correlation coefficient
PWR	pressurised-water reactor
q_0	uncertainty interval width
q_1	indicator of the position of the reference calculation within the uncertainty interval
RCC	rank (Spearman's) correlation coefficient
REF	reference calculation
REF_{min}/REF_{max}	minimum/maximum of the reference calculations provided by all participants
RFO	fuel outer radius
RIA	reactivity-initiated accident
SCC	simple (Pearson's) correlation coefficient
SCH	clad hoop stress at outer part of the clad
SSM	Strålsäkerhetsmyndigheten (Swedish Radiation Safety Authority)
TCO	temperature of clad outer surface
TFC	temperature of fuel centreline
TFO	temperature of fuel outer surface
TRACTEBEL	Tractebel (ENGIE)
TSO	Technical Support Organisation
UJV	Nuclear research institute (Czech Republic), ÚJV Řež
VTT	Teknologian Tutkimuskeskus VTT/Technical Research Centre of Finland
WGFS	Working Group on Fuel Safety (NEA/CSNI)

TABLE OF CONTENTS

LIST OF FIGURES

LIST OF TABLES

EXECUTIVE SUMMARY

Reactivity-initiated accident (RIA) fuel rod codes have been developed for a significant period of time and validated against the available specific database. However, the high complexity of the scenarios dealt with has resulted in a number of different models and assumptions adopted by code developers; additionally, databases used to develop and validate codes have been different depending on the availability of the results of some experimental programmes. This diversity makes it difficult to find the source of estimate discrepancies, when these occur.

A technical workshop on "Nuclear Fuel Behaviour during Reactivity Initiated Accidents" was organized by the NEA in September 2009. As a conclusion of the workshop, it was recommended that a benchmark (RIA benchmark Phase I) between these codes be organized in order to give a sound basis for their comparison and assessment. This recommendation was endorsed by the Working Group on Fuel Safety.

The RIA benchmark Phase I was organized in 2010-2013. It consisted of a consistent set of four experiments on very similar highly irradiated fuel rods tested under different experimental conditions (NSRR VA-1, VA-3, CABRI CIP0-1 and CIP3-1). Seventeen organizations from fourteen countries participated in the Phase I, using eight different fuel rod codes.

The main conclusions of this RIA benchmark Phase I were the following:

- With respect to the thermal behaviour, the differences in the evaluation of fuel temperatures remained limited, although significant in some cases. The situation was very different for the cladding temperatures that exhibited considerable scatter, in particular for the cases when water boiling occurred.
- With respect to mechanical behaviour, the parameter of greatest interest was the cladding hoop strain because failure during RIA transient results from the formation of longitudinal cracks. When compared to the results of an experiment that involved only PCMI, the predictions from the different participants appeared acceptable even though there was a factor of 2 between the highest and the lowest calculations. The conclusion was not so favourable for cases where water boiling had been predicted to appear: a factor of 10 for the hoop strain between the calculations was exhibited. Other mechanical results compared during the RIA benchmark Phase I were fuel stack and cladding elongations. The scatter remained limited for the fuel stack elongation, but the cladding elongation was found to be much more difficult to evaluate.
- The fission gas release evaluations were also compared. The ratio of the maximum to the minimum values appeared to be roughly 2, which is considered to be relatively moderate given the complexity of fission-gas release processes.

As a conclusion of the RIA benchmark Phase I, it was recommended to launch a second-phase exercise with the following specific guidelines:

- The emphasis should be put on deeper understanding of the differences in modelling of the different codes; in particular, looking for simpler cases than those used in the first exercise was expected to reveal the main reasons for the observed large scatter in some conditions such as coolant boiling.
- Due to the large scatter between the calculations that was shown in the RIA benchmark Phase I, it appears that an assessment of the uncertainty of the results should be performed for the different codes. This should be based on a well-established and shared methodology. This also entailed performing a sensitivity study of results to input parameters to assess the impact of initial state of the rod on the final outcome of the power pulse.

The Working Group on Fuel Safety endorsed these recommendations and a second phase of the RIA fuel-rod-code benchmark (RIA benchmark Phase II) was launched early in 2014. This RIA benchmark Phase II has been organized as two complementary activities:

- The first activity is to compare the results of different simulations on simplified cases in order to provide additional bases for understanding the differences in modelling of the concerned phenomena;
- The second activity is focused on the assessment of the uncertainty of the results and sensitivity study. In particular, the impact of the initial states and key models on the results of the transient are to be investigated and the most influential input uncertainties are to be identified.

The conclusions and recommendations from the first activity have been documented in an official OECD/NEA report.

The present report provides a summary and documents the conclusions and recommendations from the second activity. It is important to notice that all uncertainties have been considered as statistical or random ones. The identification and treatment of epistemic uncertainties, if any, is beyond the scope of the current project.

Participation in the RIA benchmark Phase II has been very large: fourteen organizations representing twelve countries have provided the lower and upper bounds associated with all specified output parameters for uncertainty analysis, and the partial rank correlation coefficients associated to each uncertain input for each specified output parameter at each specified time and for their maximum values for sensitivity analysis.

In terms of computer codes used, the spectrum was also large as analyses were performed with ALCYONE, BISON, FRAPTRAN, RANNS, SCANAIR, TESPA-ROD, and TRANSURANUS.

The second activity studies confirmed the conclusions from the first activity but also offered some new insights:

- Regarding fast transient thermal-hydraulic post-DNB behaviour, there are major differences in the different modelling approaches resulting in significant deviations between simulations. Unfortunately there are currently no simple and representative experimental results that could allow to validate or not the different approaches;
- The models of fuel and clad thermo-mechanical behaviour and the associated materials properties, should be improved and validated in RIA conditions;

- The different influential input parameters are identified for fresh fuel. For instance, injected energy, fuel enthalpy, parameters related to the rod geometry (fuel and clad roughness, cladding inside diameter), fuel thermal expansion model and Full width at half maximum come out as influential regarding the maximum value of each output parameter of interest. But, the parameters with significant influence on the results for irradiated fuel could be different;
- Uncertainties cannot fully explain the scatter observed in first activity results and during the Phase I of this benchmark exercise;
- The specifics of used codes and user effects could play a more important role than uncertainties.

Based on the conclusions summed up above, the following recommendations can be made:

- To reduce user effect and code effect, the code development teams should provide recommendations regarding the version of their codes to be used, the models and also the numerical parameters to be used (mesh size, time step, …) as much as possible;
- A complement of the RIA benchmark should be launched. This activity should be limited in time and should be focused on uncertainty and sensitivity analyses on an irradiated case, in order to identify the corresponding influential input parameters. In particular uncertainties regarding fission gases distribution, fuel microstructure, clad corrosion state and gap conductance should be investigated;
- This information (most influential input parameters for an irradiated case) will be useful in the perspective of a possible establishment of the Phenomena Identification and Ranking Table (PIRT) for RIA and could guide the future RIA tests and code improvements;
- Cooperation between existing experimental teams should be established in the area of clad-to-coolant heat transfer during very fast transients as well as in the area the relevant fuel and clad thermo-mechanical modelling. The main objectives of this cooperation should be to collect and share all existing data and to formulate specific proposals in order to reduce the lack of knowledge and achieve common understanding on the subjects. This activity should address both out-of-pile and in-pile tests.

Finally, the conclusions of this work support the main recommendations proposed in the final report of first activity of the WGFS RIA fuel codes benchmark Phase II:

- Fuel and clad thermomechanical models (with the associated material properties) should be further improved and validated more extensively against a sound RIA database;
- Build-up of a comprehensive and robust database consisting of both separate-effect tests and integral tests should be pursued in the short term. In this way, both individual model validation and model integration into codes would be feasible. The database could be shared by the modellers, whenever possible, to ease the comparison of simulation results from various codes;
- The clad-to-coolant heat transfer in the case of water boiling during very fast transients is of particular interest, and capabilities related to modelling this phenomenon should be improved. To achieve this target regarding clad-to-coolant heat transfer, more separate-effect tests and experiments seem necessary;
- Models related to the evolution of the fuel-to-cladding gap should be improved and validated for RIA conditions as this has been shown to have a significant effect on fuel rod response. To reach this objective, in-reactor measurements of cladding strain during RIA simulation tests should be done (or at least attempted).

1. BACKGROUND AND INTRODUCTION

Reactivity-initiated accident (RIA) fuel rod codes have been developed for a significant period of time and validated against the available specific database. However, the high complexity of the scenarios dealt with has resulted in a number of different models and assumptions adopted by code developers; additionally, databases used to develop and validate codes have been different depending on the availability of the results of some experimental programmes. This diversity makes it difficult to find the source of estimate discrepancies, when these occur.

A technical workshop on "Nuclear Fuel Behaviour during Reactivity Initiated Accidents" was organized by the NEA in September 2009. A major highlight from the session devoted to RIA safety criteria was that RIA fuel rod codes are now widely used, within the industry as well as the technical safety organizations (TSOs), in the process of setting up and assessing revised safety criteria for the RIA design basis accident. This turns mastering the use of these codes into an outstanding milestone, particularly in safety analyses. To achieve that, a thorough understanding of the codes' predictability is mandatory.

As a conclusion of the workshop, it was recommended that a benchmark (RIA benchmark Phase I) between these codes be organized in order to give a sound basis for their comparison and assessment. This recommendation was endorsed by the Working Group on Fuel Safety.

In order to maximize the benefits from this RIA benchmark Phase I exercise, it was decided to use a consistent set of four experiments on very similar high burnup fuel rods, tested under different experimental conditions:

- low temperature, low pressure, stagnant water coolant, very short power pulse (NSRR VA-1),
- high temperature, medium pressure, stagnant water coolant, very short power pulse (NSRR VA-3),
- high temperature, low pressure, flowing sodium coolant, larger power pulse (CABRI CIP0-1),
- high temperature, high pressure, flowing water coolant, medium width power pulse (CABRI CIP3-1).

A detailed and complete RIA benchmark Phase I specification was prepared in order to assure, as much as possible, the comparability of the calculated results. The main conclusions of the RIA benchmark Phase I are presented below [1]:

- With respect to the thermal behaviour, the differences in the evaluation of fuel temperatures remained limited, although significant in some cases. The situation was very different for the cladding temperatures that exhibited considerable scatter, in particular for the cases when water boiling occurred.
- With respect to mechanical behaviour, the parameter of largest interest was the cladding hoop strain, because failure during RIA transient results from the formation of longitudinal cracks. When compared to the results of an experiment that involved only PCMI, the predictions from

the different participants appeared acceptable even though there was a factor of 2 between the highest and the lowest calculated hoop strain. The conclusion was not so favourable for cases where water boiling had been predicted to appear: a factor of 10 for the hoop strain between the calculations was exhibited. Other mechanical results compared during the RIA benchmark Phase I were fuel stack and cladding elongations. The scatter remained limited for the fuel stack elongation, but the calculated cladding elongation was found to vary significantly.

- The fission-gas release evaluations were also compared. The ratio of the maximum to the minimum values appeared to be roughly 2, which is considered to be relatively moderate given the complexity of fission gas release processes.
- Failure predictions, which may be considered as the ultimate goal of fuel codes dedicated to the behaviour in RIA conditions, were compared: it appears that the failure/no failure predictions are fairly consistent between the different codes and with experimental results. However, when assessing the code qualification, one should rather look at predictions in terms of enthalpy at failure because it is a parameter that may vary significantly between different predictions (and is also of interest in practical reactor applications). In the frame of this RIA benchmark Phase I, the calculated failure enthalpies among the different codes were within a +/- 50 % range.

As a conclusion of the RIA benchmark Phase I, it was recommended to launch a second phase exercise with the following specific guidelines:

- The emphasis should be put on deeper understanding of the differences in modelling of the different codes; in particular, looking for simpler cases than those used in Phase I, is expected to reveal the main reasons for the observed large scatter in some conditions, such as coolant boiling.
- Due to the large scatter between the calculations that was shown in the RIA benchmark Phase I, it appears that an assessment of the uncertainty of the results should be performed for the different codes. This should be based on a well-established and shared methodology. This also entailed performing a sensitivity study of results to input parameters to assess the impact of initial state of the rod on the final outcome of the power pulse.

The Working Group on Fuel Safety endorsed these recommendations and a second phase of the RIA fuel-rod-code benchmark (RIA benchmark Phase II) was launched early in 2014. This RIA benchmark Phase II has been organized as two complementary activities:

- The first activity is to compare the results of different simulations on simplified cases in order to provide additional bases for understanding the differences in modelling of the concerned phenomena.
- The second activity is focused on assessing the uncertainty of the results. In particular, the impact of the initial states and key models on the results of the transient are to be investigated.

The first activity has been completed in 2015 and documented in an OECD report (see [2] and [3]).

The present report provides a summary and documents the conclusions and recommendations from the second activity.

A detailed and complete specification of the second activity of RIA benchmark Phase II was prepared in order to ensure, as much as possible, the comparability of the calculated results. The specifications regarding the second activity are compiled in the Appendix of the present report.

The complete set of solutions provided by all the participants are compiled in an unpublished report (available to benchmark participants and to WGFS members).

This document is organized as follows:

- Chapter 1 (this Chapter) is a short introduction to the WGFS RIA fuel codes benchmark, and in particular, to Phase II of it;
- Chapter 2 gives a short description of the specifications for the second activity of the RIA benchmark Phase II;
- Chapter 3 presents the participants and the their adopted codes;
- Chapter 4 discusses the main findings of the second activity, which are illustrated by selected plots comparing the solutions provided by the participants;
- Chapter 5 gives the conclusions of the second activity of RIA benchmark Phase II exercise and provides some recommendations for follow-up activities.

2. SUMMARY OF SPECIFICATIONS

The objective of this second activity of the RIA benchmark Phase II was to assess the uncertainty of the results. In particular, the impact of the initial states and key models on the results of the transient were investigated. All uncertainties were considered as statistical or random ones. The identification and treatment of epistemic uncertainties, if any, was beyond the scope of the current project.

In addition, a sensitivity study was performed to identify or confirm the most influential input uncertainties.

2.1 Description of the Reference Case

Considering the feedback from Phase I of the RIA benchmark, the uncertainty analysis was initially intended to be performed on the foreseen CABRI international programme test CIP3-1, on an irradiated ZIRLO cladded UO_2 fuel rodlet in PWR representative conditions. This Case was also considered in Phase I of the benchmark and resulted in the largest differences in the predictions from the different codes [1].

However, in the first activity of Phase II, it appeared that, despite simplifications in the defined Cases, a significant spread of results were still present. The original thought to use CIP3-1 Case (interesting due to its high burnup) seemed too ambitious for the reference Case due to:

- Complex initial rod state evaluation;
- Large effort required from participants;
- Risk of non-conclusive outcomes.

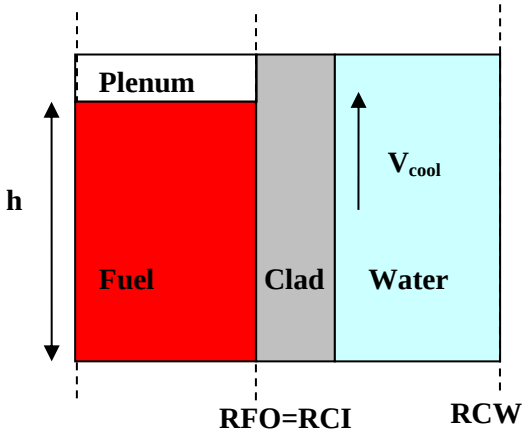

Fuel outer radius (RFO) = 4.13 mm
Clad inner radius (RCI) = 4.13 mm
Clad thickness = 570 µm
Water canal radius (RCW) = 7.5 mm
Upper plenum volume =2 cm^3
Fuel height (h) = 10 cm
Coolant velocity (V_{cool}) = 4.0 m/s

Figure 2-1: Rod design

Therefore, it was agreed that the numerical reference case should be "Case 5" of the first activity (see [2] and [3]). To limit the differences linked to the initial state of the fuel, the case is limited to a fresh 17x17 PWR type fuel rodlet as described in Figure 2-1 with standard UO_2 fuel and Zircloy-4 cladding. It is also assumed that there is no initial gap between the fuel and the clad which are considered perfectly bonded. The upper plenum is pressurized with helium at a typical pressure of a PWR rod (2 MPa at 20°C).

The thermal-hydraulic conditions during the transient are representative of water coolant in nominal PWR hot zero power (HZP) conditions (coolant inlet conditions: P_{cool}=155 bar, T_{cool}=280 °C and V_{cool}=4 m/s). These conditions are established by letting the coolant pressure and temperature increase linearly from ambient conditions during 50 s, after which a 50 s pre-transient hold time is postulated to establish steady-state conditions. At t=100 s, the reference pulse starts from zero power and it is considered to have a triangular shape, with 30 ms of Full Width at Half Maximum (FWHM) and a high value for the rod maximal power in the fuel is considered to provoke departure from nucleate boiling (DNB).

2.2 Methodology

2.2.1 *Uncertainty analysis methodology*

Among all the available uncertainty analysis methods, the probabilistic input uncertainty propagation method is, so-far, the most widely used in nuclear safety analysis [4]. In this method, the fuel codes are treated as "black boxes", and the input uncertainties are propagated to the simulation model output uncertainties via the code calculations, with sampled data from known or assumed distributions for key input parameters [5]. The input parameters of interest may also include uncertain material properties, model parameters, etc.

The method consists in the following steps:

1) Specification of the problem: All relevant code outputs and corresponding uncertain parameters for the codes, plant modelling schemes, and plant operating conditions are identified.
2) Uncertainty modelling: the uncertainty of each uncertain parameter is quantified by a probability density function (PDF) based on engineering judgment and experience feedback from code applications to separate and integral effect tests and to full plants simulation. If dependencies between uncertain parameters are known and judged to be potentially important, they can be quantified by correlation coefficients.
3) Uncertainty propagation through the computer code: the propagation is represented by Monte-Carlo simulations [6]. In Monte-Carlo simulations, the computer code is run repeatedly, each time using different values for each of the uncertain parameters. These values are drawn from the probability distributions and dependencies chosen in the previous step. In this way, one value for each uncertain parameter is sampled simultaneously in each repetition of the simulation. The results of a Monte-Carlo simulation lead to a sample of the same size for each output quantity.
4) Statistical analysis of the results: the output sample is used to get any typical statistics of the code response such as mean or variance and to determine the cumulative distribution function (CDF). The CDF allows deriving the percentiles of the distribution.

A simple way to get information on percentiles is to use order statistics [7] which is a well-established and shared methodology in the nuclear community, and hence, is recommended for this activity.

The principle of order statistics is to derive results from the ranked values of a sample. If $(X^1,\ldots,X^N)$ denotes a sample of any random variable, X, and $(X^{(1)},\ldots,X^{(N)})$ the corresponding ranked one, order statistics first provides an estimation of the percentile of interest since the α-percentile can be estimated by $X^{(\alpha N)}$. Moreover, it turns out that the CDF of $X^{(k)}$, $F_X(X^{(k)})$, follows the Beta law $\beta(k,N-k+1)$, which does

not depend on the distribution of X. This key result allows quantifying the probability that any ranked value is smaller than any percentile by the following formula:

$$P(X^{(k)} \leq X_{\alpha}) = F_{\beta(k,N-k+1)}(\alpha)$$

where $F_{\beta(k,N-k+1)}$ denotes the CDF of the Beta law $\beta(k,N-k+1)$.

This equation can then be used to derive:

1) lower and upper bounds of a percentile of interest, given the sample size N and the confidence level β that controls the probability that $X(k) \leq X_{\alpha}$. For this purpose, it is necessary to solve the equation $F_{\beta}(k,N-k+1)(\alpha)= \beta$.
2) the minimal sample size (and therefore the minimal number of computer runs) to perform in order to obtain a lower or upper bound of a given percentile with a given confidence level. It leads to the so-called Wilk's formula [8]:

$$N = \ln(1-\beta)/\ln(\alpha)$$

and Guba's estimate in case of multiple output parameters in [9].

Order statistics are widely used since no information is needed on the distribution of the random variable. Moreover, this method is very simple to implement, which makes it extremely interesting for licensing applications to nuclear safety analyses.

The probabilistic input uncertainty propagation method was selected due to its simplicity, robustness and transparency. The highly recommended sample size is set to 200 (i.e. 200 code runs must be performed). Strong justifications should be given if a lower number of code runs is performed. The sample is constructed according to the selected PDFs coming from the uncertainty modelling step and assuming independence between input parameters following a Simple Random Sampling (SRS).

We focus on the estimation of a lower, resp. upper, bound of the 5 %, resp. 95 %, percentiles (α) at confidence level (β) higher than 95 %.

For N = 200 and $\alpha = 0.05$ or 0.95, previous equations lead to:

$$P(X^{(5)} \leq X_{5\%}) = 0.97$$

$$P(X^{(196)} > X_{95\%}) = 0.97$$

the lower, resp. upper, bound is defined in this benchmark by $X^{(5)}$, resp. $X^{(196)}$. Note that a one-sided approach is used here and that the bounds are estimated separately.

2.2.2 *Sensitivity analysis methodology*

Besides uncertainty analysis, a complementary study was performed to get qualitative insight on the most influential input parameters.

This work was done based on a sensitivity analysis using the 200 code runs previously obtained. More precisely, if Y denotes the response of interest and $\{X_i\}_{i=1,\ldots,p}$ the set of p uncertain input parameters (also called regressors), it required to estimate the following classical correlation coefficients:

- Linear (or Pearson's) simple correlation coefficients (SCC): for each i,

$$\rho_i = \frac{\mathrm{cov}(Y, X_i)}{\sigma_X \sigma_Y}$$

where σ_X and σ_Y are the empirical standard deviations of X and Y.

They correspond to the p correlation coefficients between the response and each of the p regressors. They measure the degree of linear dependence between the response and each of the p regressors taken separately. In multiple regression the regressors are not always orthogonal and partial correlation coefficients (PCC) are sometimes preferred to SCC, since in this case, the correlation is not evaluated with the response but with the response from which linear trends associated with other input variables are removed [10]. PCC might lead to higher number than the Pearson's simple correlation coefficient.

- Spearman's rank correlation coefficient (RCC): same definition as SCC but replacing input and output values by their respective ranks. Working with ranks allows one to extend the previous underlying linear regression model to a monotonic non-linear one. In the presence of nonlinear but monotonic relationships between the response and each of the p regressors, use of the rank transform can substantially improve the resolution of sensitivity analysis results [11].

Similarly to PCC, the partial rank correlation coefficient (PRCC) can be introduced in order to remove trends associated with other variables [10]. Again, the PRCC might lead to higher number than the Spearman's rank correlation coefficient.

Based on this information (Pearson's SCC or Spearman's RCC, PCC or PRCC), the most influential uncertain input parameters can be identified, if the input and corresponding output parameters show monotonic relation.

2.3 Identification of Uncertainty parameters

The uncertainties from the Phase I and activity 1 of Phase II of the RIA benchmark, as well as the OECD UAM benchmark [12], were identified and classified into four categories:

- Uncertainties in the fuel rod design, bounded by allowable manufacturing tolerances,
- Thermal hydraulic boundary conditions,
- Core power boundary conditions,
- Physical Properties/Key models.

Table 2-1 provides the specified input parameters as well as the information related to their uncertainty. For each input parameter, the information includes a mean value, a standard deviation and a type of distribution. In order to avoid unphysical numerical values, a range of variation (lower and upper bounds) was also provided. The sampling was performed between the upper and lower bounds, i.e. the PDFs were truncated. In order to simplify the current benchmark application, a normal distribution was assigned to all the considered input parameters. Their standard deviation was taken as the half of the maximum of the absolute value of the difference between their nominal value and their upper or lower bound. The effect of the uncertainty modelling (i.e. the choice of a normal distribution) has not been studied in this benchmark. Although this effect it could have some impact on the derived uncertainty bands, the conclusions of this exercise are expected to be similar for other distributions.

It should be recalled that, as the study is limited to fresh fuel, classical uncertainty parameters for irradiated fuel (such as fission gases distribution, cladding corrosion, gap conductance,…) are not considered here.

Finally, although the dependency between the pulse width and the injected energy was well known, it was not considered.

2.4 Output specification

As a result from the uncertainty analysis, each participant gave lower and upper bounds associated with all the time trend of output parameters listed in Table 2-2. In addition, the results of the calculation with the nominal value of the input parameters, also called reference calculation were provided.

The reference, lower and upper bound values were provided for the following scalar outputs:

- Maximum value for each parameter in Table 2-2,
- Time to Maximum value for each parameter in Table 2-2,
- Boiling duration: difference between time of critical heat flux achievement and time of reaching the rewetting heat flux.

Regarding sensitivity analysis, the partial rank correlation coefficients (or Spearman's if PRCC is not available) associated to each uncertain input for each output at the times defined in Table 2-3 as well as for their maximal value were also provided.

Input uncertainty parameter	Distribution				
	Mean	**Standard Deviation**	**Type**	**Lower bound**	**Upper bound**
1. Fuel rod manufacturing tolerances					
Cladding outside diameter (mm)	9.40	0.01	Normal	9.38	9.42
Cladding inside diameter (mm)	8.26	0.01	Normal	8.24	8.28
Fuel theoretical density (kg/m^3 at 20 °C)	10970	50	Normal	10870	11070
Fuel porosity %	4	0.5	Normal	3	5
Cladding roughness (µm)	0.1	1.	Normal	10.$^{-6}$	2.
Fuel roughness (µm)	0.1	1.	Normal	10.$^{-6}$	2.
Filling gas pressure (MPa)	2.0	0.05	Normal	1.9	2.1
2. Thermal hydraulic boundary conditions					
Coolant pressure (MPa)	15.500	0.075	Normal	15.350	15.650
Coolant inlet temperature (°C)	280	1.5	Normal	277	283
Coolant velocity (m/s)	4.00	0.04	Normal	3.92	4.08
3. Core power boundary conditions					
Injected energy in the rod (Joule)	30000	1500	Normal	27000	33000
Full width at half maximum (ms)	30	5	Normal	20	40
4. Physical Properties/Key models					
Fuel thermal conductivity model (Mult. Coef.)	1.00	5 %	Normal	0.90	1.10
Clad thermal conductivity model (Mult. Coef.)	1.00	5 %	Normal	0.90	1.10
Fuel thermal expansion model (Mult. Coef.)	1.00	5 %	Normal	0.90	1.10
Clad thermal expansion model (Mult. Coef.)	1.00	5 %	Normal	0.90	1.10
Clad Yield stress (Mult. Coef.)	1.00	5 %	Normal	0.90	1.10
Fuel enthalpy / heat capacity (Mult. Coef.)	1.00	1.5 %	Normal	0.97	1.03
Clad to coolant heat transfer (Mult. Coef. - Same Coef. applied for all flow regimes)	1.00	12.5 %	Normal	0.75	1.25

Table 2-1: List of input uncertainty parameters for statistical uncertainty analysis.

Parameter	Unit	Description
DHR	cal/g	Variation of radial average enthalpy with respect to initial conditions of the transient in the rodlet as a function of time (at z = h/2) (please note that: DHR(t = 0) = 0)
TFC	°C	Temperature of fuel centreline as a function of time (at z = h/2)
TFO	°C	Temperature of fuel outer surface as a function of time (at z = h/2)
TCO	°C	Temperature of clad outer surface as a function of time (at z = h/2)
ECTH	%	Clad total (thermal + elastic + plastic) hoop strain at the outer part of the clad as a function of time (at z = h/2)
ECT	mm	Clad total axial elongation as a function of time
EFT1	mm	Fuel column total axial elongation as a function of time
SCH	MPa	Clad hoop stress at outer part of the clad as a function of time (at z = h/2)
RFO	mm	Fuel outer radius as a function of time (at z = h/2)

Table 2-2: List of time-dependent parameters to be provided

Time parameters	t_1	t_2	t_3	t_4	t_5
Definition	Beginning of power pulse	Time of maximum power pulse	End of power pulse	101 s	End of calculation
Value	100.000 s	between 100.020 s and 100.040 s	between 100.040 s and 100.080 s	101.000 s	200.000 s

Table 2-3: List of different times for scalar sensitivity analysis output

3. PARTICIPANTS AND CODES USED

The participation to the RIA benchmark Phase II has been very important, because 14 organizations provided solutions for some or all the Cases that were defined.

The participants, which represented 12 countries, are listed below:

- Tractebel (ENGIE) from Belgium,
- ÚJV Řež (UJV) from the Czech Republic,
- Institut de Radioprotection et de Sûreté Nucléaire (IRSN) and Commissariat à l'énergie atomique et aux énergies alternatives (CEA) from France,
- Gesellschaft für Anlagen- und Reaktorsicherheit (GRS) GmbH from Germany,
- Centre of Energy Research, Hungarian Academy of Sciences (MTA-EK) from Hungary,
- Nuclear and INdustrial Engineering (NINE) from Italy,
- Japan Atomic Energy Agency (JAEA) from Japan,
- Korea Institute of Nuclear Safety (KINS) from Korea,
- Centro de Investigaciones Energéticas, Medioambientales y Tecnológicas (CIEMAT) and Consejo de Seguridad Nuclear (CSN) from Spain,
- Strålsäkerhetsmyndigheten (Swedish Radiation Safety Authority – SSM) represented by Quantum Technologies from Sweden,
- Nuclear Regulatory Commission (USNRC) and Idaho National Laboratory (INL) from the Unites States,
- VTT Technical Research Centre of Finland (VTT) from Finland.

As it can be seen, research institutions, utilities, technical safety organizations and safety authorities are well represented among the participants.

In terms of computer fuel rod codes used, the spectrum was also large as solutions were provided with ALCYONE, BISON, FRAPTRAN[1], RANNS, SCANAIR, TESPA-ROD and TRANSURANUS. Brief descriptions of these computer codes are given in Appendix I of reference [2].

Table 3-1 summarizes the contributions provided by the participants and the codes used for transient simulation as well as for sensitivity and uncertainty analyses.

Organization	Codes	
SSM	SCANAIR V_7_5	SUNSET
	SCANAIR V_7_5 + TH-2P	SUNSET
VTT	SCANAIR V_7_5	SUSA
IRSN	SCANAIR V_7_6	SUNSET
CIEMAT	SCANAIR V_7_5	Internal tool
USNRC	FRAPTRAN V2.0	DAKOTA
UJV	FRAPTRAN V_1_5	internal tool
KINS	FRAPTRAN V2.0	SUNSET
TRACTEBEL	FRAPTRAN V2.0-Beta	DAKOTA
MTA-EK	FRAPTRAN 1.4.-TRABCO_unc	Internal tool
NINE	TRANSURANUS	Internal tool
JAEA	RANNS	DAKOTA
GRS	TESPA-ROD	SUSA
CEA	ALCYONE 1.4	URANIE
INL	BISON	DAKOTA

Table 3-1: Benchmark collected contributions (code combinations used for the second activity of Phase II)

[1] For this benchmark, FRAPTRAN V2.0 is the version of the code recommended for use by the NRC. The official released versions of FRAPTRAN-1.4 and FRAPTRAN-1.5 did not contain uncertainty input options, and the heat transfer correlations and thermal solution scheme have since been improved upon in FRAPTRAN-2.0. The FRAPTRAN-2.0 Beta was created before the release of FRAPTRAN-2.0 specifically for code users in this benchmark exercise, but was not fully tested and was discovered to have an error in the code's ability to change between the clad-to-coolant heat transfer regimes and did not properly apply the uncertainty parameter on fuel enthalpy calculations

4. RESULTS SUMMARY AND ANALYSIS

4.1 Methodology

This section provides an overview on the methods and tools that were used to analyse participants' results.

4.1.1 *Uncertainty analysis*

A first study is performed on the time trend outputs. Then, the formal method of information synthesis developed by IRSN [10] is applied to get quantitative insight on the results associated with scalar outputs.

Time trend outputs

For each output, the analysis is focused on the uncertainty interval ([LUB, UUB]) as well as on the position of the reference calculation (REF) within this interval.
Concerning the first point, two kinds of synthesis have been performed. They are based on the evolution with respect to time of:

- the union of all participants' intervals i.e. of [LUBmin,UUBmax] with LUBmin (resp. UUBmax) defined as the minimum (resp. maximum) of all the LUBs (resp. UUBs) (Figure 4-1)
- the uncertainty interval (or band) width of each participant:

$$q_0 = UUB - LUB$$

As for the position of the reference calculation, it is studied through the computation with respect to time of the following quantity:

$$q_1 = \frac{UUB - REF}{UUB - LUB}$$

Note that:

- If q1<0: the reference calculation is outside the uncertainty interval (REF > UUB)
- If 0< q1 <0.5: the reference calculation is closer to the upper bound
- If 0.5< q1 <1: the reference calculation is closer to the lower bound
- If q1>1: the reference calculation is outside the uncertainty interval (REF<LUB)

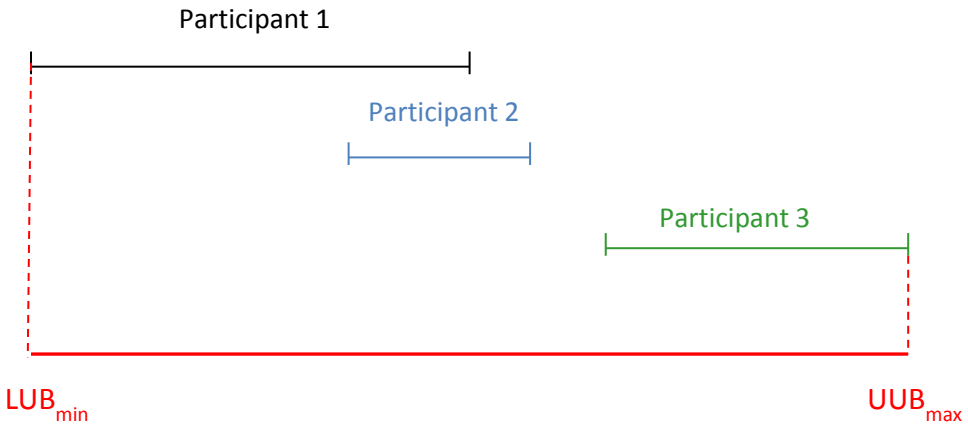

Figure 4-1: Example of union of participants' intervals

Scalar outputs

The formal approach of information synthesis developed by IRSN is used for this type of output. In the frame of this benchmark, the uncertainty analysis performed by each participant was regarded as an information source on the outputs of interest. The IRSN methodology was applied to combine all these information sources and to detect agreements or conflicts (if any) between them. This approach has been introduced in [13] and already applied during the PREMIUM benchmark [14]. It is composed of three steps, fully described in [10], and related to:

1) information modelling
2) information evaluation
3) information fusion

In this benchmark, the second step has not been performed, since it requires computing a criterion based on the discrepancy between reference calculations and experimental values that are not available. Therefore, we restrict the overview of the IRSN method to Steps 1 and 3 when the available state of knowledge on uncertainties is summarized by an interval ($[LUB,UUB]$) and a reference value (REF) as it was requested in the benchmark specifications.

Information modelling: a triangular model as displayed in the Figure 4-2 is associated with each output of interest and each contribution. For a source s (i.e. a contribution) and an output variable v, its parameterization is denoted $\pi_{s,v}(t)$ and defined by

$$\pi_{s,v}(t) = \begin{cases} \dfrac{1}{REF - LUB}(t - LUB), & if\ t \in [LUB, REF], \\ \dfrac{1}{REF - UUB}(t - UUB), & if\ t \in [REF, UUB] \end{cases}$$

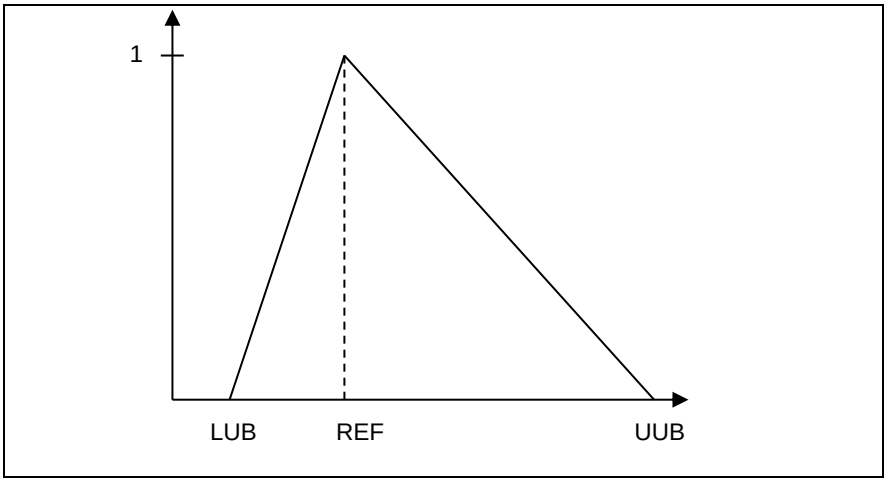

Figure 4-2: Information modelling associated with a source

Information fusion: for each output variable v, the goal is here to aggregate the information provided by p sources $\{s_i\}_{i=1,...,p}$. The IRSN methodology distinguishes three kinds of aggregation operators, but we recall only the first two that have been considered during this benchmark. The first one is equivalent to taking the intersection between the information. More precisely, starting from the p models $\{\pi_{s_i,v}\}_{i=1,...,p}$ given by each source, it leads to $\pi^{\cap}{}_v$ that can be formally written as

$$\pi^{\cap}{}_v = \min_{i=1,...,\ p} \pi_{s_i,v}$$

In order to evaluate agreement and disagreement between sources, it allows computing a quantitative measure called the conflict indicator that is written

$$CI_v = 1 - \max_{t \in IR} \pi^{\cap}{}_v(t)$$

The disagreement (resp. agreement) corresponds to an indicator close to 1 (resp. 0).
The second operator is equivalent to taking the union between the information provided by the sources:

$$\pi^{\cup}{}_v = \max_{i=1,...,\ p} \pi_{s_i,v}$$

It offers a relevant representation of the uncertainty results including reference values and therefore allows to compare them. As clarified in the next section, it is complementary to the first kind of fusion and can be helpful by providing more insight on the reasons why disagreements appear.

Figure 4-3displays an example of these kinds of aggregation in the case of two sources.

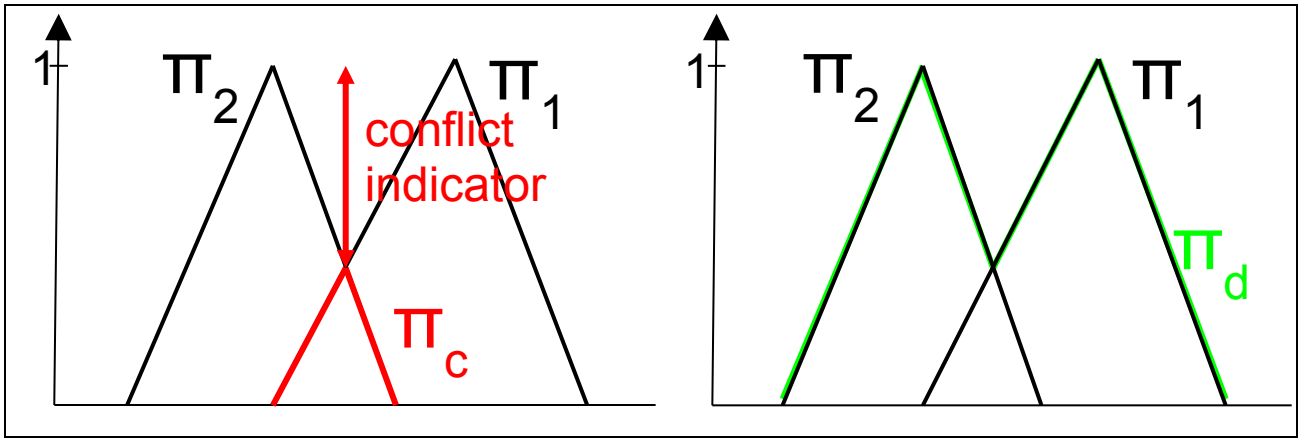

Figure 4-3: Aggregation of the information provided by two sources. The black lines stand for the model representing each source of information, whereas the red and green ones are the aggregated result after intersection (left) and union (right). The red arrow represents the conflict indicator

4.1.2 *Sensitivity analysis*

This section begins with a quick recall of the used method that has been already described in the specifications. Then, a criterion is introduced in order to exhibit, for each participant, the most influential input parameters according to the computed sensitivity measures.

Choice of the method

Several approaches are available to perform sensitivity analysis [15]. However, their mathematical treatment follows the same steps as for uncertainty analysis: input sampling, propagation through the evaluation model and analysis of the results leading to a qualitative insight on the most influential input parameters.

In this benchmark, the input sample comes from the random sample constructed after uncertainty analysis and the analysis step consists in evaluating correlation coefficients. This approach has been already successfully applied during the BEMUSE benchmark [16].

As mentioned in the specifications, the most classical correlation coefficient is the Pearson one, which is based on a linear assumption to connect the input parameters $\{X_i\}_{i=1,\ldots,p}$ (called regressors) to the output Y. In this study, we consider a more generic class of models of type isotonic (monotonic with respect to each input parameter) and non-linear. In this case, the sensitivity measures are based on Spearman rank correlation coefficient (RCC), whose definition is similar to the Pearson coefficient as the numerical values of X_i and Y are replaced by their ranks[2]. In multiple regression, the regressors are not always orthogonal and (Spearman) partial rank correlation coefficients (PRCC) are sometimes preferred to RCC, since in this case, for a given regressor, the correlation is not evaluated with all the responses, but only with the response from which the explained part by all other regressors has been removed. PRCC is the indicator considered in this work.

[2] For a N-sample, the rank ranges from 1 to N. Rank 1 is associated with the smallest value of the sample and rank N with the largest one

When analysing the results produced by this method, it is important to mention that:

- the use of the correlation coefficients is based on several assumptions related to the model connections between inputs and outputs that have to be kept in mind in the interpretation of the "influence" of each input parameter;
- this study is restricted to the evaluation of the main effects, i.e. interactions between input parameters are not considered. In the same framework, an alternative approach to exhibit the sensitivity to input parameters and associated interactions without aliasing could apply the theory of design of experiments [17]. However this is out of the scope of this benchmark.

Criterion for the identification of the most influential input parameters

This section presents the identification of the most influential parameters after the correlation coefficients have been computed. The identification is based on the introduction of a significance threshold. The method to quantify this threshold relies on classical statistical results [7] and is briefly recalled in the sequel in the case of the Pearson correlation coefficient. This quantification still holds when working with ranks as soon as the sample is sufficiently large (>100).

The objective is to evaluate from a correlation coefficient associated with N observations $\{(x_i , y_i)\}_{i=1,\dots,N}$, denoted r for simplicity, the "strength" of the relationship between an input parameter X and an output Y. We start with the statement that X and Y are linearly independent. Under this hypothesis, one can exhibit the likely (or the unlikely) values of the correlation coefficient r corresponding to a N-sample, or more precisely, the probability distribution of the associated random variable R. For a sufficiently large sample (>100), this distribution can be approximated by the normal law (Figure 4-4):

$$N\left(0, \frac{1}{\sqrt{N-1}}\right)$$

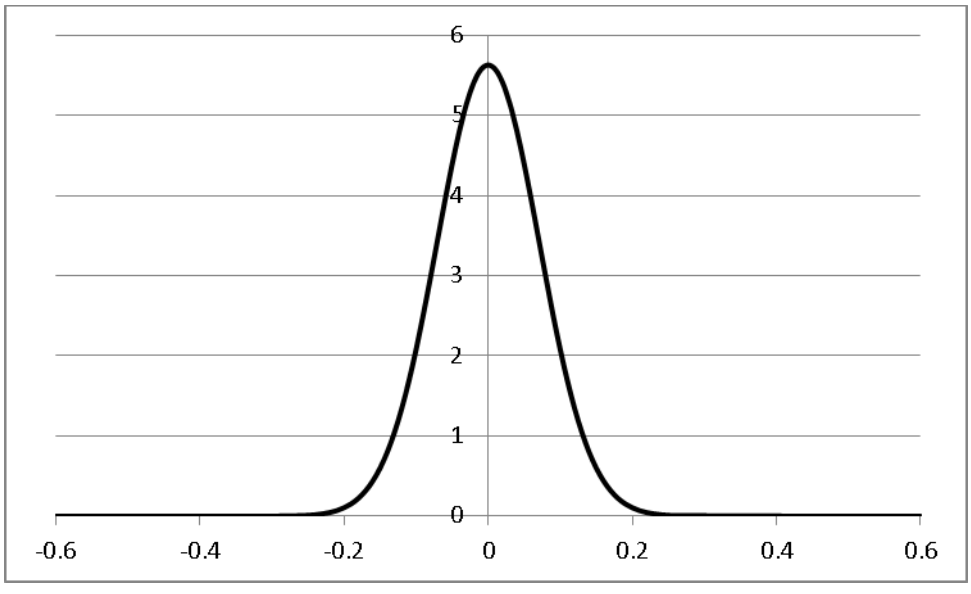

Figure 4-4: Probability distribution function of the normal law for N=200

Significance thresholds are then related to its extreme percentiles and are therefore associated with different confidence levels. Table 4-1: Examples of percentiles for the normal law with N=200 displays some examples of these percentiles.

Percentiles (r*)	Confidence level	P(R>r*) or P(R<-r*)
0.09	90.00 %	0.1000
0.14	97.50 %	0.0250
0.16	99.00 %	0.0100
0.22	99.90 %	0.0010
0.27	99.99 %	0.0001

Table 4-1: Examples of percentiles for the normal law with N=200

In practice, given a value of a correlation coefficient, the previous figure and table can then be used to estimate the likelihood of occurrence for this value assuming linear independence. In this benchmark, we set the significance threshold to 0.25 (which corresponds to a high confidence level, i.e. > 99.9%, or in other words, to a very low risk of rejecting the assumption of linear independence, i.e. P(R>r*) < 0.001) and consider an input parameter as influential as soon as its correlation coefficient is in absolute value larger than that threshold.

4.2 Results

This analysis is based on the methodology recalled in the previous section and is therefore similarly structured with respect to the type of studies (uncertainty or sensitivity analysis) and to the type of outputs (time trend or scalar).

4.2.1 *Uncertainty analysis: Time trend outputs*

Following Section 4.1.1, the evolution of [LUB_{min},UUB_{max}], q_0 and q_1 are plotted for the 9 outputs of Table 2-2 as well as of the corresponding reference calculations.

The evolution of [LUB_{min},UUB_{max}] and of the uncertainty band width (q_0) for fuel enthalpy increase (DHR) are represented in

Figure 4-5 and

Figure 4-6.

From these figures, four phases can be identified:

- Before the transient ($t \leq 100$ s),
- During the power pulse ($100 \text{ s} < t \leq 100.1$ s),
- After the power pulse and before 120 s ($100.1 \text{ s} < t \leq 120$ s),
- After the transient ($t > 120$ s).

Therefore, the analysis is performed for each of these phases with a focus on:

- Reference calculation evolution with respect to time for each participant,
- Uncertainty band width evolution with respect to time for each participant,
- Maximum of the uncertainty band width for each participant as a function of the corresponding reference calculation. **Note that this reference calculation is taken at the same time as the maximum uncertainty band width and does not always coincide with the maximum of the reference value during each time period**.

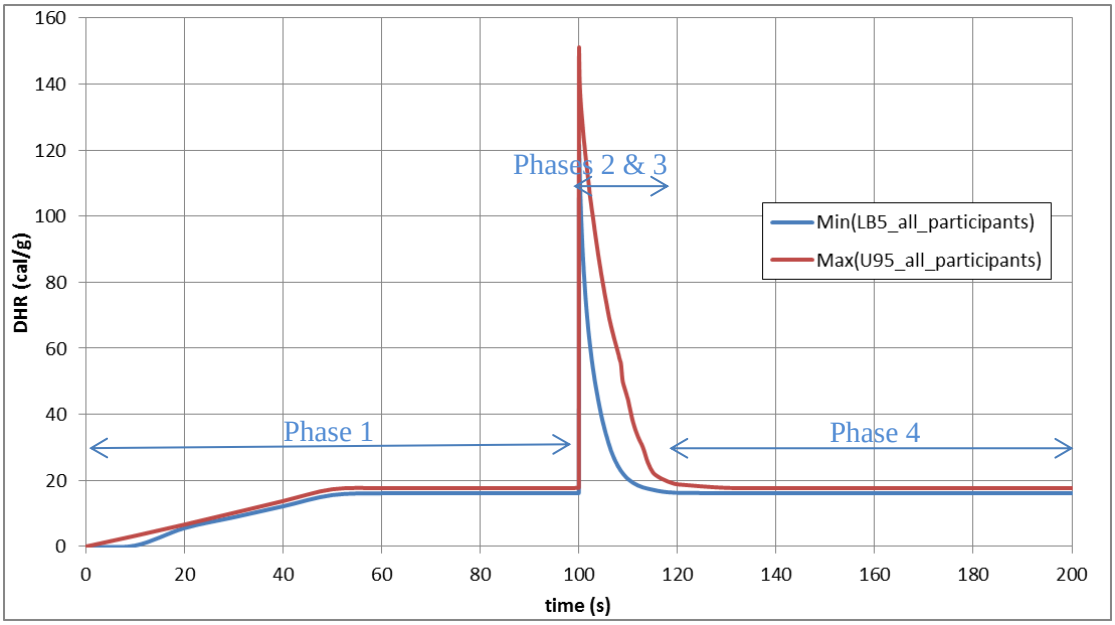

Figure 4-5: Evolution of [LUB_{min},UUB_{max}] for fuel enthalpy increase (DHR) (all participants)

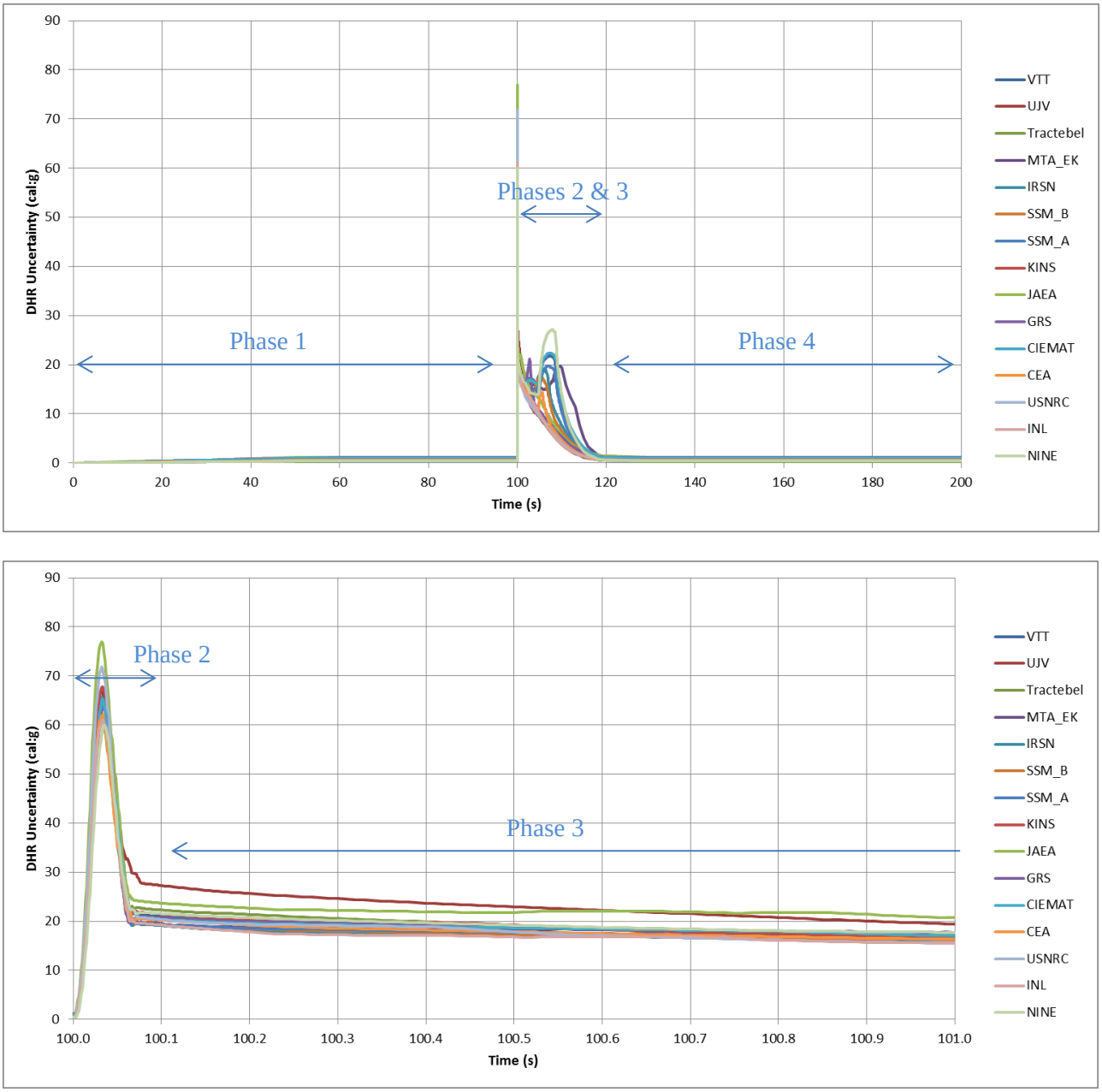

Figure 4-6: Uncertainty band widths of fuel enthalpy increase (DHR) for all the participants

4.2.1.1 *Analysis of the results before the transient (t < 100 s)*

The results clearly show that the uncertainty is low on the thermal behaviour of fuel and clad before the transient and that the discrepancies between the different participants are limited.

As an example, the DHR uncertainty ($max(q_0)$) is lower than 6 % (~1 cal/g for a reference value of 17 cal/g), see

Figure 4-7, and the uncertainty on clad temper ature (TCO) is around 5 °C, see

Figure 4-8, mostly resulting from the initial uncertainty on coolant temperature (3 °C).

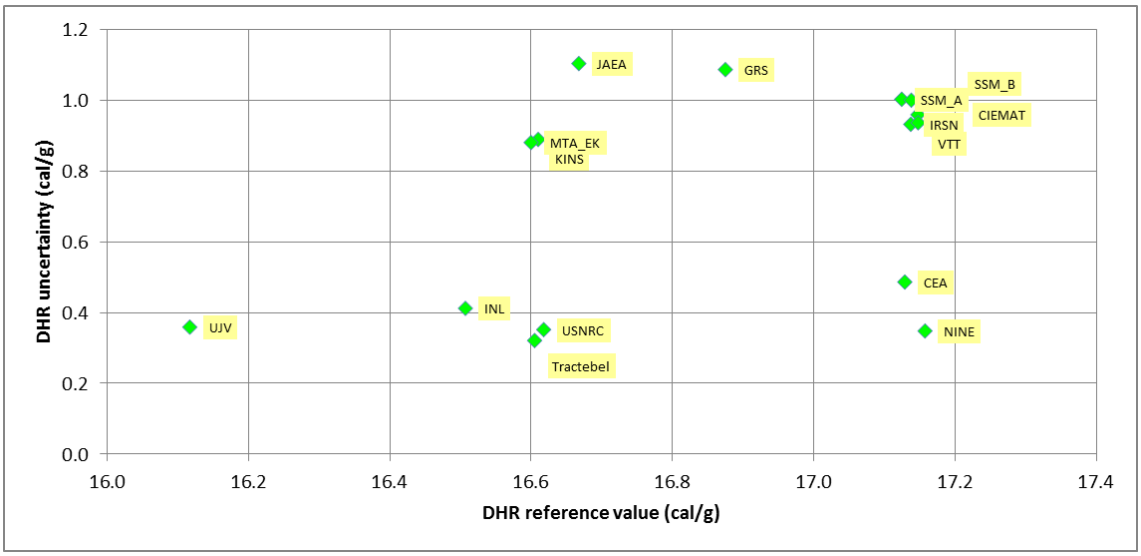

Figure 4-7: DHR uncertainty ($max(q_0)$) before the transient as a function of the corresponding reference value

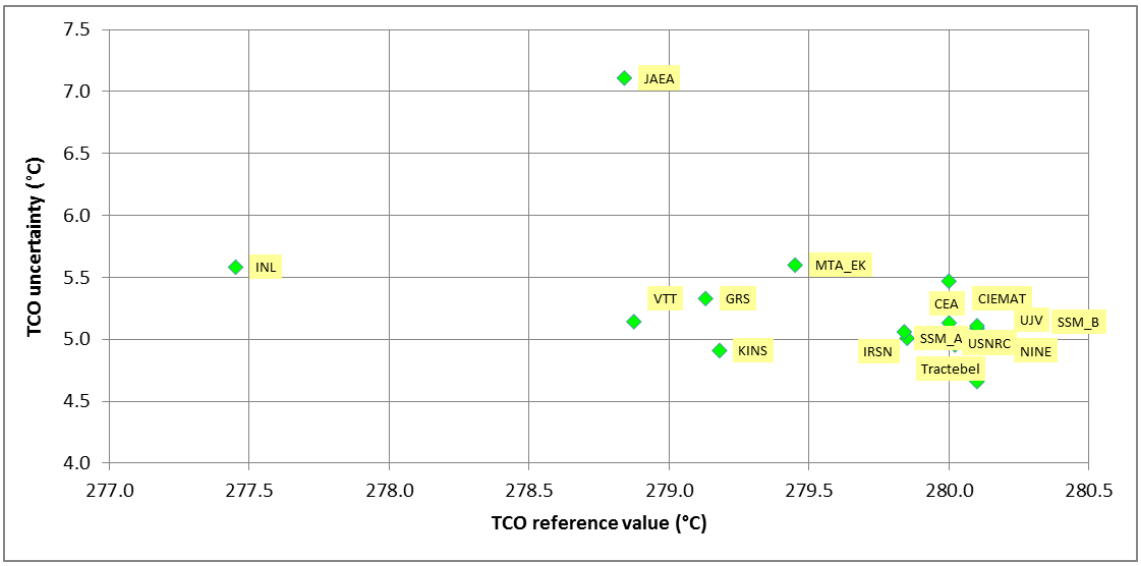

Figure 4-8: TCO uncertainty (*max(q_0)*) before the transient as a function of the corresponding reference value

The outputs parameters linked to the mechanical behaviour present a higher initial uncertainty: the initial uncertainty on the clad total hoop strain (ECTH) represents ~20 % of the reference value (cf. Figure 4-9) and the uncertainty on the clad hoop stress (SCH) is of the same order of magnitude of the reference value (~30 to 100 MPa, cf. Figure 4-10). Moreover, from Figure 4-10, it is worth noting that there are two well differentiated groups with a factor 3 between the two groups for the SCH reference values and a code effect is observed (~30 MPa for SCANAIR and TRANSURANUS, ~100 MPa for other codes). However, their uncertainty is of the same order of magnitude.

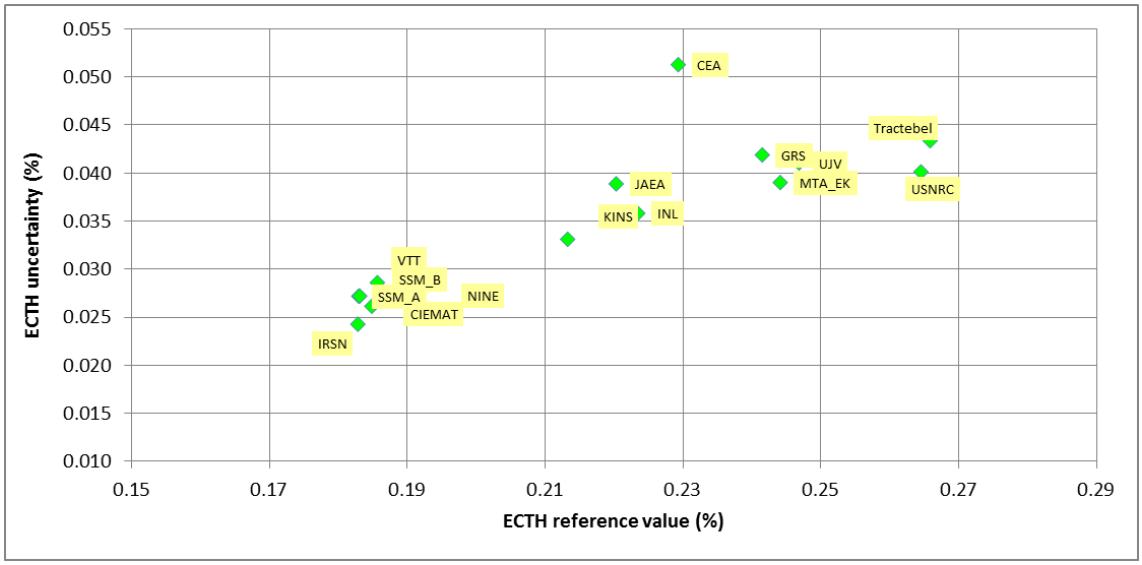

Figure 4-9: ECTH uncertainty (*max(q_0)*) before the transient as a function of the corresponding reference value

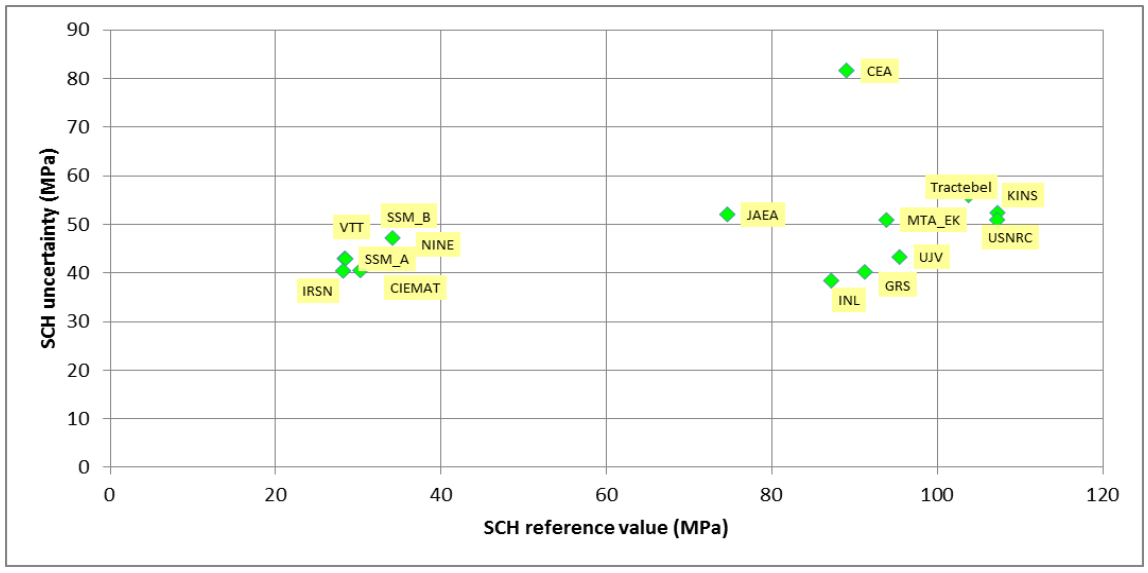

Figure 4-10: SCH uncertainty (*max(q_0)*) before the transient as a function of the corresponding reference value

4.2.1.2 *Analysis of the results during the power pulse (100 – 100.1 s)*

Fuel thermal and mechanical behaviour

During the power deposit, there is a very good agreement between all the participants for fuel thermal behaviour. As an example, concerning the reference calculations, the discrepancy for the maximal fuel central temperature (TFC) is lower than 40 °C (see Figure 4-11).

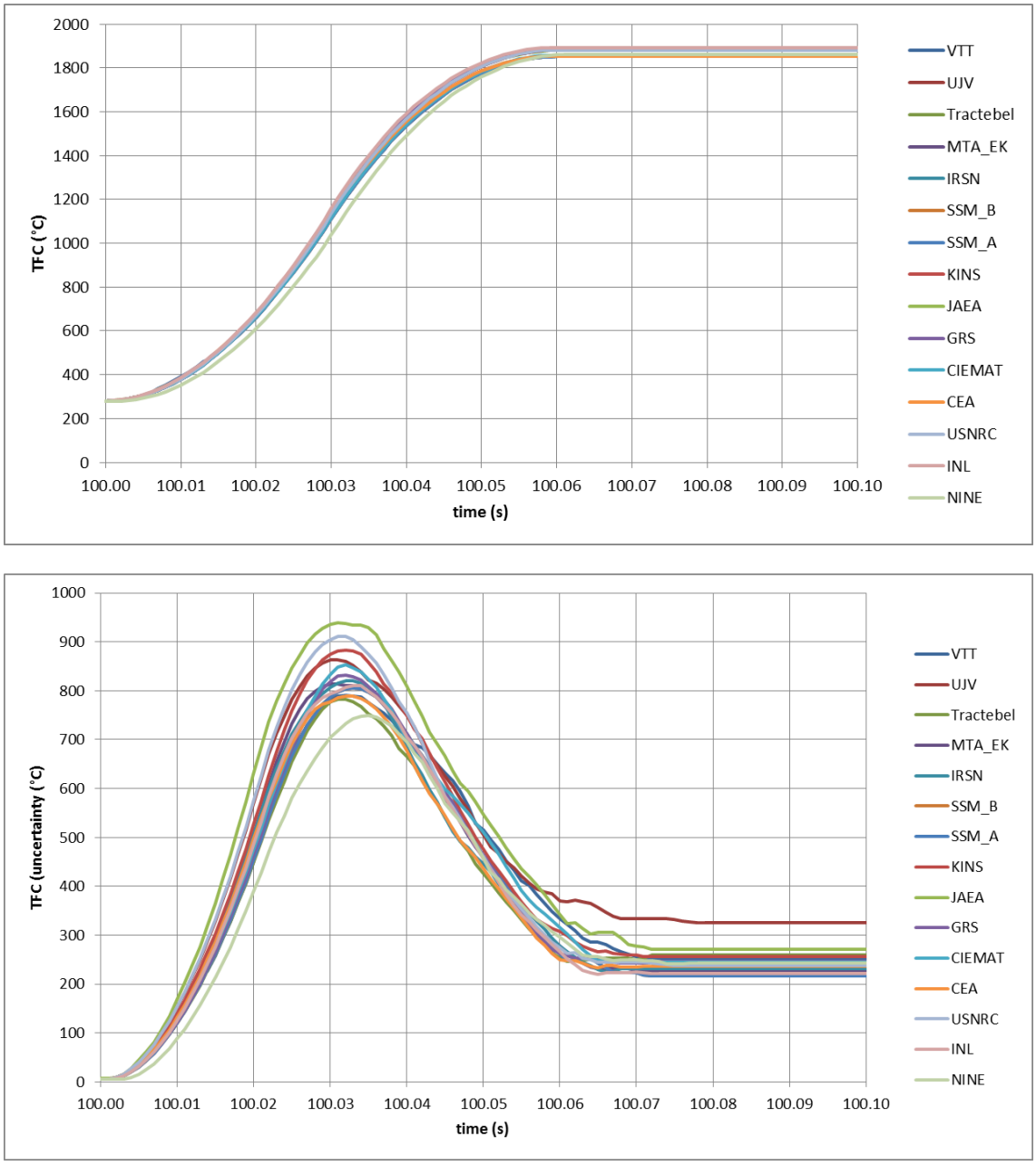

Figure 4-11: TFC reference calculations (up) and uncertainty band widths (down) during the power pulse

The TFC uncertainty assessment with respect to time is also quite consistent between all the participants. During the power deposit, the uncertainty band width can be very high, around 800 °C. This result is linked to the fact that the uncertainty on the pulse width is very large (+/-10 ms). Thus, even with

the same final injected energy, the injected energy 40ms after the beginning of the transient can vary by a factor of two in the two extreme cases of pulse half width (20ms and 40ms) that can lead to large thermal differences during the transient. Just after the power deposit, the TFC uncertainty is significantly lower, 200-300 °C, which is 10-15 % of the TFC reference value (~1850 °C).

The same "pulse width uncertainty effect" can be seen on the fuel elongation (EFT1) during the transient: very large during the power deposit, much less after the pulse. Nevertheless, compared to the reference value, the uncertainty is rather significant (~0.6 mm compared to ~2 mm), see Figure 4-12.

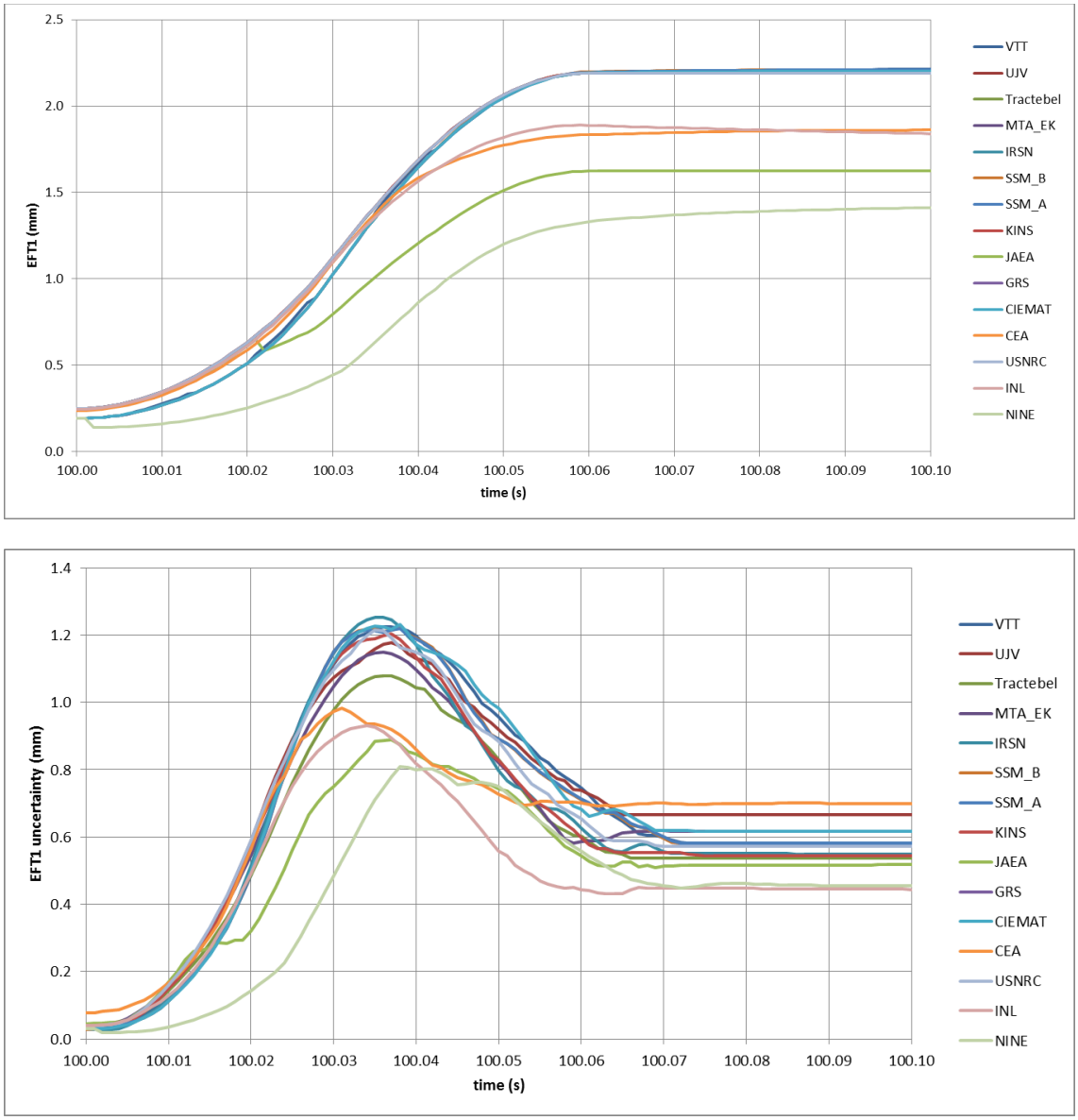

Figure 4-12: EFT1 reference calculations (up) and uncertainty band widths (down) during the power pulse

Clad mechanical and thermal behaviour

The clad hoop strain (ECTH) reference value and uncertainty band width as a function of time during the power pulse are represented in the Figure 4-13. The trends are very similar to those observed for fuel elongation (EFT1).

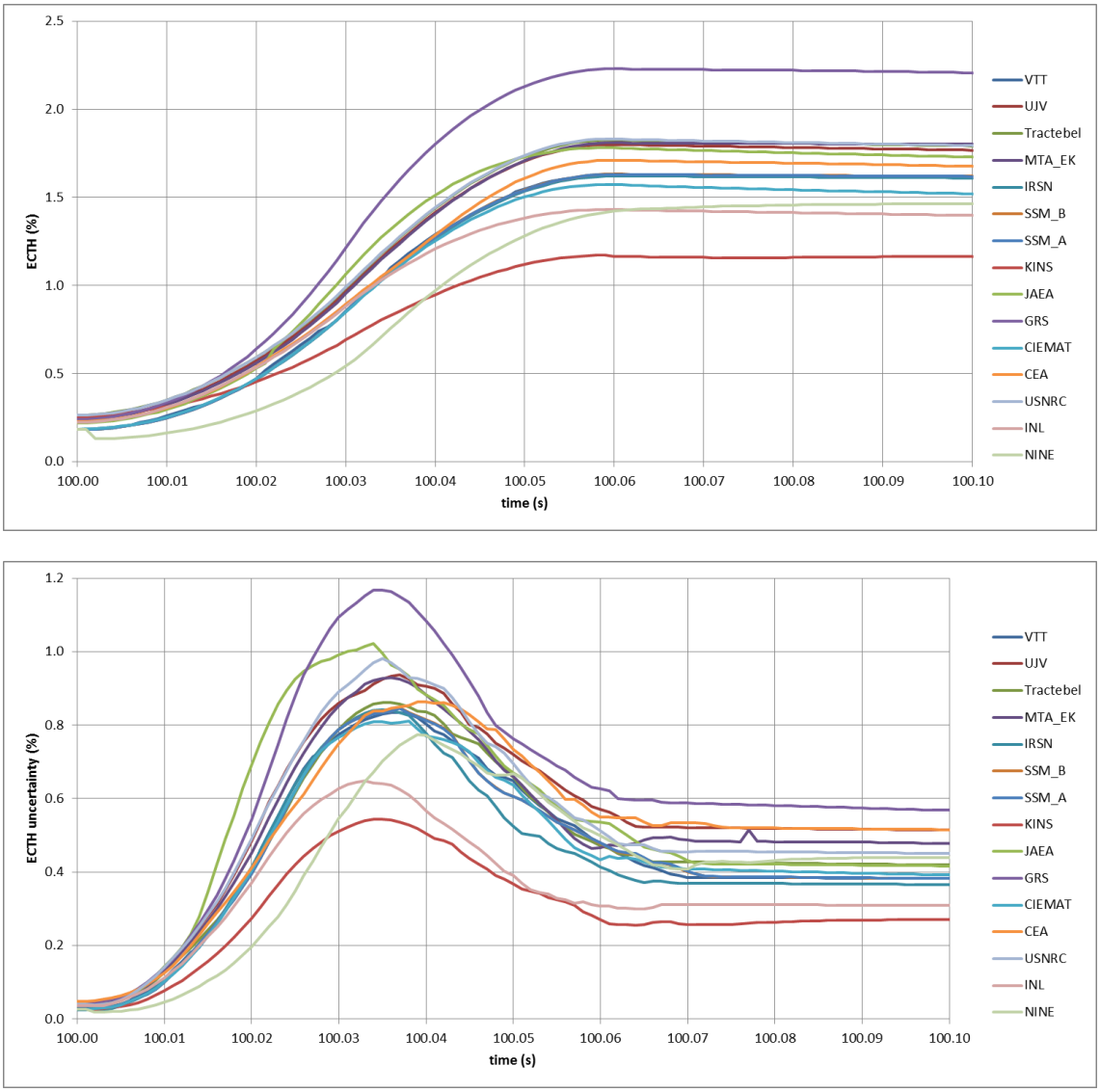

Figure 4-13: ECTH reference calculations (up) and uncertainty band widths (down) during the power pulse

The clad outer temperature (TCO) at the end of this phase is very high, because the boiling crisis is reached in all the calculations, Figure 4-14. The discrepancy between participants is high for the clad outer temperature uncertainty as it is already the case for the reference calculation. These discrepancies are linked to the differences in clad to coolant heat exchange modelling in the codes. It is worth noticing that the maximal uncertainty is reached later for the clad temperature than for fuel output parameters (temperature or elongation). Furthemore the maximal uncertainty band width is linearly increasing with the reference value, see Figure 4-15.

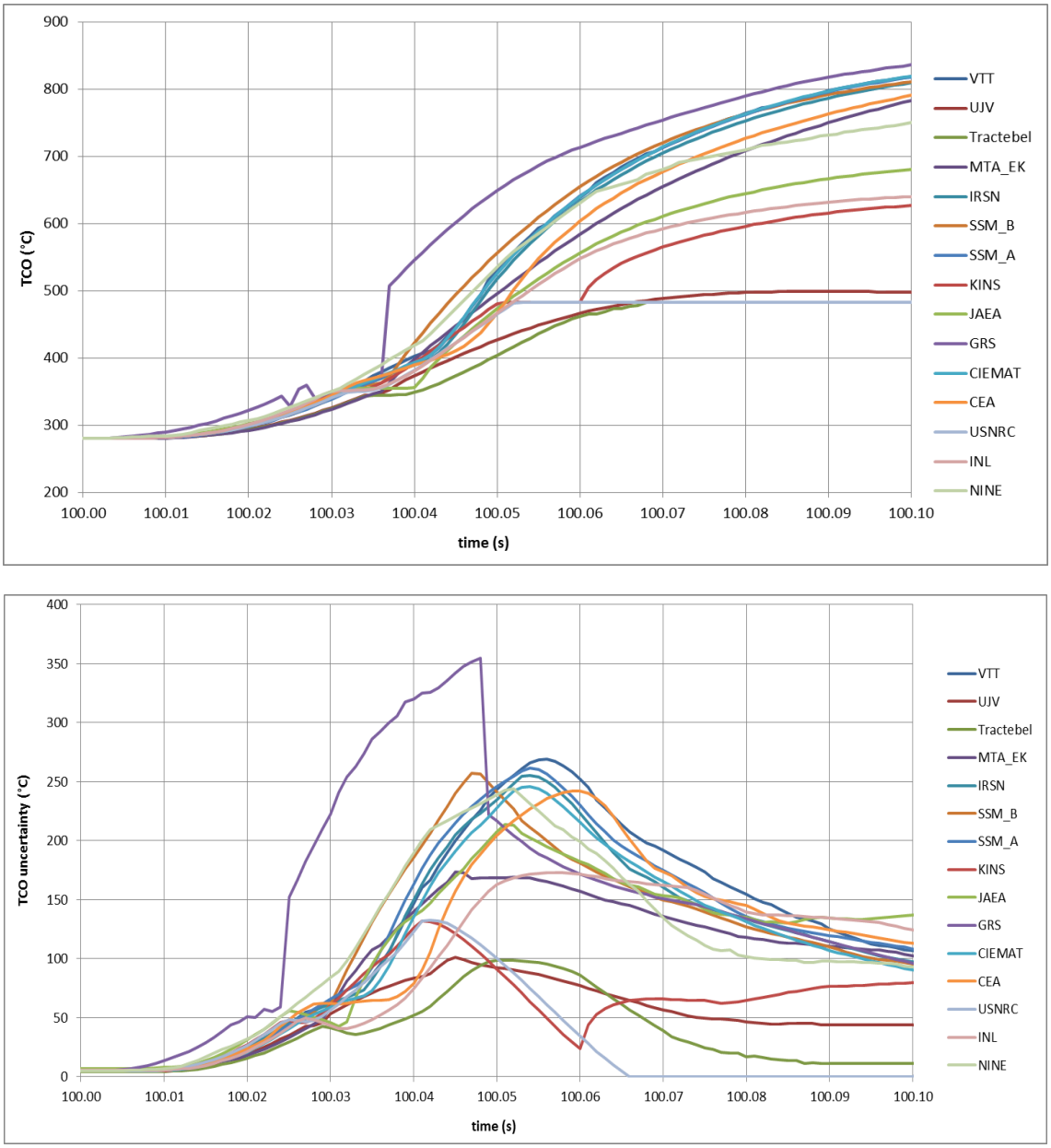

Figure 4-14: TCO reference calculations (up) and uncertainty band widths (down) during the power pulse

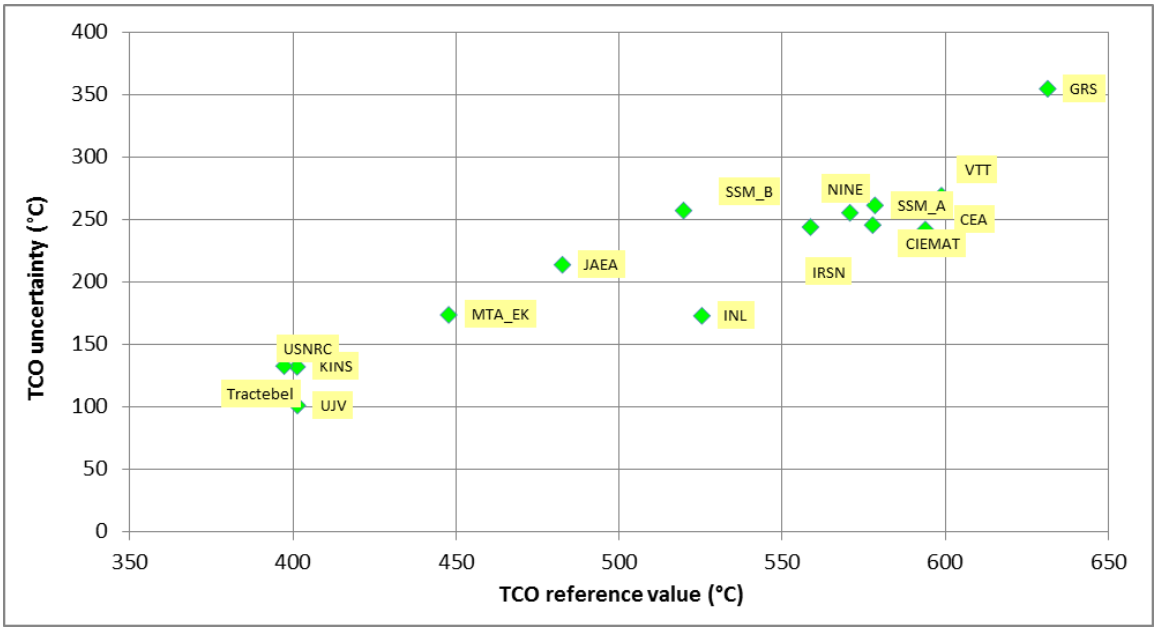

Figure 4-15: TCO uncertainty ($max(q_0)$) during the power pulse as a function of the corresponding reference value

4.2.1.3 *Analysis of the results after the power pulse (100.1 s – 120 s)*

After the power deposit, all participants calculate boiling at the clad-to-coolant interface. The thermo-mechanical behaviour of the rod will mainly depend on the clad to coolant heat exchange coefficient and on the quenching time.

The uncertainty evolutions of fuel thermal and mechanical results are represented in Figure 4-16. After the power pulse, the DHR uncertainty globally decreases from ~20 cal/g to ~1 cal/g. During this phase the uncertainty depends on the quenching time. The participant results are quite consistent for the uncertainty evolution of the fuel pellet outer radius (RFO).

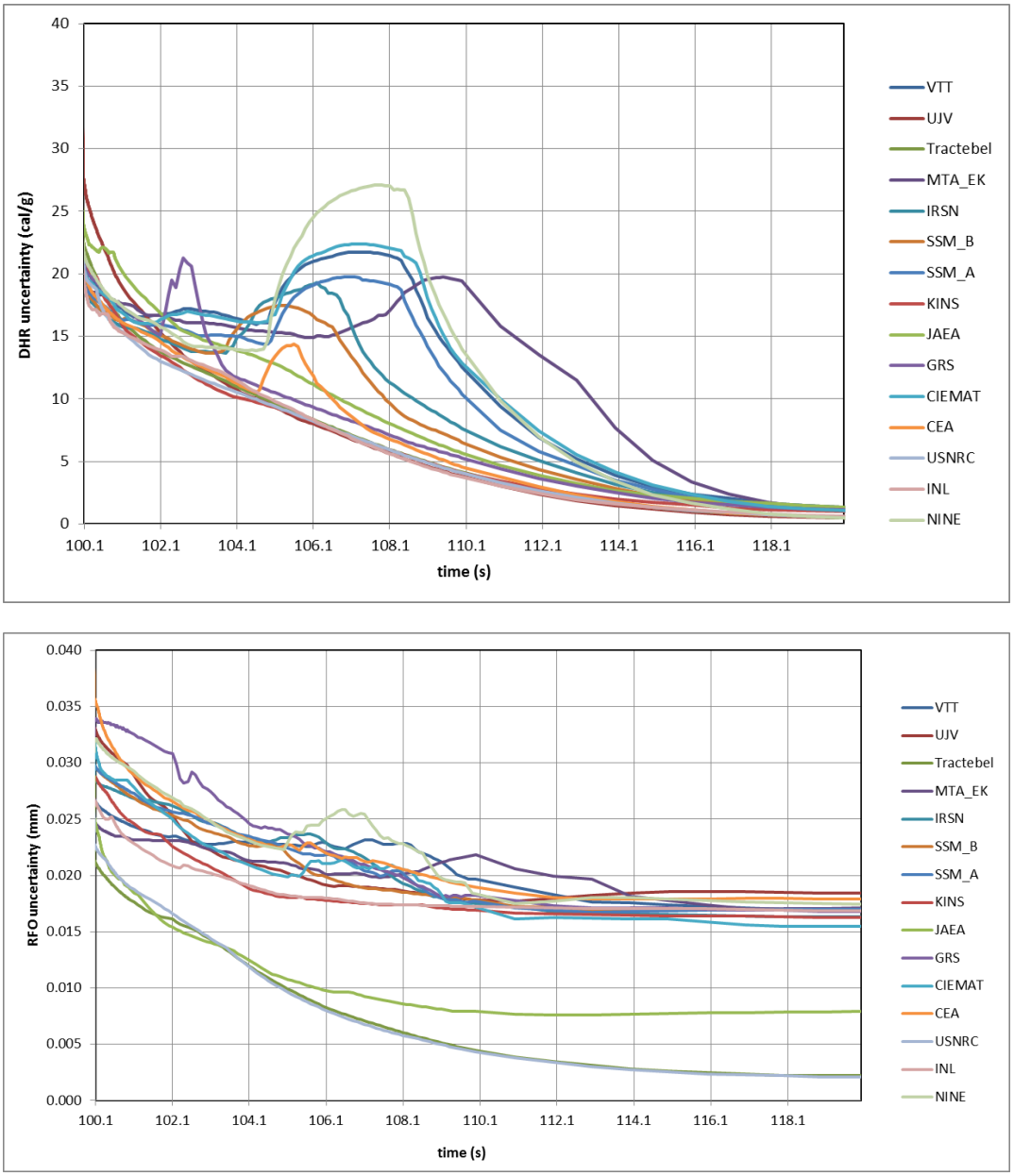

Figure 4-16: DHR (up) and RFO (down) uncertainty band widths after the power pulse (100.1 s to 120 s)

The uncertainty evolutions of the clad thermal and mechanical results are represented in

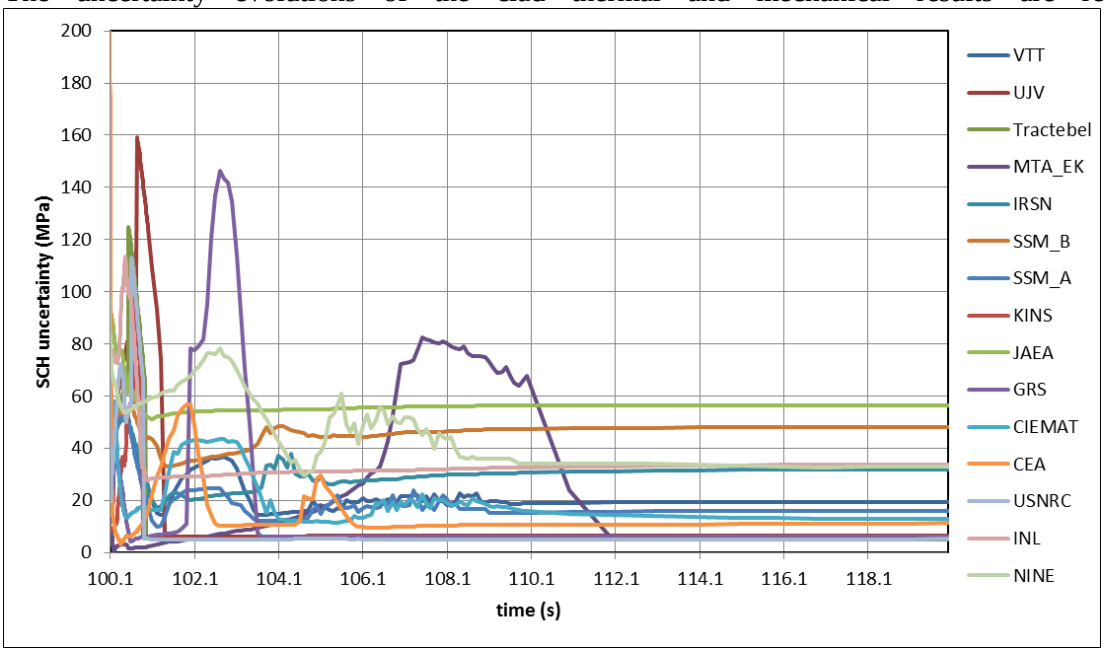

Figure 4-17. The uncertainty is still large after the power deposit for all the participants, both for thermal (TCO) and mechanical output (SCH). The discrepancies between participants are significant, mainly due to different modelling of the heat exchange during the boiling phase and to significant difference in quenching time. SCH uncertainty is also affected by the mechanical approach (i.e. different yield stress laws).

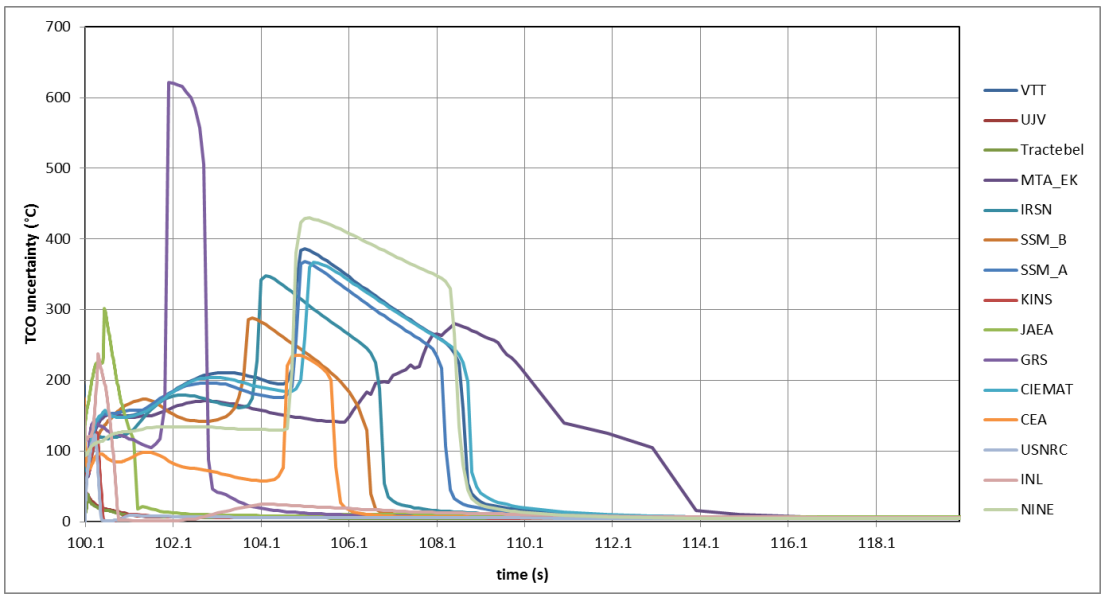

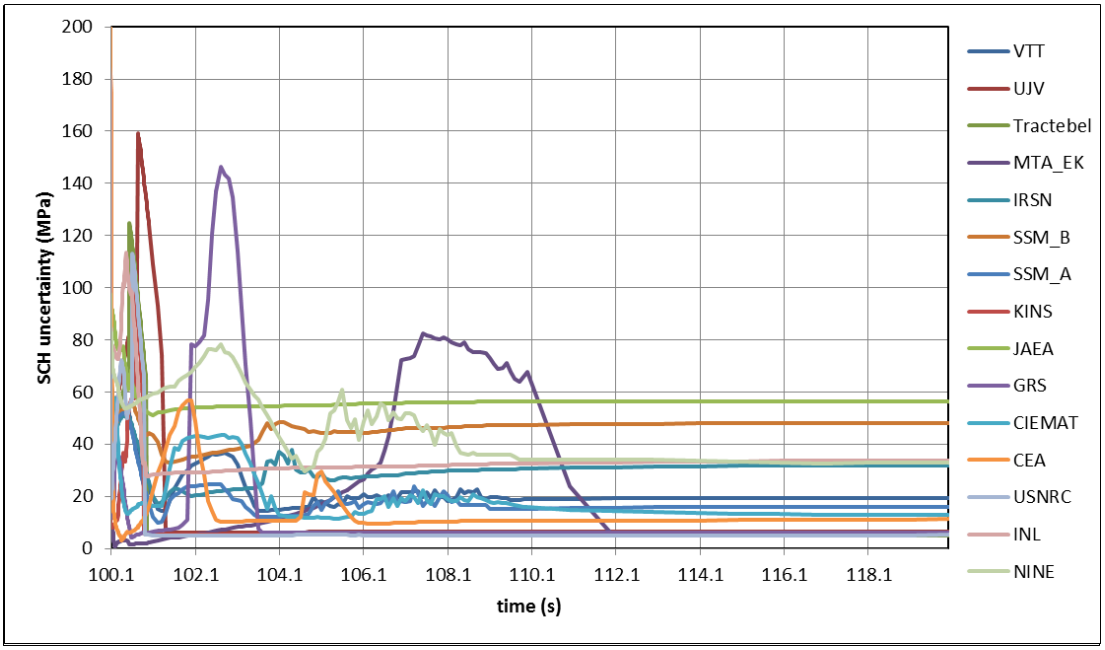

Figure 4-17: TCO (up) and SCH (down) uncertainty band widths after the power pulse (100.1 s to 120 s)

The position of reference calculations in the uncertainty band is presented in Figure 4-18 for RFO and TCO. While for the fuel outer radius (RFO), the reference calculations are centred in the uncertainty band (q1~0.5) and vary only slightly, the clad outer temperature (TCO) position varies significantly in the uncertainty band.

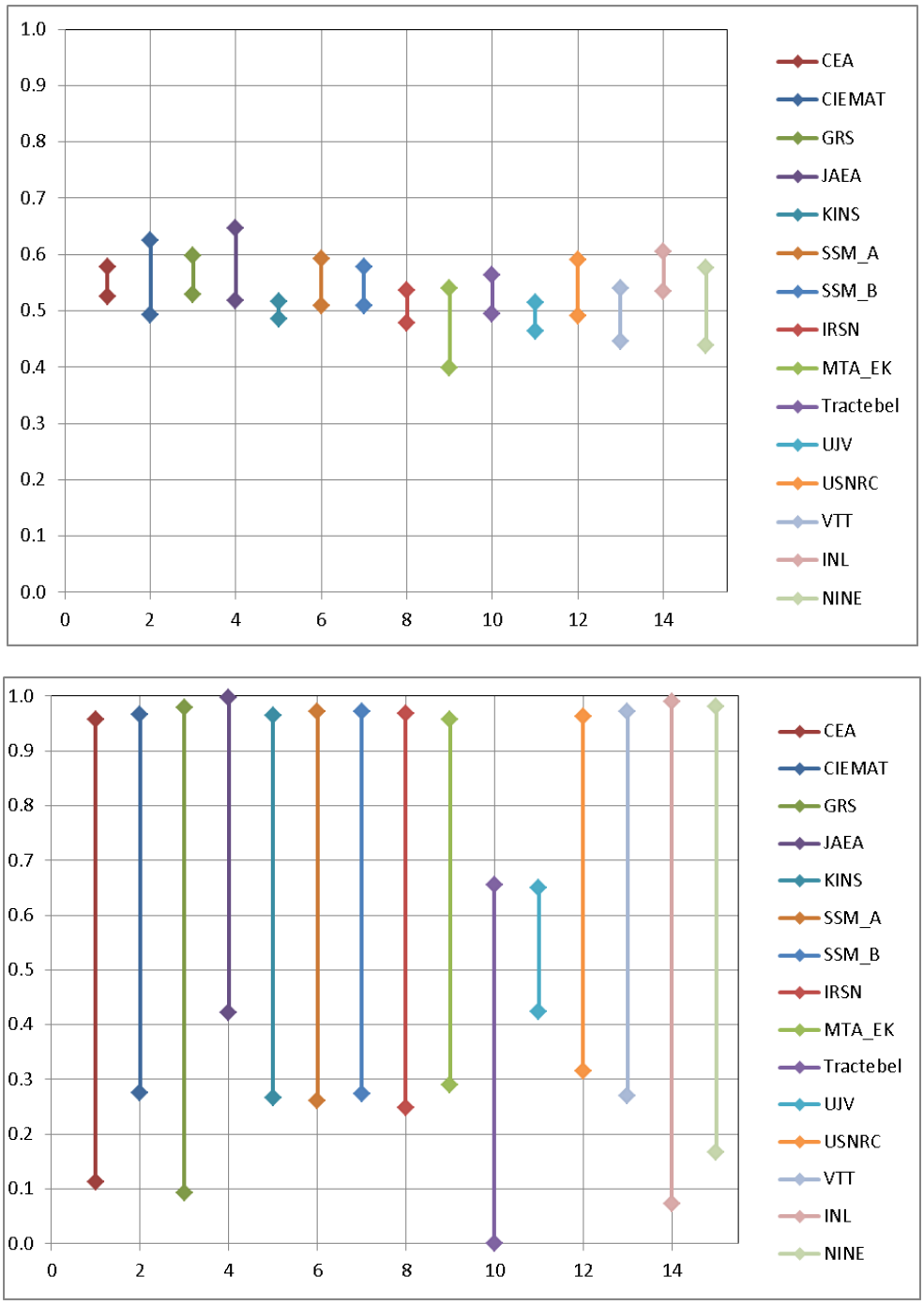

Figure 4-18: Position of the reference calculation within the uncertainty band for RFO (up) and TCO (down)

4.2.1.4 *Analysis of the results after the transient (t > 120 s)*

The results are very similar to the ones observed before the transient, the uncertainty on the thermal behaviour is rather low and the participants' results are consistent. The uncertainty on mechanical behaviour is nevertheless higher than before the transient: the uncertainties on clad residual hoop strain and elongation are high compared to the reference value (~50 %) and the discrepancies between participants are significant (see Figure 4-19).

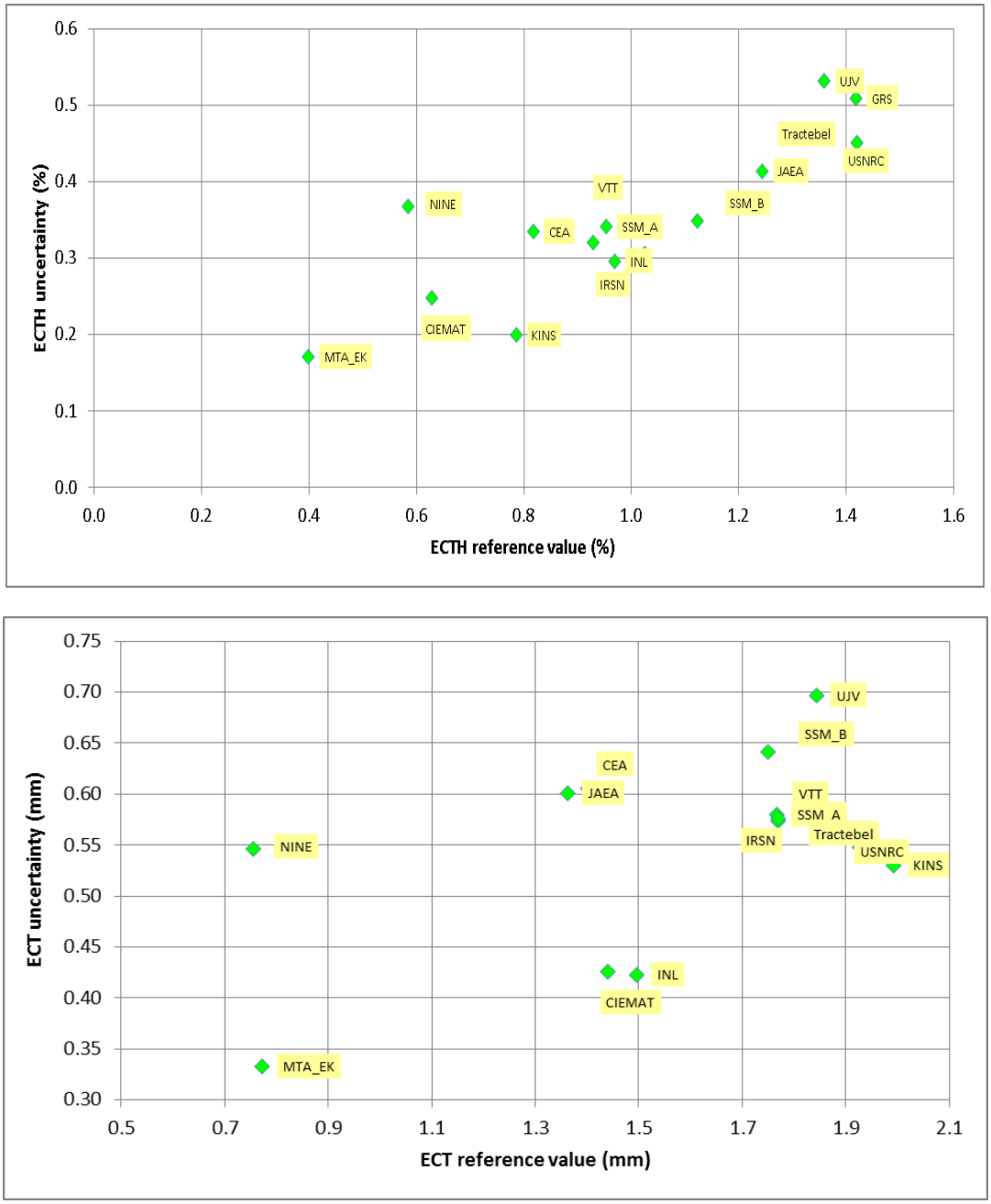

Figure 4-19: ECTH (up) and ECT (down) uncertainty ($max(q_0)$) after the transient as a function of the corresponding reference value

4.2.1.5 *Comparison between the union of all uncertainty intervals and reference calculation dispersion*

The union of all uncertainty intervals introduced in Section 4.1.1 is $[LUB_{min},UUB_{max}]$ where LUB_{min} (resp. UUB_{max}) is the minimum (resp. maximum) of all the LUBs (resp. UUBs). For the sake of clarity, we define the global uncertainty width as the difference between these two quantities.

Similarly, we also consider in the sequel the union of all the reference calculations $[REF_{min},REF_{max}]$ where REF_{min} (resp. REF_{max}) is the minimum (resp. maximum) of all the reference calculations. The reference calculation dispersion is then defined as the difference between these two quantities.

Figure 4-20, respectively Figure 4-21, shows these quantities for fuel enthalpy variation (DHR), respectively clad outer temperature (TCO). The global uncertainty width is close to the reference calculation dispersion. The code effect is very significant here. As illustrated for TCO on Figure 4-21, for several outputs, the reference calculation dispersion is larger than the typical uncertainty resulting from input parameter variations calculated by each participant individually.

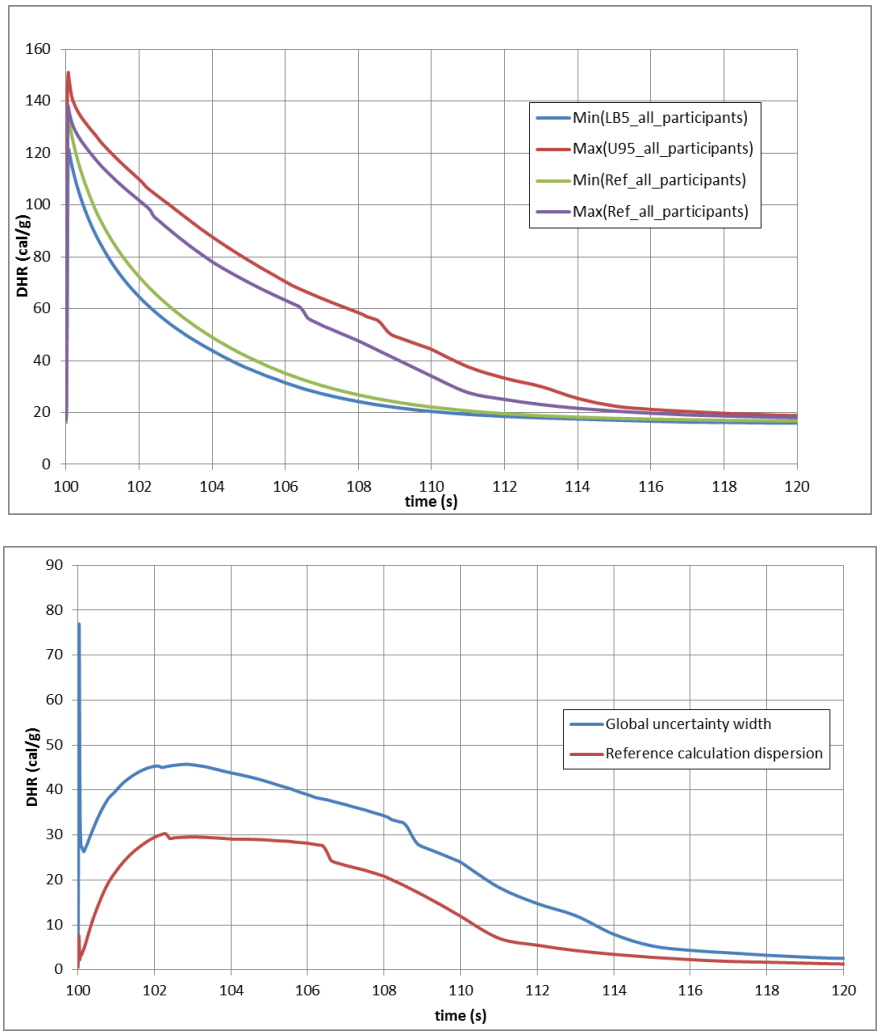

Figure 4-20: DHR uncertainty (up) and reference calculation dispersion (down)

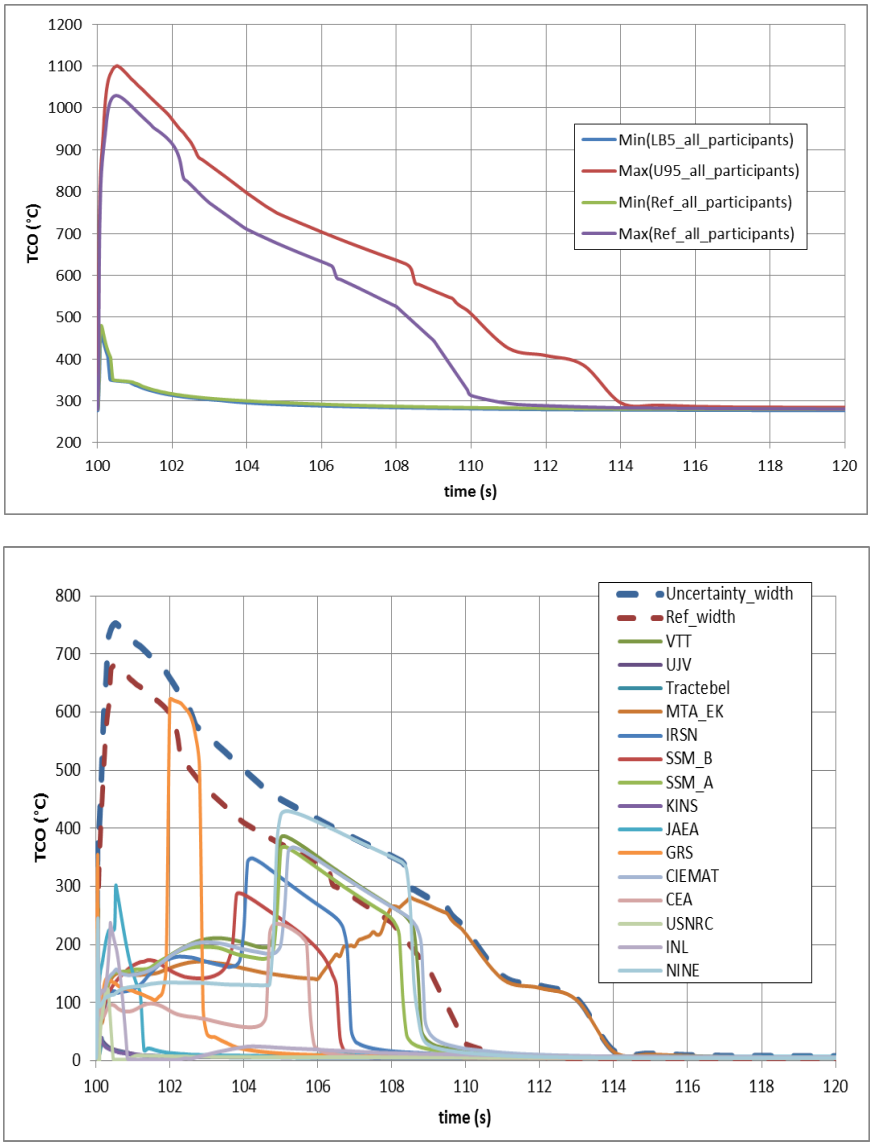

Figure 4-21: TCO uncertainty (up) and reference calculation dispersion (down)

4.2.2 *Uncertainty analysis: Scalar outputs*

Figure 4-22 first displays the relative global uncertainty associated with each scalar output parameter related to maximum values and boiling duration taking into account the contributions of all participants (see Table 2-2). It has been obtained by dividing LUB_{min} and UUB_{max} by the average of all reference calculations.

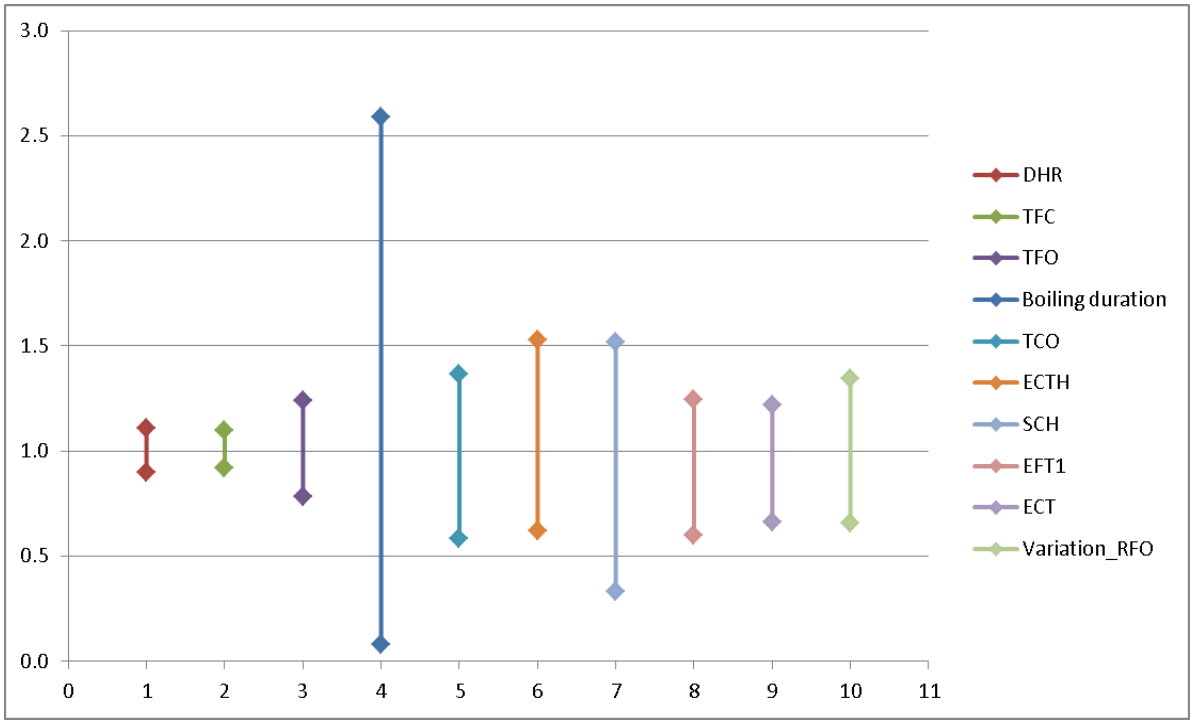

Figure 4-22: Relative global uncertainty interval associated with each output associated with maximum values and boiling duration

The results show that the global uncertainty interval width depends on the type of parameter observed. More precisely, the narrowest relative uncertainty intervals are obtained for fuel thermal behaviour outputs (DHR, TFC and TFO with a factor less than 1.5 between upper and lower bounds). The uncertainty interval width increases slightly for fuel mechanical outputs and clad elongation (RFO, EFT1 and ECT with a factor between 2 and 2.5) and more significantly for other clad mechanical outputs and clad temperature (ECTH, SCH and TCO). Concerning this last group, SCH exhibits a larger uncertainty (a factor ~5) than ECTH (a factor ~2.5). Finally, the largest uncertainty interval is observed for the boiling duration (a factor ~30).

The formal method recalled in Section 4.1.1 is then used to analyse the results. This work has been done with the SUNSET software [18] developed at IRSN. In order to evaluate the agreement or disagreement between participants' contributions, the intersection-based aggregation operator has been applied and Figure 4-23 provides the conflict indicator for each output.

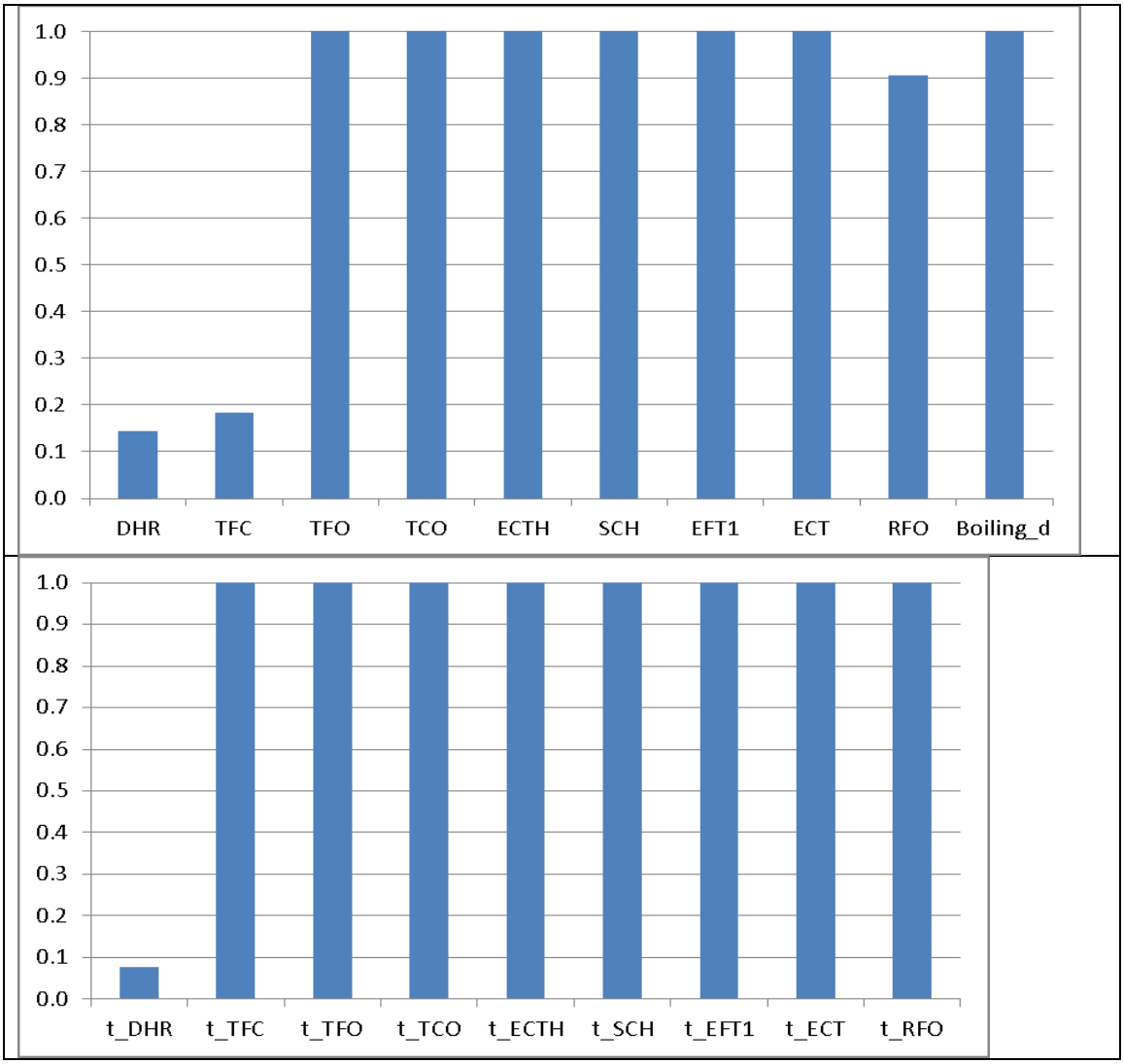

Figure 4-23: Conflict indicator associated with each output (maximum values, boiling duration and time of maximum values)

It appears that the results are highly conflicting, except for fuel thermal behaviour. However, since by construction, this indicator is equal to 1 as soon as two participants fully disagree (i.e. empty intersection between their uncertainty intervals), it is interesting to investigate the reasons why this lack of coherence is so noticeable. This is achieved by considering the union-based operator that leads to a representation of participants' contributions including the associated reference calculations. More precisely, the distributions coming from this type of aggregation are plotted for the maximal values of boiling duration that are the most relevant to study. For the sake of clarity, this section only provides this quantity for some outputs (Figure 4-24) in order to illustrate the main features of the results. We recall that, by construction, the distribution reaches 1 for each participant's reference calculation and its support is the union of all uncertainty intervals. The other points in the figures have no physical meaning and are associated with a non-regular discretization defined for the plot of the distributions. For a better understanding, we also add next to each distribution the raw data that have been used for its construction (i.e. uncertainty intervals and reference calculation of each participant).

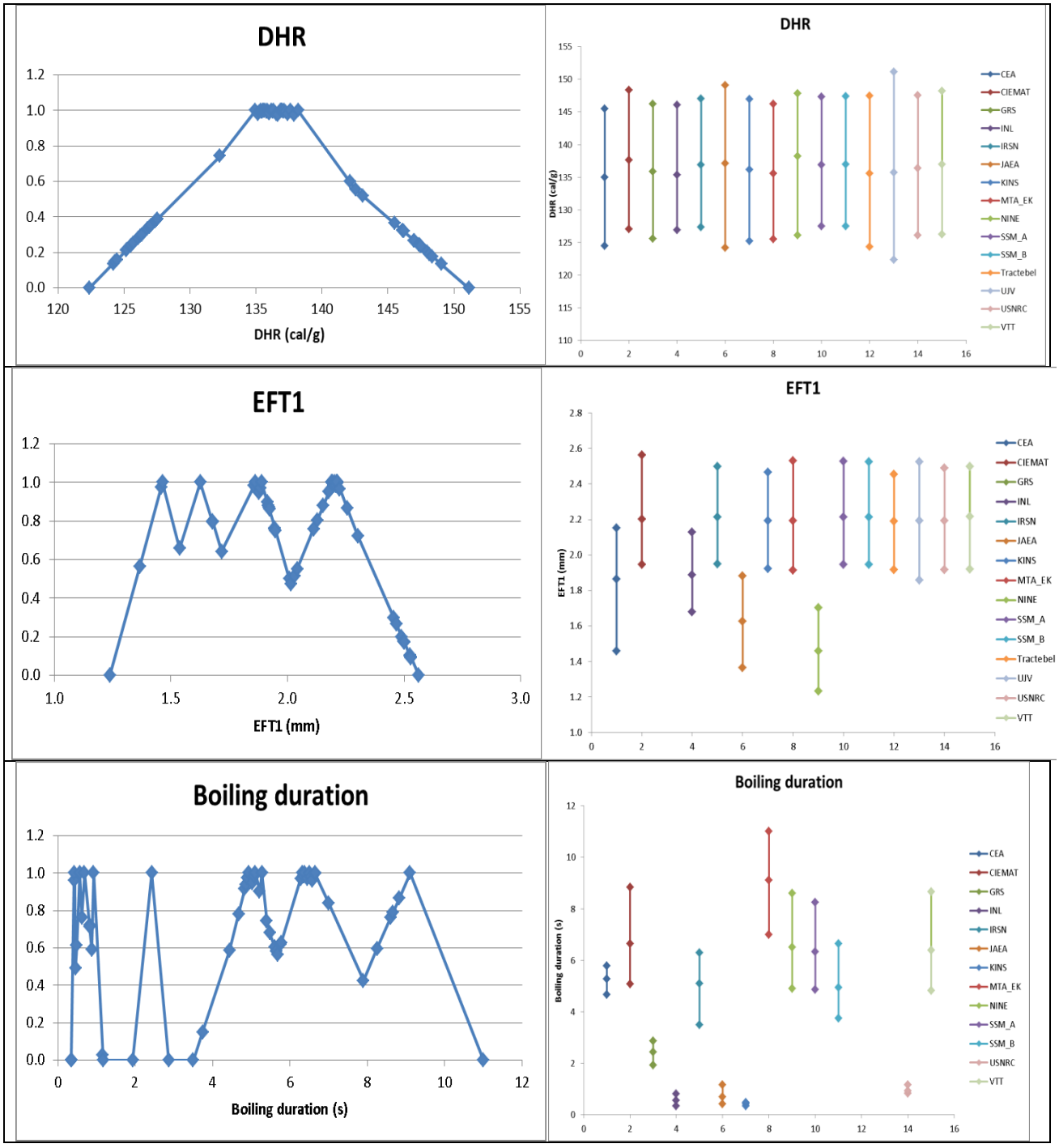
DHR
DHR (cal/g)
EFT1
EFT1 (mm)
Boiling duration
Boiling duration (s)
CEA
CIEMAT
GRS
INL
IRSN
JAEA
KINS
MTA_EK
NINE
SSM_A
SSM_B
Tractebel
UJV
USNRC
VTT

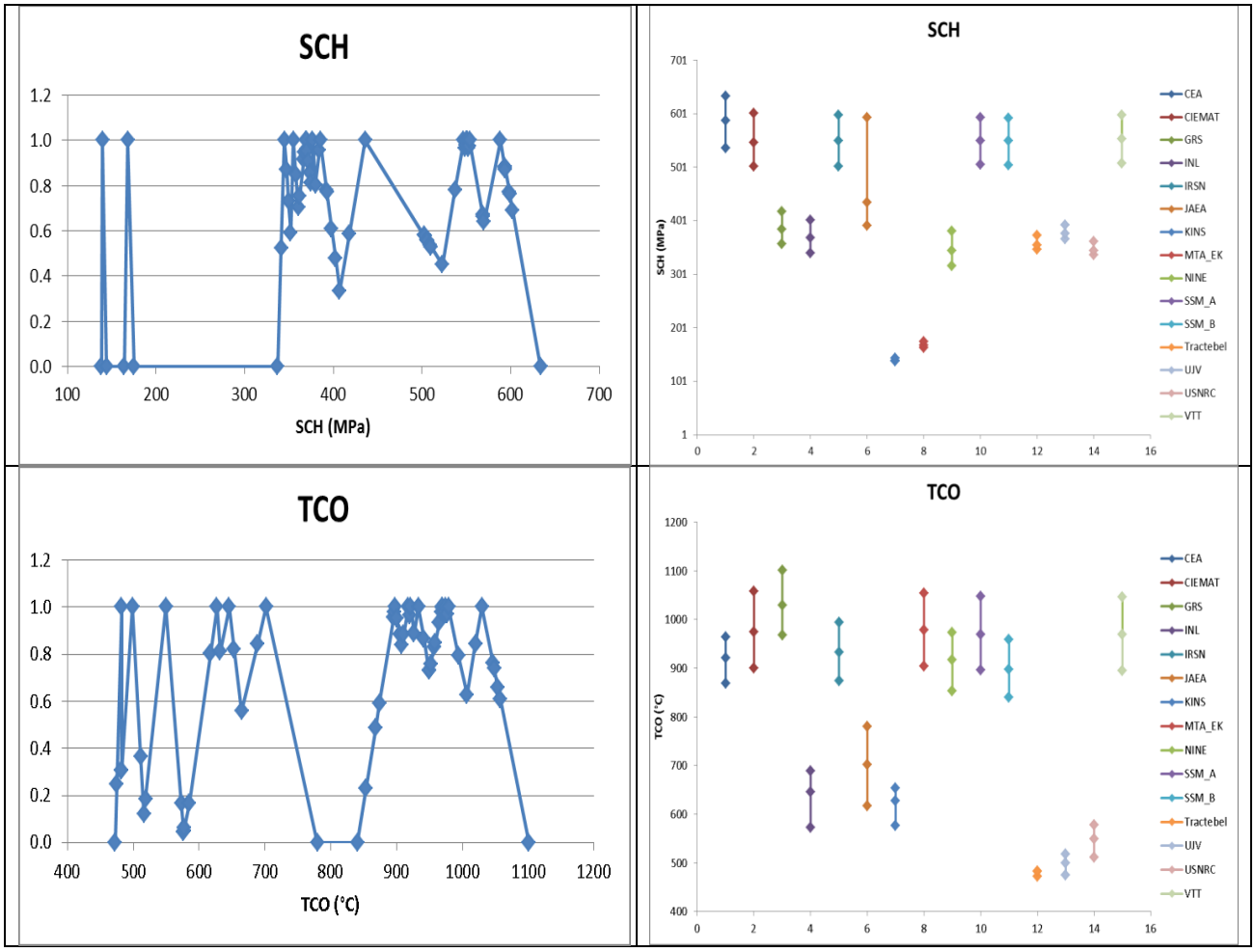

Figure 4-24: Union-based aggregation of the uncertainty results associated to DHR, EFT1, Boiling duration, SCH and TCO (from top to bottom)

The above figures point out the same three groups of results as in the Figure 4-22. They correspond to different levels of coherence:

- High coherence: it includes participants' results that are in strong agreement for uncertainty intervals and reference calculations. It corresponds to fuel thermal behaviour outputs,
- Low coherence: it concerns participants' results with a conflict indicator equal to 1 but exhibiting coherent reference calculations and uncertainty intervals for a large majority of participants (i.e. the empty intersection is due to few participants that do not agree with the others). It is the case for fuel and clad mechanical behaviour output except for SCH,
- No coherence: it concerns participants' results with a conflict indicator equal to 1 where the incoherence cannot be reduced by removing just a few contributions. It corresponds to thermal-hydraulic behaviour output (TCO, Boiling duration) and SCH. This strong lack of coherence can be explained by the combination of a large dispersion of reference calculations and narrow uncertainty bands, which is particularly noticeable for TCO and SCH.

It is also interesting to focus on subgroups of participants, based on the computer codes they use. Since FRAPTRAN and SCANAIR are the most used codes in this benchmark, we evaluate the coherence among the ten participants using these two codes (Figure 4-25). It appears that restricting the results to two subgroups strongly increases the coherence only for clad mechanical behaviour outputs, keeping in mind that the reduced number of participants (10 compared to the 15 contributions) has not been taken into account.

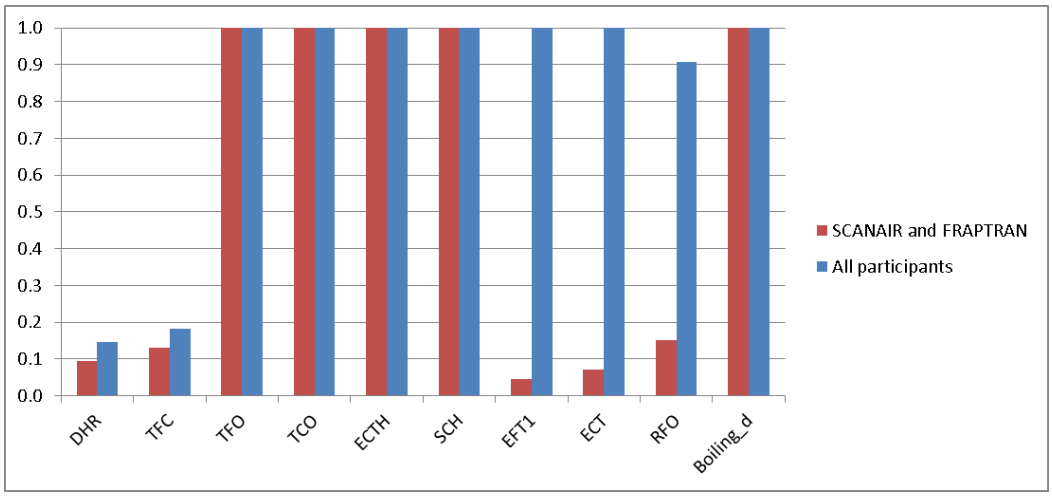

Figure 4-25: Conflict indicator associated with each output (maximum values and boiling duration) for the subgroup of SCANAIR and FRAPTRAN users

Finally, the same study has been performed for FRAPTRAN and SCANAIR users separately. In order to investigate a user effect, the contributions of SSM_B (SCANAIR) and MTA_EK (FRAPTRAN) that did not use standard thermal-hydraulic models (two-phase coolant channel model for SSM_B and coupling with TRABCO for MTA_EK) have not been considered. The conflict indicator shown by Figure 4-26 illustrates that the user effect is not negligible, especially for FRAPTRAN users for thermal-hydraulic parameters (TFO, TCO, Boiling duration) and mechanical parameters (ECTH, SCH). This deviation is not solely a user effect and is likely significantly influenced by the different code versions used in this benchmark study. It was determined the FRAPTRAN-2.0 Beta did contain an error in the clad-to-coolant heat transfer coefficient.

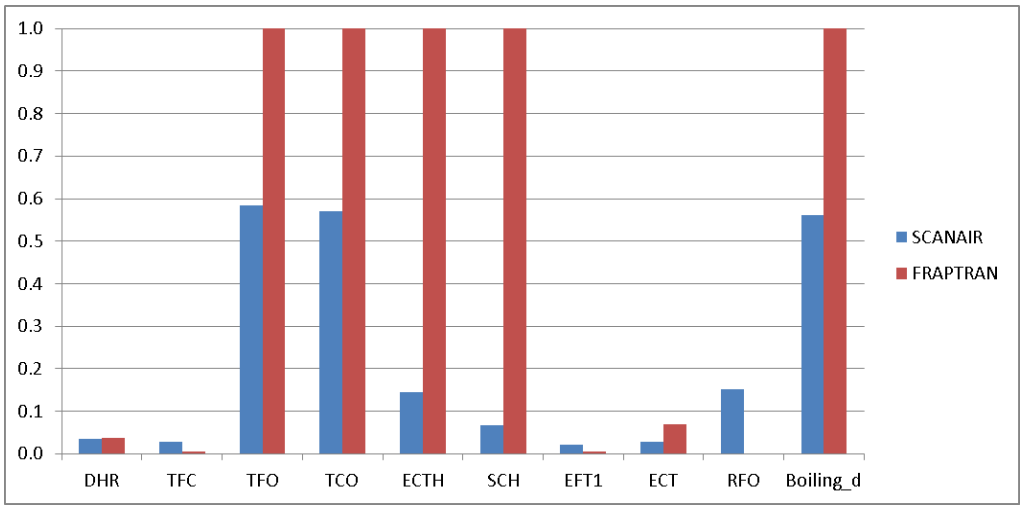

Figure 4-26: Conflict indicator for maximum values outputs and boiling duration with respect to the used code (SCANAIR or FRAPTRAN)

4.2.3 *Sensitivity analysis*

The most influential input parameters have been identified for each participant, based on their calculated correlation coefficients and using a fixed significance threshold of 0.25. Two kinds of synthesis have been performed.

The first one (Table 4-2 to Table 4-9) intends to exhibit a general trend of the most influential parameters, taking into account all participants' results. It has been achieved by averaging the number of participants that consider a given parameter as influential. This short calculation has been repeated for the five fixed times (see Table 2-3) when the outputs of interest were evaluated and for maximum values, as required in the specifications.

In the second one, in order to draw conclusions for practical issues, the results have been summarized with respect to groups of outputs corresponding to a type of behaviour (Figure 4-27 to Figure 4-32). More precisely, for each to Table 4-2 to Table 4-9, several columns have been aggregated following the rule that if an input parameter is influential for an output associated with a given behaviour, it is considered as influential for the whole group.

- **Before the transient** (t < 100 s):

Before the transient there is a strong agreement on influential parameters (very high or very low percentage). At that time, the coolant inlet temperature is influential for all type of behaviour. Fuel thermal expansion model is identified as influential for mechanical behaviour (for fuel and clad) by almost all the participants. To a smaller extent, cladding inside diameter, clad thermal expansion model and fuel enthalpy, are also identified as influential parameters. (see Figure 4-27 and Table 4-2).

	Fuel thermal (DHR, TFC)	Clad thermal (TCO)	Clad mechanical (ECTH, SCH)	Fuel mechanical (EFT1, RFO)
Cladding outside diameter				
Cladding inside diameter				
Fuel theoretical density				
Fuel porosity				
Cladding roughness				
Fuel roughness				
Filling gas pressure				
Coolant pressure				
Coolant inlet temperature				
Coolant velocity				
Injected energy in the rod				
Full mid height width				
Fuel thermal conductivity model				
Clad thermal conductivity model				
Fuel thermal expansion model				
Clad thermal expansion model				
Clad Yield stress				
Fuel enthalpy				
Clad to coolant heat transfer				

Figure 4-27: Influential input parameters with respect to the type of behaviour when focusing on the before the transient.

A coloured bar means that more than 50 % of the participants have identified the corresponding input parameter as influential for the type of behaviour.

Input \ Output	DHR	TFC	TFO	TCO	ECTH	ECT	EFT1	SCH	RFO
Cladding outside diameter	0	0	0	0	0	0	0	0	**7**
Cladding inside diameter	0	0	0	0	0	**7**	0	0	**93**
Fuel theoretical density	0	0	0	0	0	0	0	0	0
Fuel porosity	**7**	0	0	0	0	0	**7**	0	**7**
Cladding roughness	0	0	0	0	0	0	0	0	**7**
Fuel roughness	0	0	0	0	0	0	0	0	**7**
Filling gas pressure	0	0	0	0	0	**21**	0	**7**	0
Coolant pressure	0	**13**	**13**	**13**	**7**	**7**	**7**	0	**7**
Coolant inlet temperature	**93**	**100**	**100**	**100**	**73**	**64**	**71**	**7**	**33**
Coolant velocity	0	0	0	0	0	0	0	0	0
Injected energy in the rod	0	0	0	0	0	0	0	0	0
Full width at half maximum	0	0	0	0	0	0	0	0	**7**
Fuel thermal conductivity model	0	0	0	0	**7**	0	**7**	**13**	**7**
Clad thermal conductivity model	0	0	0	0	0	0	**7**	**7**	**7**
Fuel thermal expansion model	0	0	0	0	**100**	**100**	**100**	**100**	**73**
Clad thermal expansion model	0	0	0	0	**67**	**43**	**43**	**100**	**7**
Clad Yield stress	0	0	0	0	0	0	0	0	**7**
Fuel enthalpy	**67**	0	0	0	0	0	0	0	**7**
Clad to coolant heat transfer	0	0	0	0	0	0	0	0	0

Table 4-2: Percentage of participants that have identified a given input parameter as influential for each output of interest at the beginning of the power pulse.

The orange colour is associated with a percentage larger than 50 %, the blue colour with a percentage between 0 and 50 % and the green colour with a zero percentage.

- **At the time of maximum power pulse**

At the maximum power pulse, there is a lower agreement between participants than before the pulse. Injected energy is identified as influential for almost all the outputs. Fuel enthalpy, thermal expansion model and pulse width are also in influential for several thermal and mechanical outputs. The fuel and clad roughness are identified as influential for cladding thermal and mechanical behaviour. On this last point it needs to be stressed that the effect would certainly be different with irradiated fuel where the impact of roughness on fuel to clad heat exchange is lower than for fresh fuel. It's also worth noticing that, at that time, the fuel thermal conductivity has a low impact on fuel thermal behaviour because the fuel behaviour is close to adiabatic during the first part of power pulse. (Figure 4-28 and Table 4-3).

	Fuel thermal (DHR, TFC)	Clad thermal (TCO)	Clad mechanical (ECTH, SCH)	Fuel mechanical (EFT1, RFO)
Cladding outside diameter				
Cladding inside diameter				
Fuel theoretical density				
Fuel porosity				
Cladding roughness				
Fuel roughness				
Filling gas pressure				
Coolant pressure				
Coolant inlet temperature				
Coolant velocity				
Injected energy in the rod				
Full mid height width				
Fuel thermal conductivity model				
Clad thermal conductivity model				
Fuel thermal expansion model				
Clad thermal expansion model				
Clad Yield stress				
Fuel enthalpy				
Clad to coolant heat transfer				

Figure 4-28: Influential input parameters with respect to the type of behaviour when focusing on the time of maximum power pulse values.

A coloured bar means that more than 50 % of the participants have identified the corresponding input parameter as influential for the type of behaviour.

Input \ Output	DHR	TFC	TFO	TCO	ECTH	ECT	EFT1	SCH	RFO
Cladding outside diameter	0	0	0	**67**	0	**7**	**7**	**13**	0
Cladding inside diameter	0	0	**7**	**40**	0	**7**	**7**	0	**93**
Fuel theoretical density	**13**	**20**	0	0	**7**	**7**	**7**	0	**7**
Fuel porosity	**7**	**13**	0	0	**7**	**7**	**7**	**7**	**7**
Cladding roughness	**7**	0	**100**	**67**	**13**	0	0	**73**	**7**
Fuel roughness	**7**	0	**93**	**71**	0	0	0	**79**	**7**
Filling gas pressure	**7**	**7**	0	0	0	0	0	**7**	0
Coolant pressure	0	0	0	**7**	0	0	0	**7**	**7**
Coolant inlet temperature	0	0	0	**67**	0	0	0	**47**	0
Coolant velocity	0	0	0	0	0	0	0	0	0
Injected energy in the rod	**93**	**93**	**93**	**73**	**93**	**93**	**93**	**47**	**80**
Full width at half maximum	**60**	**27**	**67**	**93**	**33**	**36**	**36**	**87**	**27**
Fuel thermal conductivity model	0	0	**67**	**40**	**7**	0	0	**20**	**7**
Clad thermal conductivity model	0	0	**47**	**73**	0	0	0	**47**	0
Fuel thermal expansion model	**7**	**7**	0	0	**93**	**93**	**93**	**53**	**87**
Clad thermal expansion model	0	0	0	0	**7**	0	0	**13**	**7**
Clad Yield stress	0	0	0	0	**7**	**14**	**14**	**60**	**13**
Fuel enthalpy	**40**	**80**	**53**	**20**	**80**	**71**	**71**	**13**	**73**
Clad to coolant heat transfer	**7**	0	0	**53**	0	0	0	**40**	0

Table 4-3: Percentage of participants that have identified a given input parameter as influential for each output of interest at the time of maximum power pulse.

The orange colour is associated with a percentage larger than 50 %, the blue colour with a percentage between 0 and 50 % and the green colour with a zero percentage.

- **At the end of power pulse**

At the end of power pulse the trend is similar to that at the time of maximal power. Injected energy is identified as influential for almost all the outputs. Fuel enthalpy is also influential for fuel and clad thermal and mechanical outputs. Fuel thermal conductivity model is now identified as influential for fuel and clad outer temperature and clad stress (see Figure 4-29 and Table 4-4.)

	Fuel thermal (DHR, TFC)	Clad thermal (TCO)	Clad mechanical (ECTH, SCH)	Fuel mechanical (EFT1, RFO)
Cladding outside diameter				
Cladding inside diameter				
Fuel theoretical density				
Fuel porosity				
Cladding roughness				
Fuel roughness				
Filling gas pressure				
Coolant pressure				
Coolant inlet temperature				
Coolant velocity				
Injected energy in the rod				
Full mid height width				
Fuel thermal conductivity model				
Clad thermal conductivity model				
Fuel thermal expansion model				
Clad thermal expansion model				
Clad Yield stress				
Fuel enthalpy				
Clad to coolant heat transfer				

Figure 4-29: Influential input parameters with respect to the type of behaviour when focusing on the end of the power pulse.

A coloured bar means that more than 50 % of the participants have identified the corresponding input parameter as influential for the type of behaviour.

Input \ Output	DHR	TFC	TFO	TCO	ECTH	ECT	EFT 1	SCH	RFO
Cladding outside diameter	0	0	**7**	**73**	**7**	**7**	**7**	**53**	**7**
Cladding inside diameter	**60**	**53**	**7**	**33**	0	**14**	**14**	**20**	**87**
Fuel theoretical density	**40**	**40**	0	0	**20**	**21**	**21**	0	**13**
Fuel porosity	**33**	**33**	0	0	**27**	**29**	**29**	0	**7**
Cladding roughness	**53**	0	**100**	**60**	**7**	0	0	**67**	**7**
Fuel roughness	**43**	0	**100**	**71**	0	0	0	**64**	0
Filling gas pressure	**7**	**7**	0	0	0	0	0	0	0
Coolant pressure	0	0	**7**	**13**	0	0	0	**7**	0
Coolant inlet temperature	**33**	0	0	**27**	**0**	**7**	**7**	**27**	0
Coolant velocity	0	0	0	0	0	0	0	0	0
Injected energy in the rod	**100**	**100**	**100**	**93**	**100**	**93**	**93**	**93**	**100**
Full width at half maximum	**73**	**13**	**67**	**100**	**33**	**29**	**29**	**93**	**33**
Fuel thermal conductivity model	**33**	0	**93**	**67**	**7**	0	0	**73**	0
Clad thermal conductivity model	0	0	**73**	**67**	0	0	0	**53**	0
Fuel thermal expansion model	**7**	**7**	0	0	**100**	**100**	**100**	**7**	**93**
Clad thermal expansion model	**7**	0	0	0	**33**	0	0	0	0
Clad Yield stress	0	0	0	0	**7**	**7**	**7**	**53**	**13**
Fuel enthalpy	**73**	**87**	**80**	**60**	**80**	**79**	**79**	**40**	**73**
Clad to coolant heat transfer	**7**	0	**27**	**53**	0	0	0	**47**	**7**

Table 4-4: Percentage of participants that have identified a given input parameter as influential for each output of interest at the end of power pulse.

The orange colour is associated with a percentage larger than 50 %, the blue colour with a percentage between 0 and 50 % and the green colour with a zero percentage.

- **During the boiling phase** (t = 101 s):

Similarly to the previous time, the injected energy is still influential (for a large majority of participants) for all outputs. Fuel properties (enthalpy, conductivity and thermal expansion model) are influential for fuel and clad mechanical properties.
Surprisingly, the clad to coolant heat transfer has been identified as influential by at most two thirds of the participants depending on the type of output. This can be due to the difference between reported SCANAIR and FRAPTRAN results. More precisely, according to Table 4-6 and Table 4-7, it appears that this parameter is influential for a very large majority of SCANAIR users but for less than 40 % of FRAPTRAN users, likely caused by the different code versions used. One also notes that for FRAPTRAN, there is no reported correlation between the clad yield stress and SCH for all considered time positions (see Figure 4-30 and Table 4-5).

	Fuel thermal (DHR, TFC)	Clad thermal (TCO)	Clad mechanical (ECTH, SCH)	Fuel mechanical (EFT1, RFO)
Cladding outside diameter				
Cladding inside diameter				
Fuel theoretical density				
Fuel porosity				
Cladding roughness				
Fuel roughness				
Filling gas pressure				
Coolant pressure				
Coolant inlet temperature				
Coolant velocity				
Injected energy in the rod				
Full mid height width				
Fuel thermal conductivity model				
Clad thermal conductivity model				
Fuel thermal expansion model				
Clad thermal expansion model				
Clad Yield stress				
Fuel enthalpy				
Clad to coolant heat transfer				

Figure 4-30: Influential input parameters with respect to the type of behaviour when focusing on the time 101 s.

A coloured bar means that more than 50 % of the participants have identified the corresponding input parameter as influential for the type of behaviour.

Input \ Output	DHR	TFC	TFO	TCO	ECTH	ECT	EFT1	SCH	RFO
Cladding outside diameter	0	0	**13**	**7**	**7**	**7**	**7**	**27**	0
Cladding inside diameter	**53**	**60**	**27**	**7**	0	**14**	**14**	**33**	**87**
Fuel theoretical density	**40**	**47**	0	**7**	**20**	**14**	**14**	0	**13**
Fuel porosity	**40**	**40**	0	**13**	**33**	**29**	**29**	0	**13**
Cladding roughness	**27**	0	**33**	**27**	**13**	**7**	**7**	**13**	**7**
Fuel roughness	**29**	0	**43**	**21**	**7**	**8**	**8**	**14**	**14**
Filling gas pressure	**7**	**7**	0	0	**7**	0	0	**20**	**7**
Coolant pressure	0	0	**20**	**40**	0	0	0	**33**	**7**
Coolant inlet temperature	**7**	0	0	**33**	0	**7**	**7**	**7**	0
Coolant velocity	0	0	0	**29**	0	0	0	0	0
Injected energy in the rod	**100**	**100**	**100**	**100**	**100**	**93**	**93**	**87**	**100**
Full width at half maximum	**7**	0	**13**	**20**	**7**	**7**	**7**	**20**	0
Fuel thermal conductivity model	**80**	0	**87**	**80**	**20**	**14**	**14**	**67**	**33**
Clad thermal conductivity model	**7**	0	**27**	0	0	0	0	**7**	**7**
Fuel thermal expansion model	**7**	**7**	**33**	**27**	**100**	**100**	**100**	**60**	**100**
Clad thermal expansion model	0	0	**27**	**13**	**40**	**7**	0	**13**	**7**
Clad Yield stress	0	0	**7**	0	**13**	**7**	**7**	**40**	**7**
Fuel enthalpy	**87**	**87**	**80**	**47**	**87**	**79**	**86**	**53**	**80**
Clad to coolant heat transfer	**67**	0	**67**	**67**	**40**	**29**	**21**	**47**	**27**

Table 4-5: Percentage of participants that have identified a given input parameter as influential for each output of interest at t=101 s.

The orange colour is associated with a percentage larger than 50 %, the blue colour with a percentage between 0 and 50 % and the green colour with a zero percentage.

Input \ Output	DHR	TFC	TFO	TCO	ECTH	ECT	EFT1	SCH	RFO
Cladding outside diameter	0	0	**20**	**20**	**20**	0	0	0	0
Cladding inside diameter	**60**	**80**	0	0	0	0	0	0	**100**
Fuel theoretical density	**20**	**20**	0	0	0	0	0	0	0
Fuel porosity	**40**	**20**	0	0	**40**	**20**	**20**	0	0
Cladding roughness	0	0	0	**20**	0	0	0	0	0
Fuel roughness	0	0	0	0	0	0	0	0	0
Filling gas pressure	0	0	0	0	0	0	0	0	0
Coolant pressure	0	0	**40**	**40**	0	0	0	0	0
Coolant inlet temperature	0	0	0	0	0	0	0	0	0
Coolant velocity	0	0	0	0	0	0	0	0	0
Injected energy in the rod	**100**	**100**	**100**	**100**	**100**	**100**	**100**	**100**	**100**
Full width at half maximum	**20**	0	0	0	0	0	0	**20**	0
Fuel thermal conductivity model	**100**	0	**100**	**100**	0	**20**	**20**	**100**	0
Clad thermal conductivity model	0	0	0	0	0	0	0	0	0
Fuel thermal expansion model	0	0	0	0	**100**	**100**	**100**	**100**	**100**
Clad thermal expansion model	0	0	0	0	**80**	0	0	**40**	0
Clad Yield stress	0	0	0	0	0	0	0	**80**	0
Fuel enthalpy	**100**	**100**	**100**	**100**	**100**	**100**	**100**	**100**	**100**
Clad to coolant heat transfer	**100**	0	**100**	**100**	**100**	**40**	**20**	**60**	**20**

Table 4-6: Percentage of SCANAIR users that have identified a given input parameter as influential for each output of interest at t=101 s.

The orange colour is associated with a percentage larger than 50 %, the blue colour with a percentage between 0 and 50 % and the green colour with a zero percentage.

Input \ Output	DHR	TFC	TFO	TCO	ECTH	ECT	EFT1	SCH	RFO
Cladding outside diameter	0	0	**20**	0	0	0	0	**60**	0
Cladding inside diameter	**80**	**60**	**40**	0	0	0	0	**60**	**80**
Fuel theoretical density	**60**	**80**	0	**20**	**40**	**40**	**40**	0	**40**
Fuel porosity	**60**	**80**	0	**40**	**40**	**40**	**40**	0	**40**
Cladding roughness	**40**	**0**	**60**	**60**	0	0	0	0	0
Fuel roughness	**40**	**0**	**80**	**60**	0	0	0	0	**20**
Filling gas pressure	0	0	0	0	0	0	0	**60**	**20**
Coolant pressure	0	0	0	**40**	0	0	0	**60**	**20**
Coolant inlet temperature	**20**	0	0	**80**	0	0	0	0	0
Coolant velocity	0	0	0	**80**	0	0	0	0	0
Injected energy in the rod	**100**	**100**	**100**	**100**	**100**	**100**	**100**	**60**	**100**
Full width at half maximum	0	0	**20**	**60**	0	0	0	0	0
Fuel thermal conductivity model	**80**	**0**	**100**	**100**	**20**	0	0	**40**	**60**
Clad thermal conductivity model	0	0	**60**	0	0	0	0	0	**20**
Fuel thermal expansion model	0	0	**60**	**60**	**100**	**100**	**100**	**40**	**100**
Clad thermal expansion model	0	0	**60**	**40**	**40**	**20**	**0**	**0**	**20**
Clad Yield stress	0	0	0	0	0	0	0	0	0
Fuel enthalpy	**100**	**100**	**100**	**20**	**100**	**80**	**100**	**40**	**100**
Clad to coolant heat transfer	**40**	0	**20**	**20**	0	0	0	**20**	**40**

Table 4-7: Percentage of FRAPTRAN users that have identified a given input parameter as influential for each output of interest at t=101 s.

The orange colour is associated with a percentage larger than 50 %, the blue colour with a percentage between 0 and 50 % and the green colour with a zero percentage.

- **<u>At the end of calculation</u>** (t=200 s)

Same as before the transient, the coolant inlet temperature is identified as influential on most of the outputs. It is also important to point out that the injected energy, fuel properties (fuel enthalpy, thermal expansion model) and clad to coolant heat exchange during the test have some effects on the final state of the rod (clad hoop strain fuel and clad elongation) (see Figure 4-31 and Table 4-8).

	Fuel thermal (DHR, TFC)	Clad thermal (TCO)	Clad mechanical (ECTH, SCH)	Fuel mechanical (EFT1, RFO)
Cladding outside diameter				
Cladding inside diameter				
Fuel theoretical density				
Fuel porosity				
Cladding roughness				
Fuel roughness				
Filling gas pressure				
Coolant pressure				
Coolant inlet temperature				
Coolant velocity				
Injected energy in the rod				
Full mid height width				
Fuel thermal conductivity model				
Clad thermal conductivity model				
Fuel thermal expansion model				
Clad thermal expansion model				
Clad Yield stress				
Fuel enthalpy				
Clad to coolant heat transfer				

Figure 4-31: Influential input parameters with respect to the type of behaviour when focusing on the end of the calculation.

A coloured bar means that more than 50 % of the participants have identified the corresponding input parameter as influential for the type of behaviour.

Input \ Output	DHR	TFC	TFO	TCO	ECTH	ECT	EFT1	SCH	RFO
Cladding outside diameter	0	0	**7**	**7**	**7**	0	0	**67**	0
Cladding inside diameter	0	0	**7**	**7**	**7**	**14**	0	**67**	**93**
Fuel theoretical density	0	0	**7**	**7**	**27**	**21**	**7**	0	0
Fuel porosity	**7**	0	0	**7**	**20**	**21**	**7**	**13**	0
Cladding roughness	0	0	**7**	**7**	0	0	**7**	**20**	0
Fuel roughness	0	0	**7**	**7**	0	0	0	**14**	0
Filling gas pressure	0	0	**7**	**7**	0	0	0	**67**	0
Coolant pressure	0	**20**	**20**	**27**	**7**	**7**	**7**	**67**	**7**
Coolant inlet temperature	**93**	**100**	**93**	**100**	0	0	**64**	**13**	**27**
Coolant velocity	0	0	**7**	**7**	0	0	0	**14**	0
Injected energy in the rod	0	0	**13**	**7**	**87**	**86**	**36**	**80**	**20**
Full width at half maximum	0	0	**7**	**7**	0	0	0	**13**	0
Fuel thermal conductivity model	0	0	**7**	**7**	**53**	**14**	0	**40**	0
Clad thermal conductivity model	0	0	**7**	**7**	**7**	0	0	**40**	0
Fuel thermal expansion model	0	**7**	**7**	**7**	**100**	**100**	**86**	**60**	**73**
Clad thermal expansion model	0	0	**7**	**7**	**60**	**57**	**7**	**27**	**7**
Clad Yield stress	0	0	**7**	0	**33**	**36**	**21**	**47**	**27**
Fuel enthalpy	**67**	0	**7**	**7**	**67**	**64**	**7**	**27**	**20**
Clad to coolant heat transfer	0	0	**7**	**7**	**53**	**36**	**14**	**47**	**7**

Table 4-8: Percentage of participants that have identified a given input parameter as influential for each output of interest at the end of calculation (t=200 s).

The orange colour is associated with a percentage larger than 50 %, the blue colour with a percentage between 0 and 50 % and the green colour with a zero percentage.

- **For the maximum value of each output of interest**

The injected energy and fuel enthalpy (according to Figure 4-32 and Table 4-9), have been identified as influential for all types of behaviours by a majority of participants. Input parameters related to the rod geometry (fuel and clad roughness, cladding inside diameter) as well as fuel thermal expansion model and full width at half maximum are also found to be influential in this study.
On the contrary, several input parameters (clad thermal expansion and conductivity model, coolant velocity and pressure, filling gas pressure, fuel porosity and theoretical density, cladding outside diameter) do not appear on the previous figure since they have been considered as influential by a very low percentage of participants.
One can also notice that there are more influential parameters for clad mechanical behaviour than for the other types of behaviour. This can be explained by the complex modelling of clad mechanical behaviour which depends, i.e. on fuel pellet deformations and clad temperature.
It is also worth mentioning that some results associated with some input parameters are strongly affected by the used code. It is for example the case for clad to coolant heat transfer that is influential for SCANAIR and not for FRAPTRAN, likely attributed to the differences in code versions as mentioned in chapter 3. On the contrary, full width at half maximum comes out as influential for FRAPTRAN, but not for SCANAIR.

	Fuel thermal (DHR, TFC)	Clad thermal (TCO)	Clad mechanical (ECTH, SCH)	Fuel mechanical (EFT1, RFO)
Cladding outside diameter				
Cladding inside diameter				
Fuel theoretical density				
Fuel porosity				
Cladding roughness				
Fuel roughness				
Filling gas pressure				
Coolant pressure				
Coolant inlet temperature				
Coolant velocity				
Injected energy in the rod				
Full mid height width				
Fuel thermal conductivity model				
Clad thermal conductivity model				
Fuel thermal expansion model				
Clad thermal expansion model				
Clad Yield stress				
Fuel enthalpy				
Clad to coolant heat transfer				

Figure 4-32: Influential input parameters with respect to the type of behaviour when focusing on maximum values

A coloured bar means that more than 50 % of the participants have identified the corresponding input parameter as influential for the type of behaviour.

Input \ Output	DHR	TFC	TFO	TCO	ECTH	ECT	EFT1	SCH	RFO
Cladding outside diameter	**7**	**7**	**20**	**33**	**7**	**7**	**7**	**13**	**7**
Cladding inside diameter	**67**	**60**	**13**	**13**	0	**21**	**14**	**7**	**87**
Fuel theoretical density	**47**	**47**	0	**7**	**27**	**29**	**29**	0	**13**
Fuel porosity	**33**	**40**	**7**	**7**	**33**	**21**	**29**	**7**	**7**
Cladding roughness	**60**	**7**	**40**	**40**	**7**	0	0	**73**	**7**
Fuel roughness	**57**	**7**	**50**	**43**	0	0	0	**71**	0
Filling gas pressure	**13**	**13**	**7**	**7**	0	**7**	0	**13**	0
Coolant pressure	0	**13**	**13**	**20**	0	0	0	**13**	**7**
Coolant inlet temperature	**47**	**13**	**13**	**27**	**7**	**14**	**14**	**53**	0
Coolant velocity	**7**	**7**	**7**	**21**	0	0	0	0	0
Injected energy in the rod	**100**	**100**	**100**	**100**	**100**	**93**	**93**	**20**	**100**
Full width at half maximum	**73**	**20**	**27**	**20**	**33**	**29**	**29**	**80**	**33**
Fuel thermal conductivity model	**47**	**7**	**93**	**93**	**13**	0	0	**20**	**7**
Clad thermal conductivity model	**7**	0	**33**	**27**	0	0	0	**40**	0
Fuel thermal expansion model	**13**	**13**	**13**	**13**	**100**	**100**	**100**	**87**	**93**
Clad thermal expansion model	**7**	0	**13**	**13**	**47**	**7**	**7**	**33**	**7**
Clad Yield stress	**7**	**7**	**7**	**7**	**13**	**14**	**14**	**67**	**20**
Fuel enthalpy	**80**	**87**	**87**	**80**	**87**	**86**	**86**	**7**	**80**
Clad to coolant heat transfer	**7**	**7**	**67**	**67**	0	0	0	**27**	**7**

Table 4-9: Percentage of participants that have identified a given input parameter as influential for the maximum value of each output of interest.

The orange colour is associated with a percentage larger than 50 %, the blue colour with a percentage between 0 and 50 % and the green colour with a zero percentage.

5. CONCLUSIONS AND RECOMMENDATIONS

The second activity of the WGFS RIA fuel codes benchmark Phase II was focused on the uncertainty assessment of the calculation results. In particular, the impacts of the initial states and key models on the results of the transient have been investigated. All uncertainties were considered as statistical or random ones. The identification and treatment of epistemic uncertainties, if any, was beyond the scope of the current project. In addition, sensitivity study was performed to identify or confirm the most influential input parameters.

Participation in the RIA benchmark Phase II has been very large: fourteen organizations representing twelve countries have provided the lower and upper bounds associated with all specified output parameters for uncertainty analysis; the partial rank correlation coefficients associated to each uncertain input for each specified output parameter at each specified time; and for their maximum values for sensitivity analysis.

In terms of computer codes used, the spectrum was also large as analyses were performed with ALCYONE, BISON, FRAPTRAN, RANNS, SCANAIR, TESPA-ROD, and TRANSURANUS.

The results supplied by all participants were used in synthesis analyses performed according to the commonly agreed methodology. The uncertainty analysis has resulted in the following main observations:

- The pulse width uncertainty has a strong effect on the uncertainty results during the power pulse;
- The uncertainty band width is similar for all codes in the case of fuel thermal behaviour outputs and a high coherence is obtained for those parameters (participants' results are in strong agreement for uncertainty intervals and reference calculations);
- Large uncertainty band width is observed for clad mechanical and thermal behaviour outputs and fuel mechanical behaviour outputs;
- A low coherence is observed for fuel and clad mechanical behaviour outputs (except for stresses in the clad), but coherent reference calculations and uncertainty intervals are obtained for a large majority of participants;
- No coherence is observed for clad stress and thermal-hydraulic behaviour outputs due to the combination of a large dispersion of reference calculations and narrow uncertainty bands for those parameters.

The sensitivity analyses for the maximum values of the main output parameters of interest, have resulted in the following observations:

- The injected energy and fuel enthalpy have been identified as influential for all types of behaviours (clad and fuel thermal and mechanical behaviours) by a majority of participants;
- Input parameters related to the rod geometry (fuel and clad roughness, cladding inside diameter) as well as fuel thermal expansion model and full width at half maximum were also identified as influential by this study;

- On the contrary, several input parameters (clad thermal expansion and conductivity model, coolant velocity and pressure, filling gas pressure, fuel porosity and theoretical density, cladding outside diameter) have been considered as influential by a very low percentage of participants;
- There are more influential parameters for clad mechanical behaviour than for the other types of behaviour.

The second activity studies confirmed the conclusions from the first activity but also offered some new insights:

- Regarding fast transient thermal-hydraulic Post-DNB behaviour, there are major differences in the different modelling approaches resulting in significant deviations between simulations. Unfortunately there are currently no simple and representative experimental results that could allow to validate or not the different approaches;
- The models of fuel and clad thermo-mechanical behaviour and the associated materials properties, should be improved and validated in RIA conditions
- The different influential input parameters are identified for fresh fuel. For instance, injected energy, fuel enthalpy, parameters related to the rod geometry (fuel and clad roughness, cladding inside diameter), fuel thermal expansion model and Full width at half maximum come out as influential regarding the maximum value of each output parameter of interest. But, the parameters with significant influence on the results for irradiated fuel could be different;

Uncertainties cannot fully explain the scatter observed in first activity results and during the Phase I of this benchmark exercise;

- The specifics of used codes and user effects could play a more important role than uncertainties.
- Based on the conclusions summed up above, the following recommendations can be made:
- To reduce user effect and code effect, the code development teams should provide recommendations regarding the version of their codes to be used, the models and also the numerical parameters to be used (mesh size, time step, …) as much as possible;
- A complement of the RIA benchmark should be launched. This activity should be limited in time and should be focused on uncertainty and sensitivity analyses on an irradiated case, in order to identify the corresponding influential input parameters. In particular uncertainties regarding fission gases distribution, fuel microstructure, clad corrosion state and gap conductance should be investigated;
- This information (most influential input parameters for an irradiated case) will be useful in the perspective of a possible establishment of the Phenomena Identification and Ranking Table (PIRT) for RIA and could guide the future RIA tests and code improvements;
- Cooperation between existing experimental teams should be established in the area of clad-to-coolant heat transfer during very fast transients as well as in the area the relevant fuel and clad thermo-mechanical modelling. The main objectives of this cooperation should be to collect and share all existing data and to formulate specific proposals in order to reduce the lack of knowledge and achieve common understanding on the subjects. This activity should address both out-of-pile and in-pile tests.

Finally, the conclusions of this work support the main recommendations proposed in the final report of first activity of the WGFS RIA fuel codes benchmark Phase II:

- Fuel and clad thermo-mechanical models (with the associated material properties) should be further improved and validated more extensively against a sound RIA database;

- Build-up of a comprehensive and robust database consisting of both separate-effect tests and integral tests should be pursued in the short term. In this way, both individual model validation and model integration into codes would be feasible. The database could be shared by the modellers, whenever possible, to ease the comparison of simulation results from various codes;
- The clad-to-coolant heat transfer in the case of water boiling during very fast transients is of particular interest, and capabilities related to modelling this phenomenon should be improved. To achieve this target regarding clad-to-coolant heat transfer, more separate-effect tests and experiments seem necessary;
- Models related to the evolution of the fuel-to-cladding gap should be improved and validated for RIA conditions as this has been shown to have a significant effect on fuel rod response. To reach this objective, in-reactor measurements of cladding strain during RIA simulation tests should be done (or at least attempted).

6. REFERENCES

[1] NEA/CSNI/R(2013)7, RIA Fuel Codes Benchmark- Volume 1, Nuclear Energy Agency, OECD, Paris, France (2013).

[2] NEA/CSNI/R(2016)6, Reactivity Initiated Accident (RIA) Fuel Codes Benchmark Phase II - Volume 1: Simplified Cases Results – Summary and Analysis, Nuclear Energy Agency, OECD, Paris, France (2016).

[3] NEA/CSNI/R(2016)6, Reactivity Initiated Accident (RIA) Fuel Codes Benchmark Phase II - Volume 2: Task No. 1 Specifications, Nuclear Energy Agency, OECD, Paris, France (2016).

[4] H. Glaeser, "GRS Method for Uncertainty and Sensitivity Evaluation of Code Results and Applications," Science and Technology of Nuclear Installations, Volume 2008, Article ID 798901, 2008.

[5] J. Zhang, J. Segurado and C. Schneidesch, "Towards an Industrial Application of Statistical Uncertainty Analysis Methods to Multi-physical Modelling and Safety Analyses," Proc. OECD/CSNI Workshop on Best Estimate Methods and Uncertainty Evaluations, Barcelona, Spain, 16-18 November 2011.

[6] E. Gentle, "Monte-Carlo Methods," Encyclopaedia of Statistics, 5, pp. 612-617, John Wiley and Sons, New-York, 1985.

[7] W. Conover, Practical non-parametric statistic, Wiley, New York, 1999.

[8] S.S. Wilks, Determination of sample sizes for setting tolerance limits, Ann. Math. Stat. 12, 91–96, 1941.

[9] A. Guba, M. Makai, L. Pal: "Statistical aspects of best estimate method-I"; Reliability.

[10] J. Baccou, E. Chojnacki, "A practical methodology for information fusion in presence of uncertainty: application to the analysis of a nuclear benchmark", Environment Systems and Decisions, 34(2), 237-248, 2014.

[11] McKay, M.D., "Sensitivity and uncertainty analysis using a statistical sample of input values," Ch. 4, Uncertainty Analysis, Ronen, Y. Editor, CRC Press, Florida, USA, 1988.

[12] Benchmark for uncertainty analysis in modelling (UAM) for design, operation and safety analysis of LWRs, Volume II: Specification and Support Data for the Core Cases (Phase II), Version 2.0, April 2014.

[13] S. Destercke, E. Chojnacki, Methods for the evaluation and synthesis of multiple sources of information applied to nuclear computer codes, Nuclear Engineering and Design, 238(9), 2484-2493 (2008).

[14] A. de Crécy, J. Baccou, OECD/NEA PREMIUM Benchmark. Phase IV: Confirmation / validation of the uncertainties found within Phase III, CEA & IRSN (France) (2014).

[15] B. Iooss, P. Lemaitre, A review on global sensitivity analysis methods, in Uncertainty management in Simulation-Optimization of Complex Systems: Algorithms and Applications (C. Meloni and G. Dellino, Eds), Springer (2015).

[16] NEA/CSNI/R(2011)4, BEMUSE Phase VI Report: status report on the area, classification of the methods, conclusions and recommendations, Nuclear Energy Agency, OECD, Paris, France (2011).

[17] S. Suard, S. Hostikka, J. Baccou, Sensitivity analysis of fire models using a fractional factorial design, Fire Safety J., 62, 115–124 (2013).

[18] J. Baccou, E. Chojnacki, SUNSET V2.1: theory manual and user guide, IRSN Technical Report SEMIA-2013-173 (2013).

APPENDIX: TASK NO. 2 SPECIFICATIONS

ACKNOWLEDGEMENTS

These specifications were prepared by the RIA Benchmark Phase II Task Group of the Working Group of Fuel Safety (WGFS). Special thanks go to Olivier Marchand (IRSN, France), Jean Baccou (IRSN, France), Vincent Georgenthum (IRSN, France), Jinzhao Zhang (Tractebell, Belgium) and Marco Cherubini (NINE, Italy) for this preparation and drafting this appendix. Luis Enrique Herranz (CIEMAT, Spain), Lars Olof Jernkvist (Quantum Technologies, Sweden), and Ian Porter (NRC, USA) reviewed the specifications and provided valuable comments.

Table of Appendix Contents

A.1 INTRODUCTION

Reactivity-initiated accident (RIA) fuel rod codes have been developed for a significant period of time and validated against the available specific database. However, the high complexity of the scenarios dealt with has resulted in a number of different models and assumptions adopted by code developers; additionally, databases used to develop and validate codes have been different depending on the availability of the results of some experimental programmes. This diversity makes it difficult to find the source of estimate discrepancies, when these occur.

A technical workshop on "Nuclear Fuel Behaviour during Reactivity Initiated Accidents" was organized by the NEA in September 2009. A major highlight from the session devoted to RIA safety criteria was that RIA fuel rod codes are now widely used, within the industry as well as the technical safety organizations (TSOs), in the process of setting up and assessing revised safety criteria for the RIA design basis accident. This turns mastering the use of these codes into an outstanding milestone, particularly in safety analyses. To achieve that, a thorough understanding of the codes' predictability is mandatory.

As a conclusion of the workshop, it was recommended that a benchmark (RIA benchmark Phase I) between these codes be organized in order to give a sound basis for their comparison and assessment. This recommendation was endorsed by the Working Group on Fuel Safety.

In order to maximize the benefits from this RIA benchmark Phase I exercise, it was decided to use a consistent set of four experiments on very similar high burnup fuel rods, tested under different experimental conditions:

- low temperature, low pressure, stagnant water coolant, very short power pulse (NSRR VA-1),
- high temperature, medium pressure, stagnant water coolant, very short power pulse (NSRR VA-3),
- high temperature, low pressure, flowing sodium coolant, larger power pulse (CABRI CIP0-1),
- high temperature, high pressure, flowing water coolant, medium width power pulse (CABRI CIP3-1).

A detailed and complete RIA benchmark Phase I specification was prepared in order to assure, as much as possible, the comparability of the calculated results. The main conclusions of the RIA benchmark Phase I are presented below [1]:

- With respect to the thermal behaviour, the differences in the evaluation of fuel temperatures remained limited, although significant in some cases. The situation was very different for the cladding temperatures that exhibited considerable scatter, in particular for the cases when water boiling occurred.
- With respect to mechanical behaviour, the parameter of largest interest was the cladding hoop strain, because failure during RIA transient results from the formation of longitudinal cracks. When compared to the results of an experiment that involved only PCMI, the predictions from the different participants appeared acceptable even though there was a factor of 2 between the highest and the lowest calculated hoop strain. The conclusion was not so favourable for cases where water boiling had been predicted to appear: a factor of 10 for the hoop strain between the calculations was exhibited. Other mechanical results compared during the RIA benchmark Phase I were fuel stack and cladding elongations. The scatter remained limited for the fuel stack elongation, but the calculated cladding elongation was found to vary significantly.

- The fission-gas release evaluations were also compared. The ratio of the maximum to the minimum values appeared to be roughly 2, which is considered to be relatively moderate given the complexity of fission gas release processes.
- Failure predictions, which may be considered as the ultimate goal of fuel codes dedicated to the behaviour in RIA conditions, were compared: it appears that the failure/no failure predictions are fairly consistent between the different codes and with experimental results. However, when assessing the code qualification, one should rather look at predictions in terms of enthalpy at failure because it is a parameter that may vary significantly between different predictions (and is also of interest in practical reactor applications). In the frame of this RIA benchmark Phase I, the calculated failure enthalpies among the different codes were within a +/- 50 % range.

As a conclusion of the RIA benchmark Phase I, it was recommended to launch a second phase exercise with the following specific guidelines:

- The emphasis should be put on deeper understanding of the differences in modelling of the different codes; in particular, looking for simpler cases than those used in Phase I, is expected to reveal the main reasons for the observed large scatter in some conditions, such as coolant boiling.
- Due to the large scatter between the calculations that was shown in the RIA benchmark Phase I, it appears that an assessment of the uncertainty of the results should be performed for the different codes. This should be based on a well-established and shared methodology. This also entailed performing a sensitivity study of results to input parameters to assess the impact of initial state of the rod on the final outcome of the power pulse.

The Working Group on Fuel Safety endorsed these recommendations and a second phase of the RIA fuel-rod-code benchmark (RIA benchmark Phase II) was launched early in 2014. This RIA benchmark Phase II has been organized as two complementary activities:

- The first activity is to compare the results of different simulations on simplified cases in order to provide additional bases for understanding the differences in modelling of the concerned phenomena.
- The second activity is focused on assessing the uncertainty of the results. In particular, the impact of the initial states and key models on the results of the transient are to be investigated.

The first activity was completed in 2015 and documented in an OECD report(see [2] and [3]). The complete set of solutions provided by all the participants are compiled in an unpublished report of the first activity (available to benchmark participants and to WGFS members).

The main body of this report provides a summary and documents the conclusions and recommendations from the second activity. The present Appendix provides second activity specifications that were prepared in order to ensure, as much as possible, the comparability of the calculation results submitted.

A.2 SECOND ACTIVITY: ASSESSMENT OF UNCERTAINTY OF THE RESULTS

2.1 Objectives

The objective of this second activity of the RIA benchmark Phase II is to assess the uncertainty of the results. In particular, the impact of the initial states and key models on the results of the transient will be investigated. In addition, a sensitivity study will be performed to identify or confirm the most influential input uncertainties.

All uncertainties will be considered as statistical or random ones. The identification and treatment of epistemic uncertainties, if any, is beyond the scope of the current project.

2.2 Description of the Case

Considering the feedback from Phase I of the RIA benchmark, the uncertainty analysis was initially intended to be performed on the foreseen CABRI international programme test CIP3-1, on an irradiated ZIRLO cladded UO2 fuel rodlet in PWR representative conditions. This Case was also considered in Phase I of the benchmark and resulted in the largest differences in the predictions from the different codes [1].

However, in the first activity of Phase II, it appeared that, despite simplifications in the defined Cases, a significant spread of results were still present. The original thought to use CIP3-1 Case (interesting due to its high burnup) seemed too ambitious for the reference Case due to:

- Complex initial rod state evaluation;
- Large effort required from participants;
- Risk of non-conclusive outcomes.

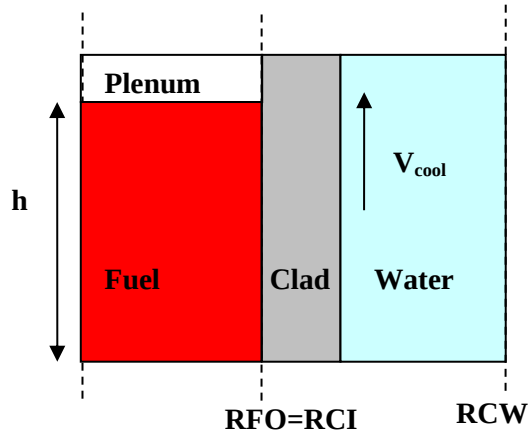

Fuel outer radius (RFO) = 4.13 mm
Clad inner radius (RCI) = 4.13 mm
Clad thickness = 570 µm
Water canal radius (RCW) = 7.5 mm
Upper plenum volume =2 cm^3
Fuel height (h) = 10 cm
Coolant velocity (V_{cool}) = 4.0 m/s

Figure 2-1: Rod design

Therefore, it has been agreed that the numerical reference case should be "Case 5" of the first activity (see [2] and [3]). To limit the differences linked to the initial state of the fuel, the case is limited to a fresh 17x17 PWR type fuel rodlet as described in Figure 2 1 with standard UO2 fuel and Zircloy-4 cladding. It is also assumed that there is no initial gap between the fuel and the clad which are considered perfectly bonded. The upper plenum is pressurized with helium at a typical pressure of a PWR rod (2 MPa at 20°C).

The thermal-hydraulic conditions during the transient are representative of water coolant in nominal PWR hot zero power (HZP) conditions (coolant inlet conditions: Pcool=155 bar, Tcool=280 °C and Vcool=4 m/s). These conditions are established by letting the coolant pressure and temperature increase linearly from ambient conditions during 50 s, after which a 50 s pre-transient hold time is postulated to establish steady-state conditions. At t=100 s, the reference pulse starts from zero power and it is considered to have a triangular shape, with 30 ms of Full Width at Half Maximum (FWHM) and a high value for the rod maximal power in the fuel is considered to provoke departure from nucleate boiling (DNB).

2.3 Uncertainty analysis methodologies

2.3.1 *Proposed methodology: input uncertainty propagation method*

Among all the available uncertainty analysis methods, the probabilistic input uncertainty propagation method is so-far the most widely used in the nuclear safety analysis [4]. In this method, the fuel codes are treated as "black boxes", and the input uncertainties are propagated to the simulation model output uncertainties via the code calculations with sampled in put data from the known distributions [5].

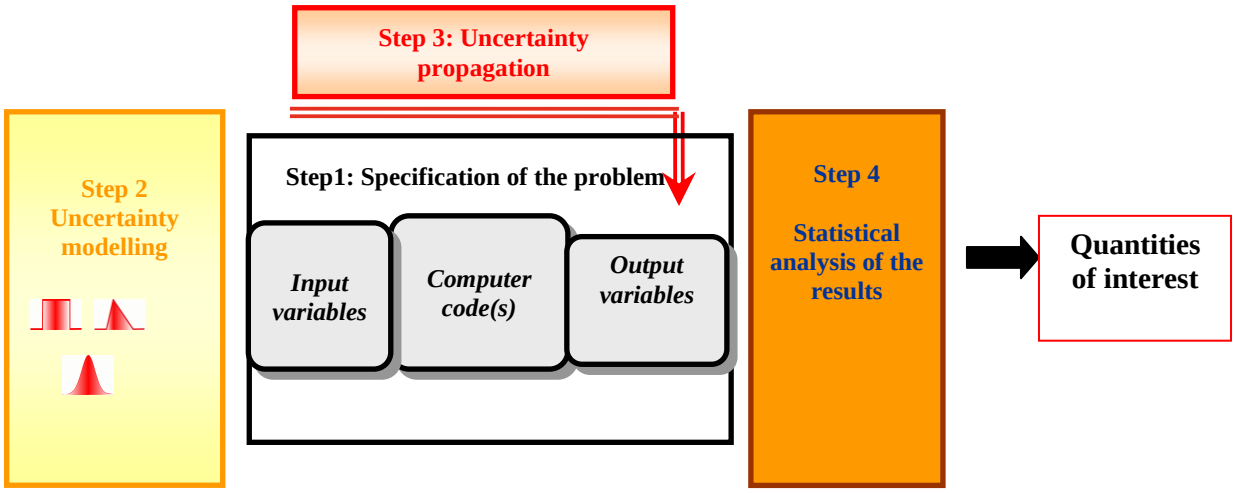

Figure 2-2: The four steps of an input uncertainty propagation method.

The method consists in the following steps (see Figure 2-2):

(1) Specification of the problem: All relevant code outputs and corresponding uncertain parameters for the codes, plant modelling schemes, and plant operating conditions are identified.

(2) Uncertainty modelling: the uncertainty of each uncertain parameter is quantified by a probability density function (PDF) based on engineering judgment and experience feedback from code applications to separate and integral effect tests and to full plants simulation. If dependencies between uncertain parameters are known and judged to be potentially important, they can be quantified by correlation coefficients.

(3) Uncertainty propagation through the computer code: the propagation is performed thanks to Monte-Carlo simulations [6]. In Monte-Carlo simulation, the computer code is run repeatedly, each time

using different values for each of the uncertain parameters. These values are drawn from the probability distributions and dependencies chosen in the previous step. In this way, one value for each uncertain parameter is sampled simultaneously in each repetition of the simulation. The results of a Monte-Carlo simulation lead to a sample of the same size for each output quantity.

(4) Statistical analysis of the results: the output sample is used to get any typical statistics of the code response such as mean or variance and to determine the cumulative distribution function (CDF). The CDF allows deriving the percentiles of the distribution (if X is a random variable and F_X its CDF, the α -percentile, $\alpha \in [0;1]$, is the deterministic value X_α such that $F_X(X_\alpha)=P(X \leq X_\alpha)=\alpha$).

A simple way to get information on percentiles is to use order statistics [7], which is a well-established and shared methodology in the nuclear community and hence is recommended for this activity.

The principle of order statistics is to derive results from the ranked values of a sample. If $(X^1,\ldots,X^N)$ denotes a sample of any random variable, X, and $(X^{(1)},\ldots,X^{(N)})$ the corresponding ranked one, order statistics first provides an estimation of the percentile of interest since the α-percentile can be estimated by $X^{(\alpha N)}$. Moreover, it turns out that the CDF of $X^{(k)}$, $F_X(X^{(k)})$, follows the Beta law $\beta(k,N-k+1)$, which does not depend on the distribution of X. This key result allows quantifying the probability that any ranked value is smaller than any percentile by the following formula:

$$P(X^{(k)} \leq X_\alpha) = F_{\beta(k,N-k+1)}(\alpha) \quad (1)$$

where $F_{\beta(k,N-k+1)}$ denotes the CDF of the Beta law $\beta(k,N-k+1)$.

Equation (1) can then be used to derive:

1) lower and upper bounds of a percentile of interest, given the sample size N and the confidence level β that controls the probability that $X(k) \leq X_\alpha$. It requires to solve the equation $F_{\beta(k,N-k+1)}(\alpha)=\beta$

2) the minimal sample size (and therefore the minimal number of computer runs) to perform in order to obtain a lower or upper bound of a given percentile with a given confidence level. It leads to the so-called Wilk's formula [8]:

$$N = \ln(1-\beta)/\ln(\alpha) \quad (2)$$

and Guba's estimate in Case of multiple output parameters in [9].

Order statistics are widely used since nothing should be known about the distribution of the random variable. Moreover, this method is very simple to implement, which makes it extremely interesting for licensing applications to nuclear safety analyses.

Due to its simplicity, robustness and transparency, this method will be used in this benchmark. The highly recommended sample size is set to 200 (i.e. 200 code runs will be performed). Strong justifications should be given if a lower number of code runs is performed. The sample is constructed according to the selected pdfs coming from the uncertainty modelling step and assuming independence between input parameters following a Simple Random Sampling (SRS) as recommended for the use of order statistics in BEMUSE [10][11].

Moreover, we focus on the estimation of a lower, resp. upper, bound of the 5%, resp. 95%, percentiles (α) at confidence level (β) higher than 95%. For N=200 and α=0.05 or 0.95, Equation (1) leads to:

$P(X^{(5)} <= X_{5\%}) = 0.97$

$P(X^{(196)} > X_{95\%}) = 0.97$

the lower, resp. upper, bound is defined in this benchmark by $X^{(5)}$, resp. $X^{(196)}$.

For a proper use of order statistics, all code runs should be successfully terminated. If not, it is therefore recommended to correct the failed code runs. As noticed during the BEMUSE project, some failures can come from a too large time step and the run can be continued after time step reduction. If there is no possible correction, a careful checking of the output evolution has to be performed in the failed runs to keep the results before the failures occur and use the previous methodology to analyse them. When the number of failures is relatively low, a conservative treatment can also be considered by assuming that the n failed runs produced the n most adverse values of the output of interest.

Participants are requested to clearly describe in their contribution their approach to handle this topic.

2.3.2 *Sensitivity analysis*

Besides uncertainty analysis, a complementary study will be performed to get qualitative insight on the most influential input parameters.

This work will be based on a sensitivity analysis using the 200 code runs previously obtained. More precisely, if Y denotes the response of interest and $\{X_i\}_{i=1,\ldots,p}$ the set of p uncertain input parameters (also called regressors), it will require to estimate the following classical correlation coefficients:

- Linear (or Pearson's) simple correlation coefficients (SCC): for each i,

$$\rho_i = \frac{\mathrm{cov}(Y, X_i)}{\sigma_X \sigma_Y}$$

  where σ_x and σ_y are the empirical standard deviations of X and Y.
  They correspond to the p correlation coefficients between the response and each of the p regressors. They measure the degree of linear dependence between the response and each of the p regressors taken separately. In multiple regression, the regressors are not always orthogonal and partial rank correlation coefficients (PCC) are sometimes preferred to SCC since in this case the correlation is not evaluated with the response but with the response from which linear trends associated with other input variables are removed [21]. PCC might lead to higher number than the Pearson's simple correlation coefficient.
  They correspond to the p correlation coefficients between the response and each of the p regressors. They measure the degree of linear dependence between the response and each of the p regressors taken separately. A better measure of linear relation between the response and one of the p regressors is the so-called partial correlation coefficient (PCC), in which the correlation between the two variables under consideration is calculated after each is corrected for the linear contribution of the remaining variables [21]. Indeed, since this correction removes linear trends associated with other variables, the PCC would lead to higher number than the Pearson's simple correlation coefficient.
- Spearman's rank correlation coefficient (RCC): same definition as SCC but replacing input and output values by their respective ranks. Working with ranks allows one to extend the previous underlying linear regression model to a monotonic non-linear one. In the presence of nonlinear but monotonic relationships between the response and each of the p regressors, use of the rank transform can substantially improve the resolution of sensitivity analysis results [22].

Similarly to PCC, the partial rank correlation coefficient (PRCC) can be introduced in order to remove trends associated with other variables [21]. Again, the PRCC might lead to higher number than the Spearman's rank correlation coefficient.

Based on this information (Pearson's SCC or Spearman's RCC, PCC or PRCC), the most influential uncertain input parameters can be identified.

Note that the above correlation coefficients estimate the linear connection (SCC) or the monotonic one (RCC) between the input and the target output parameters. Moreover, no interaction between input parameters is taken into account [23].

As the RIA fuel rod codes are all complex models, and there are certain interactions between input parameters, these coefficients can only be considered as qualitative and relative index for screening the non-important input parameters.

Other sensitivity measures, such as the Sobol's indexes, could be obtained by using the variance-based decomposition method [15]. The Sobol's indexes provide quantitatively the contribution of the uncertainty of each input parameter to the target output parameter uncertainty. However, the variance-based decomposition method requires much more calculations efforts, therefore is not recommended for the current benchmark.

2.3.3 ***Proposed tools***

2.3.3.1 *DAKOTA (SNL)*

The DAKOTA (Design Analysis Kit for Optimization and Terascale Applications) code has been developed by the Sandia National Laboratory [12]. It can be freely downloaded from the website *http://www.cs.sandia.gov/dakota*.

As shown in Figure 2-3, DAKOTA provides a flexible, extensible interface between simulation codes and iterative analysis methods, via DAKOTA input files and executables.

Among others, DAKOTA contains algorithms for uncertainty quantification (UQ) with sampling (Monte-Carlo or Latin Hypercube), epistemic uncertainty methods (Second order probability or Dempster-Shafer theory of evidence), and sensitivity analysis. These capabilities may be used on their own or as components within advanced strategies.

For the applications presented in this activity, the input uncertainty parameters ranges and distributions, as well as the uncertainty analysis method and number of samples are defined in the DAKOTA Input File.

Based on the sampled or assigned input uncertainty parameters in the DAKOTA Parameter File, various scripts can be developed to create the code input files, to execute the simulation jobs, and to collect the code calculation output data into the DAKOTA Results File.

The DAKOTA Executable will then perform the requested statistical uncertainty and sensitivity analysis, and provide the information in the DAKOTA Output Files.

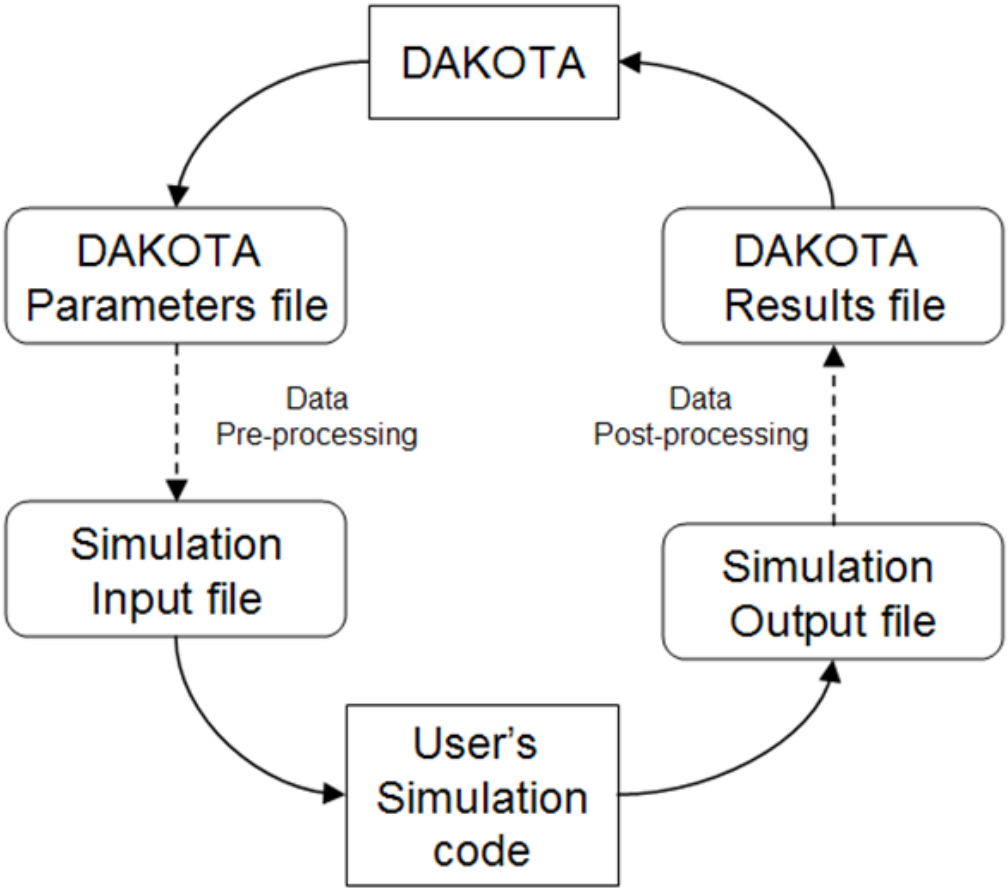

Figure 2-3: DAKOTA uncertainty analysis process

2.3.3.2 *SUNSET (IRSN)*

The SUNSET (Sensitivity and UNcertainty Statistical Evaluation Tool) software [18] is a statistical tool providing a collection of methods for information treatment in risk analysis studies.
It can be freely downloaded from the website https://gforge.irsn.fr/gf/project/sunset.

In the sequel, we provide a quick overview of the available methodologies to take into account uncertainties in risk analysis studies (see Figure 2-4). A more exhaustive description of the software can be found on http://www.irsn.fr/en/research/scientific-tools/computer-codes/pages/sunset.aspx.

SUNSET allows the user to evaluate the uncertainties associated to the results coming from risk analysis studies. It includes statistical tools to perform a probabilistic assessment of uncertainties, where the uncertainty sources are modelled using random variables. To be able to handle both aleatory and epistemic uncertainties, techniques based on the Dempster-Shafer evidence framework are available.

SUNSET can also be used for sensitivity analyses to identify the variables which have the largest contributions to the overall model response uncertainty, but also to directly study the explicit relationship between the variables and each response. The methods are based on algebraic and statistical tools combining design of experiment theory and regression techniques.

Both uncertainty analysis and sensitivity analyses require running the used model (such as a computer code) several times in order to propagate the information from its input to its outputs. Therefore, several

coupling functionalities are available in SUNSET: for analytical models, it is possible for the user to directly introduce the analytical expression in a SUNSET data deck, whereas for complex computer codes, non-intrusive (i.e. by data files) or intrusive (i.e. by developing some special coupling procedures) coupling can be performed. These functionalities have been exploited to couple SUNSET to several IRSN codes such as SCANAIR for RIA studies.

In safety assessment, different uncertainty analyses using different computer codes and implying different experts are generally performed. Each uncertainty study or expert can be viewed as an information source. Therefore, taking advantage of these analyses appears to be a question of information evaluation (i.e. how to measure the quality of provided information) and fusion (i.e. how to combine the different information given by several sources on a same output such as temperature). SUNSET provides several formal tools to address these two important questions. They will be used to analyse the results of the benchmark.

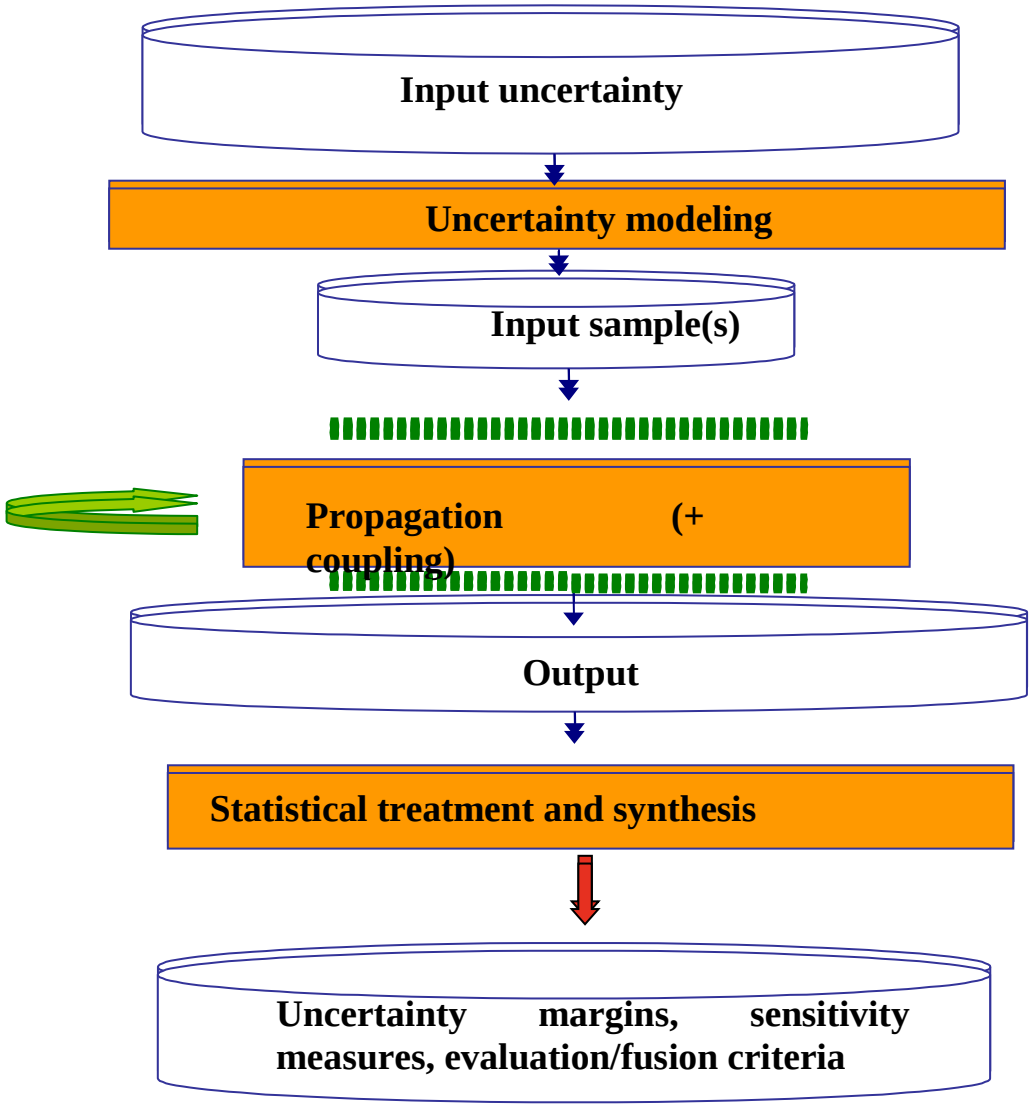

Figure 2-4: Sketch of the different steps of an uncertainty analysis with the SUNSET software.

2.4 Identification of Uncertainty parameters

The uncertainties from the Phase I and activity 1 of Phase II of the RIA benchmark, as well as the OECD UAM benchmark [14], were identified and classified into four categories:

- Uncertainties in the fuel rod design, bounded by allowable manufacturing tolerances,
- Thermal hydraulic boundary conditions,
- Core power boundary conditions,
- Physical Properties/key models.

2.4.1 *Uncertainties in the fuel rod manufacturing tolerances*

- Cladding outside/inside diameter: the manufacturing tolerance is taken into account, uncertainty = 20 µm,
- cladding roughness: between 0 and 2 µm,
- fuel pellet outside diameter: not considered (in our case equal to cladding inside diameter),
- fuel pellet roughness: between 0 and 2 µm,
- U235 enrichment: the manufacturing tolerance is very low (uncertainty = 0.003) and neglected,
- fuel theoretical density: the recommended uncertainty for the fuel density is 1 % according to Carbajo [15],
- fuel initial porosity: 3 to 5 %,
- fuel stoichiometry: for fresh fuel O/M is equal to 2, no uncertainties are considered,
- rod gas-gap fill pressure: uncertainty of 1 bar.

2.4.2 *Uncertainties in the fuel rod initial states*

The uncertainty parameters in the initial states of the fuel rod are mainly related to the uncertainties in the base irradiation operating conditions: with fresh fuel, these parameters have not to be considered in this study.

2.4.3 *Uncertainties in thermal hydraulic boundary conditions*

- System pressure: the uncertainty is low (~ 1 %),
- coolant inlet temperature: an uncertainty of 3K is considered,
- coolant flow rate: an uncertainty of 2 % is considered,
- Clad to coolant heat transfer coefficient: There is a large uncertainty on this value; an engineering uncertainty of 25% is considered.

2.4.4 *Uncertainties in core power boundary conditions*

- Power pulse width: in CABRI REPNa tests, if the measurement of core power and then power pulse width is precise, the reproducibility of the pulse width is more difficult and the uncertainty is ~ 5 ms,
- Injected energy: in the CABRI REPNa tests the uncertainty on the injected energy was ~ 7 % , an uncertainty of 10% is considered here,

- Fuel rod power: once the uncertainties on the power pulse width and the injected energy are fixed, the fuel rod power is fixed by Pmax = Injected energy/(power pulse width)
- Power distributions: axial and radial profiles in the rod are supposed flat in this study, no uncertainties considered.

2.4.5 *Uncertainties in the physical properties and key models*

- Fuel and clad thermal conductivity: 10% of uncertainty is commonly considered (Fink [16], Carbajo [15]),
- Fuel and clad thermal expansion: 10% of uncertainty is commonly considered (Fink [16], Carbajo [15]),
- Fuel enthalpy (or mass heat capacity): according to Fink [16]and Carbajo [15], analyses the uncertainty on this property is 3 %,
- Clad Yield stress: an uncertainty of 10 % is considered [17],
- Fuel Young modulus: not considered,
- Poisson's ratio: not considered.
- Fuel and clad emissivities: not considered,
- Cladding creep model: not considered ,
- Fission gas release model: not considered here (fresh fuel),
- Cladding corrosion model (initial state) : not considered in this study,
- Cladding hydrogen pickup model: not considered in this study.

2.4.6 *List of uncertain parameters*

Input uncertainty parameter	Distribution				
	Mean	**Standard Deviation**	**Type**	**Lower bound**	**Upper bound**
1. Fuel rod manufacturing tolerances					
Cladding outside diameter (mm)	9.40	0.01	Normal	9.38	9.42
Cladding inside diameter (mm)	8.26	0.01	Normal	8.24	8.28
Fuel theoretical density (kg/m3 at 20 °C)	10970	50	Normal	10870	11070
Fuel porosity %	4	0.5	Normal	3	5
Cladding roughness (µm)	0.1	1.	Normal	10.-6	2.
Fuel roughness (µm)	0.1	1.	Normal	10.-6	2.
Filling gas pressure (MPa)	2.0	0.05	Normal	1.9	2.1
2. Thermal hydraulic boundary conditions					
Coolant pressure (MPa)	15.500	0.075	Normal	15.350	15.650
Coolant inlet temperature (°C)	280	1.5	Normal	277	283
Coolant velocity (m/s)	4.00	0.04	Normal	3.92	4.08
3. Core power boundary conditions					
Injected energy in the rod (Joule)	30000	1500	Normal	27000	33000
Full width at half maximum (ms)	30	5	Normal	20	40
4. Physical Properties/Key models					
Fuel thermal conductivity model (Mult. Coef.)	1.00	5 %	Normal	0.90	1.10
Clad thermal conductivity model (Mult. Coef.)	1.00	5 %	Normal	0.90	1.10
Fuel thermal expansion model (Mult. Coef.)	1.00	5 %	Normal	0.90	1.10
Clad thermal expansion model (Mult. Coef.)	1.00	5 %	Normal	0.90	1.10
Clad Yield stress (Mult. Coef.)	1.00	5 %	Normal	0.90	1.10
Fuel enthalpy / heat capacity (Mult. Coef.)	1.00	1.5 %	Normal	0.97	1.03
Clad to coolant heat transfer (Mult. Coef. - Same Coef. applied for all flow regimes)	1.00	12.5 %	Normal	0.75	1.25

Table 2-1 provides the specified input parameters as well as the information related to their uncertainty. For each input parameter, the information includes a mean value, a standard deviation and a type of distribution. In order to avoid unphysical numerical values, a range of variation (lower and upper bounds) is also provided. The sampling will be performed between the upper and lower bounds, i.e. the PDFs will be truncated. In order to simplify the current benchmark application, a normal distribution is assigned to all the considered input parameters. Their standard deviation are taken as the half of the maximum of the absolute value of the difference between their nominal value and their upper or lower bound. The effect of the uncertainty modelling (i.e. the choice of a normal distribution) will not be studied in this benchmark. Although this effect it could have some impact on the derived uncertainty bands, the conclusions of this exercise are expected to be similar for other distributions.

It should be recalled that, as the study is limited to fresh fuel, classical uncertainty parameters for irradiated fuel (such as fission gases distribution, cladding corrosion, gap conductance,…) are not considered here.

Finally, although the dependency between the pulse width and the injected energy is well known, it is not considered.

In addition, the participants could perform sensitivity studies by using other distributions, such as uniform or histogram. These results could be reported at the workshop or the final report.

There exists several approaches to study the influence of the pdfs or to take into account the nature of uncertainties (aleatory, epistemic) ([17], [18], [19] or [20]) but these key topics was out of the scope of this benchmark.

Input uncertainty parameter	**Distribution**				
	Mean	**Standard Deviation**	**Type**	**Lower bound**	**Upper bound**
1. Fuel rod manufacturing tolerances					
Cladding outside diameter (mm)	9.40	0.01	Normal	9.38	9.42
Cladding inside diameter (mm)	8.26	0.01	Normal	8.24	8.28
Fuel theoretical density (kg/m^3 at 20 °C)	10970	50	Normal	10870	11070
Fuel porosity %	4	0.5	Normal	3	5
Cladding roughness (µm)	0.1	1.	Normal	10.$^{-6}$	2.
Fuel roughness (µm)	0.1	1.	Normal	10.$^{-6}$	2.
Filling gas pressure (MPa)	2.0	0.05	Normal	1.9	2.1
2. Thermal hydraulic boundary conditions					
Coolant pressure (MPa)	15.500	0.075	Normal	15.350	15.650
Coolant inlet temperature (°C)	280	1.5	Normal	277	283
Coolant velocity (m/s)	4.00	0.04	Normal	3.92	4.08
3. Core power boundary conditions					
Injected energy in the rod (Joule)	30000	1500	Normal	27000	33000
Full width at half maximum (ms)	30	5	Normal	20	40
4. Physical Properties/Key models					
Fuel thermal conductivity model (Mult. Coef.)	1.00	5 %	Normal	0.90	1.10
Clad thermal conductivity model (Mult. Coef.)	1.00	5 %	Normal	0.90	1.10
Fuel thermal expansion model (Mult. Coef.)	1.00	5 %	Normal	0.90	1.10
Clad thermal expansion model (Mult. Coef.)	1.00	5 %	Normal	0.90	1.10
Clad Yield stress (Mult. Coef.)	1.00	5 %	Normal	0.90	1.10
Fuel enthalpy / heat capacity (Mult. Coef.)	1.00	1.5 %	Normal	0.97	1.03
Clad to coolant heat transfer (Mult. Coef. - Same Coef. applied for all flow regimes)	1.00	12.5 %	Normal	0.75	1.25

Table 2-1: list of input uncertainty parameters for statistical uncertainty analysis

2.5 Output specification

2.5.2 *Uncertainty analysis output*

Each participant should give lower and upper bounds associated with all the time trend output parameters listed in

Table 2-2. In addition, the results of the calculation with the nominal value of the input parameters, also called reference calculation should be provided.

One formatted Excel file is expected for the uncertainty analysis results (see task-2-A_organization_case_5). In this file, the list of time where each output has to be simulated is provided. Participants are requested to keep the same format when filling the file since an excel function will be included to automatically extract the two bounds of interest.

Parameter	Unit	Description
DHR	cal/g	Variation of radial average enthalpy with respect to initial conditions of the transient in the rodlet as a function of time (at z = h/2) (please note that: DHR(t = 0) = 0)
TFC	°C	Temperature of fuel centreline as a function of time (at z = h/2)
TFO	°C	Temperature of fuel outer surface as a function of time (at z = h/2)
TCO	°C	Temperature of clad outer surface as a function of time (at z = h/2)
ECTH	%	Clad total (thermal + elastic + plastic) hoop strain at the outer part of the clad as a function of time(at z = h/2)
ECT	mm	Clad total axial elongation as a function of time
EFT1	mm	Fuel column total axial elongation as a function of time
SCH	MPa	Clad hoop stress at outer part of the clad as a function of time (at z = h/2)
RFO	mm	Fuel outer radius as a function of time (at z = h/2)

Table 2-2: list of output parameters to be provided

Moreover, the reference, lower and upper bound values for following scalar outputs shall be provided:

- Maximum value for each parameter in
- Table 2-2,
- Time to Maximum value for each parameter in
- Table 2-2,

- Boiling duration: difference between time of critical heat flux achievement and time of reaching the rewetting heat flux.

2.5.3 *Sensitivity analysis output*

The partial rank correlation coefficients (or Spearman's if PRCC is not available) associated to each uncertain input for each output at the times defined in Table 2-3 as well as for their maximal value shall also be provided.

Time parameters	t_1	t_2	t_3	t_4	t_5
Definition	**Beginning of power pulse**	**Time of maximum power pulse**	**End of power pulse**	**101 s**	**End of calculation**
Value	**100.000 s**	**between 100.020 s and 100.040 s**	**between 100.040 s and 100.080 s**	**101.000 s**	**200.000 s**

Table 2-3: list of different times for sensitivity analysis output

One formatted Excel file is expected for the sensitivity analysis results (see task-2-B_organization_case_5).

Appropriate common thresholds for measuring the importance can be defined at a later stage.

2.6 Synthesis of the participants' results

Regarding the uncertainty analysis, besides plotting the uncertainty results for each participant, IRSN will perform a more detailed synthesis for both time depending parameters and scalar outputs in order to exhibit relevant conclusions making easier the analysis of the benchmark.

The elaborated synthesis will be based on the introduction of two formal tools for information evaluation and fusion. It will contribute to provide a summary of all participants' results and will also allow pointing out agreement or disagreement between groups of participants.

A full description of this methodology can be found in [21].

Regarding the sensitivity analysis, based on information provided by each participant, the most influential uncertain input parameters with respect to the Fuel Thermal Behaviour (DHR, TFC), Clad Thermal Behaviour (TCO), Clad Mechanical Behaviour (ECTH, SCH) and Fuel Mechanical Behaviour (EFT1, RFO) will be identified by IRSN.

The threshold for measuring the importance (High or Low) based on the sensitivity analysis results will be fixed at 0.25.

A.3 REFERENCES

[1] NEA/CSNI/R(2013)7, RIA Fuel Codes Benchmark - Volume 1, Nuclear Energy Agency, OECD, Paris, France (2013).

[2] NEA/CSNI/R(2016)6, Reactivity Initiated Accident (RIA) Fuel Codes Benchmark Phase II - Volume 1: Simplified Cases Results – Summary and Analysis, Nuclear Energy Agency, OECD, Paris, France (2016).

[3] NEA/CSNI/R(2016)6, Reactivity Initiated Accident (RIA) Fuel Codes Benchmark Phase II - Volume 2: Task No. 1 Specifications, Nuclear Energy Agency, OECD, Paris, France (2016).

[4] H. Glaeser, "GRS Method for Uncertainty and Sensitivity Evaluation of Code Results and Applications," Science and Technology of Nuclear Installations, Volume 2008, Article ID 798901, 2008.

[5] J. Zhang, J. Segurado and C. Schneidesch, "Towards an Industrial Application of Statistical Uncertainty Analysis Methods to Multi-physical Modelling and Safety Analyses," Proc. OECD/CSNI Workshop on Best Estimate Methods and Uncertainty Evaluations, Barcelona, Spain, 16-18 November 2011.

[6] E. Gentle, "Monte-Carlo Methods," Encyclopaedia of Statistics, 5, pp. 612-617, John Wiley and Sons, New-York, 1985.

[7] W. Conover, Practical non-parametric statistic, Wiley, New York, 1999.

[8] S.S. Wilks, Determination of sample sizes for setting tolerance limits, Ann. Math. Stat. 12, 91–96, 1941.

[9] A. Guba, M. Makai, L. Pal: "Statistical aspects of best estimate method-I"; Reliability Engineering and System Safety 80, 217-232, 2003.

[10] A. de Crécy, et al., "The BEMUSE Programme: Results of the First Part Concerning the LOFT L2-5 Test," Proceedings of 14th International Conference on Nuclear Engineering, Miami, Florida, USA, 17-20 July, 2006.

[11] BEMUSE Phase VI Report, Status report on the area, classification of the methods, conclusions and recommendations, OECD/NEA/CSNI/R(2011)4, March 2011.

[12] B. Adams, et al., "DAKOTA, A Multilevel Parallel Object-Oriented Framework for Design Optimization, Parameter Estimation, Uncertainty Quantification, and Sensitivity Analysis: Version 5.1 User's Manual", Sandia Technical Report SAND2010-2183, Updated Version 5.3, December 2013. (http://www.cs.sandia.gov/dakota).

[13] J. Baccou, E. Chojnacki, "SUNSET V2.1: theory manual and user guide", IRSN Technical Report SEMIA-2013-173, 2013.

[14] Benchmark for uncertainty analysis in modelling (UAM) for design, operation and safety analysis of LWRs, Volume II: Specification and Support Data for the Core Cases (Phase II), Version 2.0, April 2014.

[15] J. J. Carbajo, et al "A review of thermophysical properties of MOX and UO2 fuel", J. Nucl Mat, 299, pp 181-198, 2001.

[16] J. K. Fink "Thermophysical properties of uranium dioxide", J. Nucl. Mat, 279, pp 1-18, 2000.

[17] B. Cazalis et al "The PROMETRA program: cladding mechanical behaviour under hidh strain rate" Nucl. Tec., pp 215-229, vol. 157, 2007

[18] S. Ferson, L. Ginzburg, “Different methods are needed to propagate ignorance and variability”, Reliability Engineering and System Safety, 54, 133-144, 1996.

[19] C. Baudrit, D. Guyonnet, D. Dubois, “Joint propagation and exploitation of probabilistic and possibilistic information in risk assessment”, IEEE Trans. Fuzzy Syst., 14, 593-608, 2006.

[20] J.C. Helton, J.D. Johnson, W.L. Oberkampf, C.J. Sallaberry, “Sensitivity analysis in conjunction with evidence theory representations of epistemic uncertainty”, Reliability Engineering & System Safety, 91 (10-11), 1414-1434, 2006.

[21] J. Baccou, E. Chojnacki, “A practical methodology for information fusion in presence of uncertainty: application to the analysis of a nuclear benchmark”, Environment Systems and Decisions, 34(2), 237-248, 2014.

[22] McKay, M.D., “Sensitivity and uncertainty analysis using a statistical sample of input values,” Ch. 4, Uncertainty Analysis, Ronen, Y. Editor, CRC Press, Florida, USA, 1988.

[23] J.C. Helton,J.D. Johnson, C.J. Sallaberry, C.B. Storlie, “Survey of sampling-based methods for uncertainty and sensitivity analysis,” Reliability Engineering and System Safety, 91(10), 10/2006.

[24] B. Iooss and P. Lemaitre, “A review on global sensitivity analysis methods,” in Uncertainty management in Simulation-Optimization of Complex Systems: Algorithms and Applications (C. Meloni and G. Dellino, Eds), Springer, 2015, http://www.springer.com/business.